Mag.rer.nat Alexander Muhr

Design and development of an experimental process setup for *in vitro* simulation of the impact of hydrodynamic stress on protein producing cells

Dissertation

zur Erlangung des akademischen Grades eines Doktors der Naturwissenschaften

erreicht an der

Technischen Universität Graz

Univ.-Prof. Dipl.-Ing. Dr.techn. Johannes Khinast

Institut für Prozess- und Partikeltechnik
Technische Universität Graz

2011

Deutsche Fassung:

EIDESSTATTLICHE ERKLÄRUNG

Ich erkläre an Eides statt, dass ich die vorliegende Arbeit selbstständig verfasst, andere als die angegebenen Quellen / Hilfsmittel nicht benutzt, und die den benutzten Quellen wörtlich und inhaltlich entnommene Stellen als solche kenntlich gemacht habe.

Graz, am …… ……..

Datum (Unterschrift)

Englische Fassung:

STATUTORY DECLARATION

I declare that I have authored this thesis independently, that I have not used other than the declared sources / resources, and that I have explicitly marked all material which has been quoted either literally or by content from the used sources.

…… ……..

date (signature)

Acknowledgements

First and foremost I want to thank my family for their everlasting support and help.

I also want to express my gratitude to all my friends, who helped me through some difficult times and enjoyed successful moments with me.

My thanks go to Professor Khinast for his long term support with this challenging project, as well as Professor Bogner-Strauß for her help and encouragement. Furthermore, I'd like to thank all people at the Institute for Process and Particle Engineering for the wonderful and enlightening time we spent together.

Kurzfassung

Die Bedeutung von therapeutischen Proteinen hat in den letzten Jahren stark zugenommen, und damit steigt auch die Bedeutung von Säugetierzellen. Diese Zellen sind nötig, um rekombinante humane Proteine richtig zu glykosylieren, und ihnen damit volle Bioaktivität für den therapeutischen Einsatz im Menschen zu ermöglichen. Doch die Maßstabsvergrößerung der Herstellverfahren ist schwierig zu planen, da eine Vielzahl von Einflüssen auf Säugetierzellen wissenschaftlich noch nicht geklärt ist. Obwohl in den letzten Jahren viele Studien durchgeführt wurden, fehlen noch einige Zusammenhänge über die Auswirkung von Stressfaktoren auf die Lebens- und Produktionsfähigkeit von Zellen. Mehrere Effekte wurden auch noch nicht quantitativ beschrieben, obwohl gerade diese Informationen Voraussetzung für eine wissenschaftlich fundierte Planung von Produktionsbioreaktoren wären.

Der Einfluss von hydrodynamischen Kräften ist einer dieser Effekte, der gerade bei Säugetierzellen, welche keine Zellwand besitzen, große Auswirkung hat. Im Rahmen dieser Dissertation werden neue Erkenntnisse zu diesem Thema gezeigt. Teil A beschreibt den bisher noch nicht durchgeführten Aufbau einer adhärenten Maus-Leber-Epithel-Zellline (BNL-Cl.2), die humanes Erythropoetin sekretiert. In Teil B wird ein neu entwickelter Versuchsaufbau vorgestellt, der die Messung der Proteinproduktion unter konstantem Fluss ermöglicht. Die hydrodynamischen Kräfte, hier als Energiedissipationsraten (EDR) beschrieben, können verändert werden, während andere Faktoren wie Temperatur oder pH-Wert konstant gehalten werden. Teil C präsentiert die Daten von Experimenten mit vier Flussraten im Bereich von $1{,}56 \times 10^3$ bis $1{,}41 \times 10^4$ W/m^3. Diese neuartigen Daten zeigen einen Einbruch der rhEPO Produktion während der Mitosephase der Zellen für alle Durchflussgeschwindigkeiten. Darüber hinaus zeigen EDRs ab 10^4 W/m^3 Auswirkungen auf die Proteinproduktion. Dabei beschleunigt sich auch der Verlust der Zellmasse, und die rhEPO Konzentration erreicht gegen Ende der Experimente maximal ein Gleichgewicht zwischen Produktion und Zerfall. Teil D stellt im Anschluss zukünftige Aspekte und Anwendungsmöglichkeiten vor, die auf dem entwickelten Versuchsaufbau und den vorliegenden Daten basieren.

Abstract

As the importance of therapeutic proteins is increasing, so is the importance of mammalian cells as hosts of production. They are necessary to achieve correct glycosylation and therefore full bioactivity of products for therapeutic use in humans. However, the scale-up of production processes is difficult to design, as the variety of influences on mammalian cells is not scientifically resolved yet. Despite many studies that have been performed during the last years, the understanding of the impact of cell stress factors on cell viability is not complete, and several effects have not been described quantitatively, although they would be a prerequisite for a rational bioreactor scale-up. This also applies to the influence of hydrodynamic forces on the viability and productivity of cell systems.

Mechanical stress is a concern especially for mammalian cells due to their lack of cell walls, and this thesis contributes new insights towards this topic. Part A describes the previously unreported construction of an adherent mouse epithelial liver cell line (BNL-CL.2), producing human erythropoietin (hEPO). In Part B a newly developed experimental setup is introduced, allowing measuring the protein production under constant flow of medium. Moreover, the strength of hydrodynamic forces, here described as energy dissipation rates (EDR), is variable, while other factors like temperature or pH-value are kept at designated levels. Part C presents unique data achieved with this experimental setup. Experiments were done at four flow rates, ranging from 1.56×10^3 to 1.41×10^4 W/m^3. The experimental data shows loss of rhEPO production during the mitosis phase for all flow rates. Furthermore, EDRs of 10^4 W/m^3 or higher, did reveal impact on the protein production. Following an accelerated loss of cell mass, the rhEPO levels reach at best a balance between production and decomposition during the final stages of the experiments. Part D finally refers to future aspects based on the developed experimental setup and the present data.

Table of contents

Part A

Isolation of the human erythropoietin gene and cloning into eligible mammalian cell lines

1 Goals and Motivation

The production of new active pharmaceutical ingredients (API) often requires the use of recombinant proteins. These proteins (reproduced after agents in the human body) are highly effective and specific but have to be manufactured using cell cultures, since they are very complex and cannot be produced by synthetic chemical processes.

Mammalian cell cultures are the method of choice for the production of therapeutic proteins, e.g. recombinant human tissue plasminogen activator (tPA), Factor VIII, erythropoietin and monoclonal antibodies. These proteins require substantial post-translational modifications for full bioactivity and acceptable pharmacokinetics, which *Escherichia coli*, yeasts, other micro-organisms or insect cells cannot provide without substantial modification [(1)].

Mammalian cell lines are more difficult to maintain then bacteria and are especially susceptible to mechanical forces, due to their lack of a protective cell wall. This stress can result in cell death, either lysis by disruption of cell membrane (apoptosis) or direct bursting of the cells due to high hydrodynamic forces (necrosis) [(2)]. A response to sublytic levels of stress can alter the growth rate, morphology, metabolism, and genetic expression [(1)] and therefore result in downgraded quality by miss folding as well as reduced quantity of the recombinant protein yield. The mechanisms by which mammalian cells detect the presence of low-level mechanical stress and convert this force into an intracellular signal which leads to altered cellular metabolism and genetic expression have been thoroughly examined in a lot of papers. Only some of these mechanisms are fully understood yet.

Aside from this lack of scientific knowledge, most production processes are still based on empiric know-how as well as trial and error. However, a “quality by design” approach, were the process is planned prior to the start of production would greatly reduce loss of time and money in the pharmaceutical industry. Some already known drugs might even become producible based on reduced production

costs. Therefore, the whole production process has to be based upon consolidated knowledge, which is not yet available.

One part of this knowledge is to scientifically examine the behaviour of mammalian cells under different stress and production conditions. Therefore, it was necessary as a first step to develop a cell line capable of secreting a recombinant protein. The basic idea was using a well known protein with developed production methods, to allow drawing comparisons to processes already in use. Since human erythropoietin (hEPO) was one of the first recombinant proteins, which was manufactured utilizing cell cultures, it seemed one of the most appropriate choices. Recombinant human EPO is not only well known in pharmaceutical industry but also rather easy to detect, using well established methods.

This first part of the thesis describes the isolation of the human EPO gene and all necessary steps to achieve a rhEPO secreting mammalian cell line. This includes the build-up of retroviral vectors, testing of their infection and transduction eligibilities as well as comparing three mammalian cell lines with respect to their adherence capabilities after retroviral transduction. Finally a usable cell line was achieved to enable the further parts of this thesis.

2 Scientific Background

Erythropoietin (EPO) is a glycoprotein playing a vital role in haematopoiesis, the formation of blood cellular components derived from haematopoietic stem cells. EPO is an essential growth factor for the production and maturation of red blood cells (erythropoiesis). It is produced by the cortex of the kidneys in adult mammals [(2)]. During the fetal stage it is mainly produced by hepatocytes and some of these production capabilities of the liver remain active in adults [(3)].

The nucleotide sequence of the human EPO gene was first reported in 1985 [(4)] and consists of 582 bp [(5)] (base pairs). The sequence begins with the start-codon ATG (AUG in DNA code) and ends with one of the three possible stop-codons, namely TGA (UGA in DNA code). It is actually reported with the following descriptions and nucleotide sequence:

Homo sapiens erythropoietin

Data from NCBI (http://www.ncbi.nlm.nih.gov/nuccore/62240996)
LOCUS: NM_000799, 582 bp, mRNA, linear, PRI 06-APR-2008
>gi|62240996:182-763 Homo sapiens erythropoietin (EPO), mRNA

Nucleotide sequence:

ATGGGGGTGCACGAATGTCCTGCCTGGCTGTGGCTTCTCCTGTCCCTGCTGTCGCTCCCTCT
GGGCCTCCCAGTCCTGGGCGCCCCACCACGCCTCATCTGTGACAGCCGAGTCCTGGAGAGG
TACCTCTTGGAGGCCAAGGAGGCCGAGAATATCACGACGGGCTGTGCTGAACACTGCAGCTT
GAATGAGAATATCACTGTCCCAGACACCAAAGTTAATTTCTATGCCTGGAAGAGGATGGAGGT
CGGGCAGCAGGCCGTAGAAGTCTGGCAGGGCCTGGCCCTGCTGTCGGAAGCTGTCCTGCGG
GGCCAGGCCCTGTTGGTCAACTCTTCCCAGCCGTGGGAGCCCCTGCAGCTGCATGTGGATAA
AGCCGTCAGTGGCCTTCGCAGCCTCACCACTCTGCTTCGGGCTCTGGGAGCCCAGAAGGAA
GCCATCTCCCCTCCAGATGCGGCCTCAGCTGCTCCACTCCGAACAATCACTGCTGACACTTTC
CGCAAACTCTTCCGAGTCTACTCCAATTTCCTCCGGGGAAAGCTGAAGCTGTACACAGGGGA
GGCCTGCAGGACAGGGGACAGATGA

The circulating, biologically active protein (Figure 2.1) is composed of 165 amino acids with a molecular weight of 30,400 Dalton (30.4 kDa). It has three N-linked (at an asparagine) and one O-linked (at a serine) acidic oligosaccharide side chains, which account for around 40% of the entire molecular weight. These α-helical chains are responsible for the heterogeneity of EPO between different species and also contribute to the resistance of erythropoietin towards thermal inactivation [(6)], circumventing degradation of the protein, as mentioned in Part B (page 56). This would imply the loss of function through dissolving the three dimensional structure.

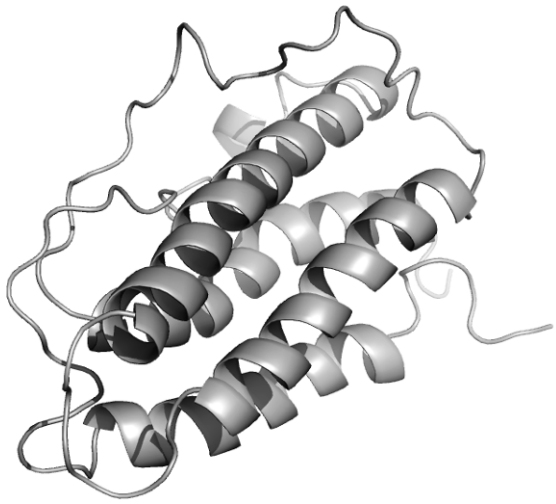

Figure 2.1 – Structure of human erythropoietin with α-helical side chains from NCBI

Experiments using plasma after a bleeding stimulus or hypoxia led to the discovery of the main effect of EPO, i.e., the maintenance or enhancement of the red blood cell concentration by inhibition of apoptosis of erythrocytic progenitors, as well as by stimulating their proliferation and differentiation to mature erythrocytes. Therefore, today rhEPO is used for treatment of anaemia, which might be caused by severe damage of the kidneys [(7)]. This resulted in EPO being one of the most interesting recombinant human proteins produced by mammalian cell cultures in pharmaceutical industry. However, the increase of the number of red blood cells resulting in enhanced oxygen transport capacity is also the reason for the doping abuse of EPO products. This illegal enhancement can lead to thromboses caused by the high amount of red blood cells in the blood vessels.

The building blocks of DNA and the rules for encoding biological information by DNA (genetic codes) are identical among different species. But as mentioned above, the post expressional modification of EPO, in this case a glycosylation, is very important for the stability and duration *in vivo* as well as biological activity of the protein. Bacteria like *Escherichia coli* are unable to modify proteins by glycosylation. A glycosylation machinery is present in the yeast *Saccharomyces cerevisiae* but different from mammalian cells. However it is highly conserved among various mammalian species [8]. Consequentially, mammalian cell cultures are the production host of choice for recombinant proteins with post expressional modifications.

Eukaryotic cells in general and mammalian cells in particular are quite complex to handle. The eukaryotic domain includes animals, plants and fungi. The cells of these domains are much more complex than prokaryotic cells. They are highly compartmentalized and a schematic of a mammalian cell can be seen in Figure 2.2 [9].

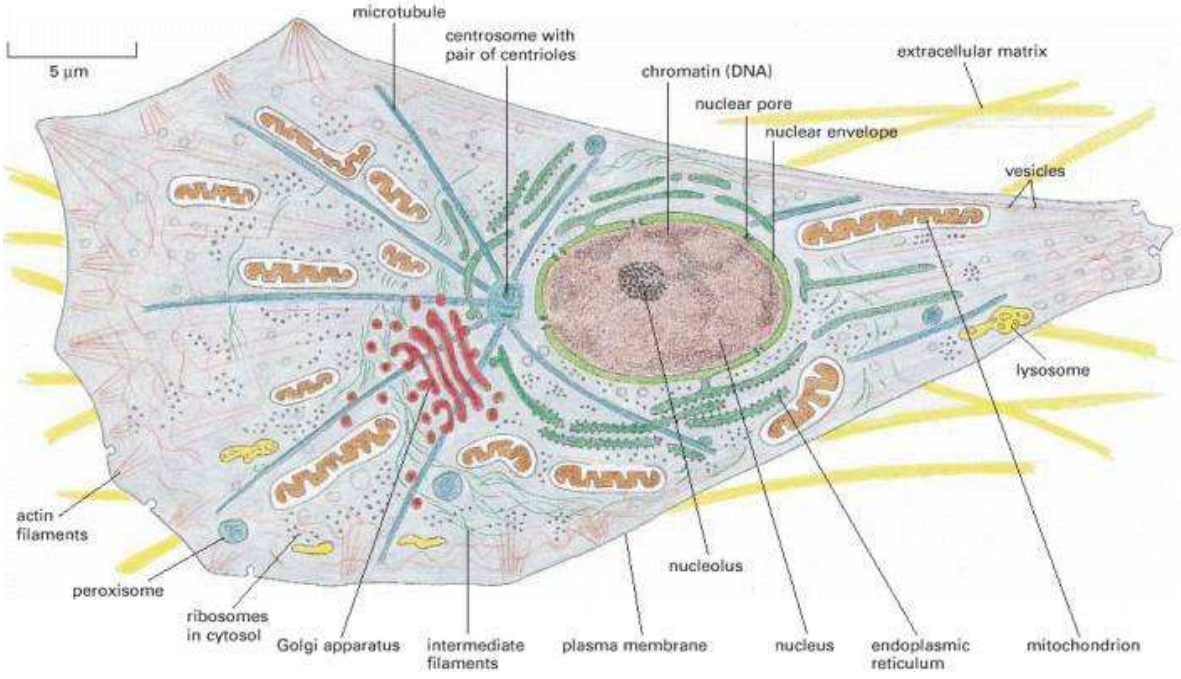

Figure 2.2 – Schematic structure and features of mammalian cells ©[9]

The largest and most prominent compartment or organelle of a mammalian cell is the nucleus. The nucleus contains the genetic information of the cell organized as linear DNA molecules or chromosomes prior to cell division [9].

Furthermore there are a variety of membrane-enclosed organelles within the cytoplasm of mammalian cells. As an example the mitochondrion and the Golgi apparatus are organelles, where different metabolic activities are localized within the separated compartments. The mitochondrion performs most cellular oxidations and produces the bulk of the cell's adenosine triphosphate (ATP), which is why it is called the “power plant” of the cell. Within the Golgi apparatus proteins are glycosylated before they are transported to their destination [(9)].

A specific feature of mammalian cells is a cytoskeleton or a system of protein filaments, which crisscrosses the cytoplasm and provides the cell with mechanical strength, controls its shape and drives and guides its movements. This system is also a critical component in forming attachment to surfaces or controlling the cell response to mechanical forces [(9)]. Since they posses a negatively charged surface, mammalian cells tend to attach to positively charged surfaces such as collagen, Fibronectin or Poly-L-Lysine.

Mammalian cells, however, do not have a cell wall, compared to plant or fungal cells. They need a quick exchange of substances and information between each other and are surrounded by a rather thin and fragile plasma membrane. This membrane is composed of proteins, lipids and carbohydrates and has significant sensitivity towards shear forces [(10)]. Moreover, mammalian cells are often anchorage dependent and have to grow on surfaces of glass, specially treated plastics, natural polymers such as collagen or other support materials.

The required nutrients for mammalian cells in culture are also very different from other cell types. A typical growth medium contains glucose, glutamine, nonessential and essential amino acids, serum (horse or calf), and mineral salts (for example Dulbecco's Modified Eagle Medium). This complex composition of nutrients, the sensitivity to temperature and mechanical forces and the oxygen demand are the main factors why the cultivation of mammalian cells for production purposes is known to be time consuming and difficult [(11)]. For all these difficulties, building a mammalian cell line secreting rhEPO was inevitable to scientifically examine the behaviour under production conditions.

3 Experimental Work

3.1 Isolation and amplification of human erythropoietin gene

The mRNA for human erythropoietin (hEPO) was the target for isolation, because it is composed of the information for the protein only in contrast to the complete gene, containing introns and exons. Aside from trying to isolate the hEPO protein coding sequence from tissues, two commercially available cell lines are reported as capable donors of hEPO mRNA. Those are the HepG2 and Hep3B cell lines [12], both isolated from human hepatocyte carcinoma patients. The isolation was made from HepG2 cells, which were in stock. This cell line was seeded in Dulbecco's Modified Eagle Medium (DMEM) containing 1% v/v glutamic acid (Glu), 10% v/v Fetal Bovine Serum (FBS).

3.1.1 RNA harvesting using trizol reagent

First PBS (phosphate buffered saline) was heated to 37°C and digital microscope images were taken from the HepG2 cells, to document the cell state. The cell culture was washed 2 times with the warmed PBS within a laminar flow clean bench. Afterwards trizol reagent was added to the cell culture vessel according to.Table 3.1.

Table 3.1 – Volumes of PBS and trizol reagent needed for the according cell culture vessels

cell culture vessel	Area [cm2]	PBS [mL]	Trizol [mL]
six well plate	9.5	2	1
60 mm diameter dish	28.3	3	2
75 cm2 flask	75	5	5
100 mm diameter dish	78.5	5	5

The liquid solution was taken up and the whole cell culture vessel was rinsed with it several times, to obtain as much material as possible. Then the solution was transferred to labelled falcon tubes. If there was too little material, some cell

culture vessels were pooled together. If the RNA extraction should be conducted later on, these tubes could be stored at -80°C.

3.1.2 RNA extraction

To start, the workspace gloves and all items used had to be cleaned with RNase-away, to prevent degradation of the isolated RNA samples. If the samples had been frozen, they were thawed and transferred to 1.5 mL microcentrifuge tubes. After briefly mixing the contents, they were left at room temperature for 5 minutes to break up the nucleoprotein complexes. 0.2 mL chloroform per used mL trizol-RNA was added under the extractor hood and the solution was mixed for 15 seconds. Next the tubes were left for 2 minutes at room temperature and then they were centrifuged for 15 minutes at 12,000 rcf (relative centrifugation force) and 4°C.

The colourless aqueous supernatant was transferred into new 1.5 mL microcentrifuge tubes. 0.5 mL isopropanol per mL trizol-RNA was added and incubated for 10 minutes at room temperature. After another centrifugation for 10 minutes at 12,000 rcf and 4°C, the supernatant was discarded and 1 mL ice-cooled 75% EtOH per mL trizol-RNA was added. The solution was put on a vortex for some seconds and then centrifuged for 5 minutes at 7,500 rcf and 4°C. This step achieved a desalting of the RNA.

The supernatant was again discarded, followed by adding 1 mL ice-cooled 100% EtOH per mL trizol-RNA without resuspending the pellet. After a centrifugation for 5 minutes at 7,500 rcf and 4°C, the supernatant was discarded and the pellet left to dry in the air at room temperature for approximately 5 to 10 minutes. It should not dry in completely. The pellet was solved in 10 µL DEPC-treated (diethylpyrocarbonate – inactivates RNases) water per mL trizol-RNA. A 1:10 dilution with DEPC-treated water was prepared to determine the RNA concentration with a NanoDrop Technologies™ ND-1000 Spectrophotometer. The RNA solution was stored at -80°C.

3.1.3 First-strand cDNA synthesis using SuperScript™ RT

To translate the isolated RNA into much more stable and usable cDNA, a first-stand cDNA synthesis is necessary. Therefore 1 µL oligo (dT) primer, 5 µg RNA, 1 µL 10 mM dNTP Mix (10 mM each dATP, dGTP, dCTP and dTTP at neutral pH) and 13 µL sterile, distilled water were added to a nuclease-free microcentrifuge tube. The mixture was heated to 65°C for 5 minutes and then quick chilled on ice. A brief centrifugation collected the contents of the tube. Next 4 µL 5x first-strand buffer and 2 µL 0.1 M DTT (dithiothreitol) were added and the contents of the tube were gently mixed and incubated for 2 minutes at 37°C. 1 µL (200 units) of SuperScript™RT from Invitrogen™ was included and mixed by pipetting gently up and down. Then incubation for 50 minutes at 37°C was conducted, followed by an inactivation of the reaction by heating the tube to 70°C for 15 minutes. The achieved cDNA solution was stored at -20°C.

3.1.4 PCR amplification of the human EPO gene

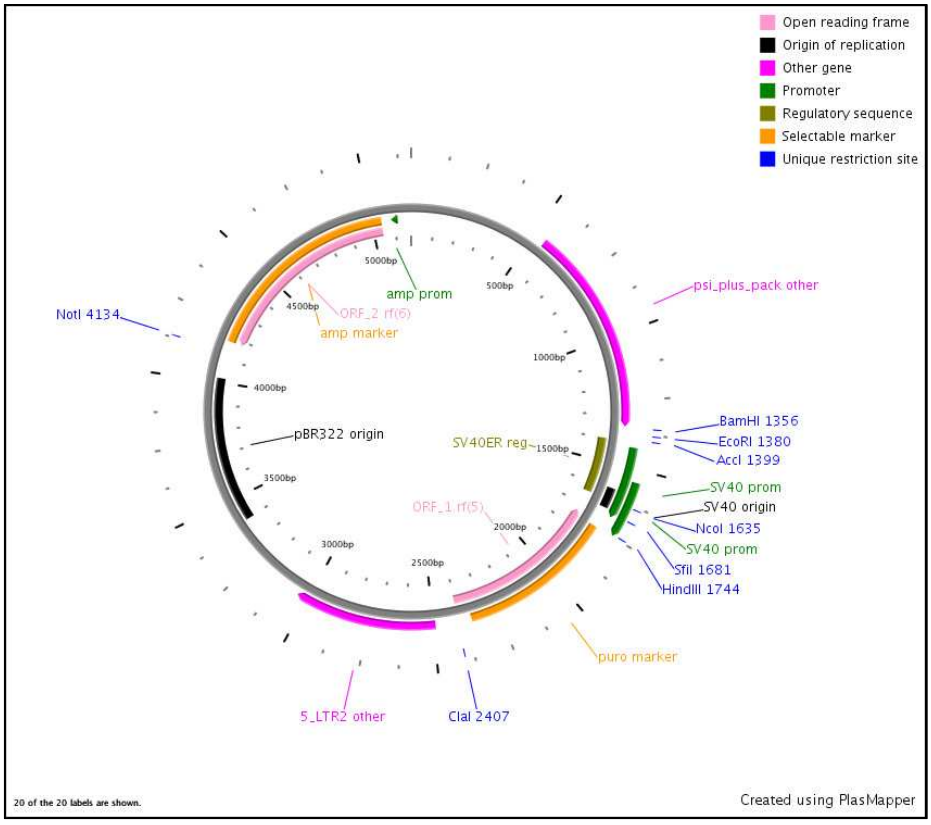

Figure 3.1 – Constructed vector map of pBABEpuro with restriction sites

The first decision to take is, which vector construct(s) will be used. Figure 3.1 displays the vector pBABEpuro (5,169 bp – from Addgene Inc.) including the restriction sites *Bam*HI and *Eco*RI (24 bp distance) and constructed with the computer program PlasMapper (http://wishart.biology.ualberta.ca/PlasMapper/).

Figure 3.2 shows the vector pMSCVpuro (6,295 bp – from Clontech-Takara Bio Europe) including the restriction sites *Xho*I and *Eco*RI (20 bp distance), also constructed with the program PlasMapper.

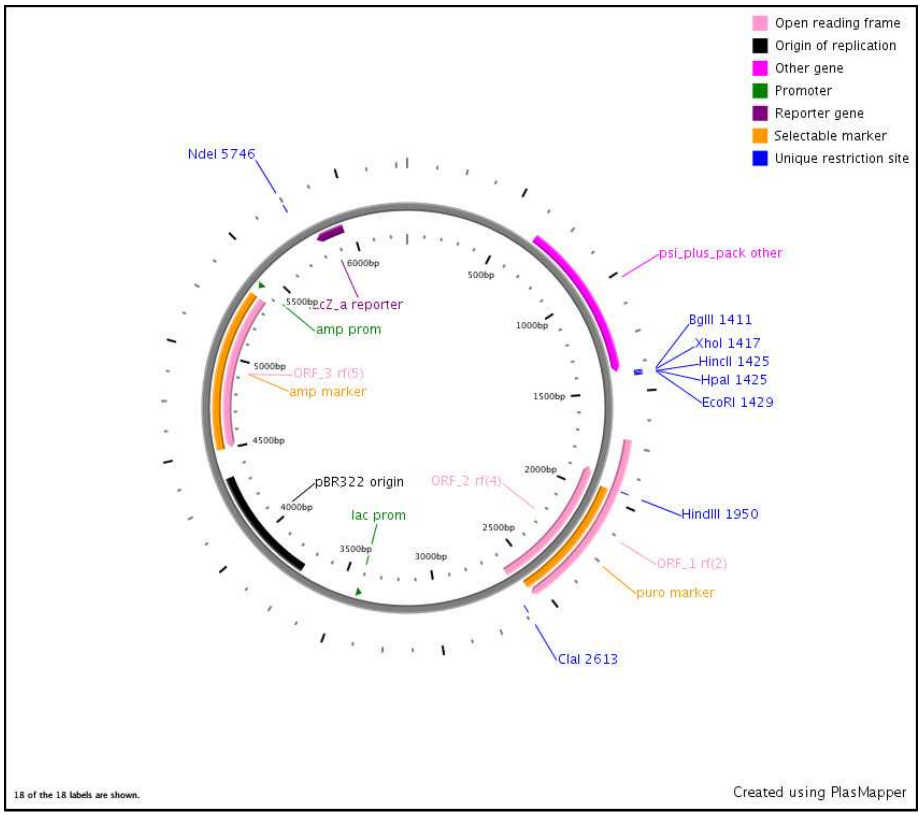

Figure 3.2 – Constructed vector map of pMSCVpuro with restriction sites

These 2 retroviral vectors seemed fit to implement the hEPO gene permanently into mammalian cell lines. The vector construct pBABEpuro is derived from a moloney murine leukemia virus while pMSCVpuro is derived from a murine stem cell virus. Both hold resistance information against ampicillin and puromycin.

But first, in order to isolate the human EPO gene, PCR amplification of the cDNA samples with the correct primers had to be conducted. These primers would have to include the start and end of the hEPO gene, as well as the forward and

accordingly reverse restriction sites of the corresponding vector, to enable inserting of the gene into the vector. The cutting enzymes for the restriction sites mentioned above were available, so the corresponding sites have been checked with NEBcutter V2.0 (http://tools.neb.com/NEBcutter2/index.php) previously. They were reported to be not cutting within the human EPO nucleotide sequence and therefore have been used for the primer design.

The forward primers for the human EPO gene and the restriction site *Bam*HI for pBABEpuro and *Xho*I for pMSCVpuro have been designed with the following sequences (from 5' to 3'):

hEPO / Fw-*Bam*HI: CGG GAT CCA TGG GGG TGC ACG AAT GTC CTG CC
hEPO / Fw-*Xho*I: CCG CTC GAG ATG GGG GTG CAC GAA TGT CCT GCC

The reverse primer for the human EPO gene and the restriction site *Eco*RI for both vectors has been designed with the following sequences (from 5' to 3'):

hEPO / Rev-*Eco*RI: GCG AAT TCT CAT CTG TCC CCT GTC CTG CAG GCC TC

These primers have been ordered from Invitrogen™ and were stored at -20°C upon reception.

To prepare the PCR-Reaction, 13 µL sterile, distilled water were filled into a PCR tube. Then 3 µL cDNA, 1 µL of the corresponding forward and reverse primers for the pBABEpuro or the pMSCVpuro vector from Invitrogen™, 1 µL 10 mM dNTP Mix (10 mM each dATP, dGTP, dCTP and dTTP at neutral pH), 2 µL 10x Buffer + $MgSO_4$ and 0.5 µL *Pfu*-polymerase from Fermentas GmbH were added to the tube. After gently mixing, the tube was inserted into a PCR machine and the cycles were programmed according to Table 3.2 for the primers designed for the pBABEpuro vector and Table 3.3 for the primers designed for the pMSCVpuro vector. The PCR product, namely a human EPO insert, was stored at -20°C.

Table 3.2 – Time and temperature settings for PCR reactions using pBABEpuro primers

reaction step	temperature [°C]	time [min]	
denaturation	98	2	
denaturation	98	0.5	x 55
annealing	57	0.75	
extension	72	1	
extension	72	10	
cooling	4	∞	

Table 3.3 – Time and temperature settings for PCR reactions using pMSCVpuro primers

reaction step	temperature [°C]	time [min]	
denaturation	98	2	
denaturation	98	0.5	x 55
annealing	63	0.75	
extension	72	1	
extension	72	10	
cooling	4	∞	

3.1.5 Human EPO insert purification by agarose gel electrophoresis

A 1.5% w/v agarose gel with ethidium bromide was prepared, using 1 µL of ethidium bromide stock (5.25 mg/mL in H_2O) per 10 mL gel solution. The gel was covered with 1x TAE buffer solution (Tris base, acetic acid and EDTA) and a 100 bp ladder was applied as standard. After thawing, the PCR samples were mixed with 4 µL loading dye (to achieve a 1:6 solution) and applied to the gel. Current and time were set according to the size of the gel and the current was stopped when the coloured dye reached the end of the gel. The gel was analyzed under ultraviolet light and digital pictures were taken. The band of the insert at approximately 600 bp was identified, cut out (Figure 3.3) and put it into previously weighted 1.5 mL microcentrifuge tubes.

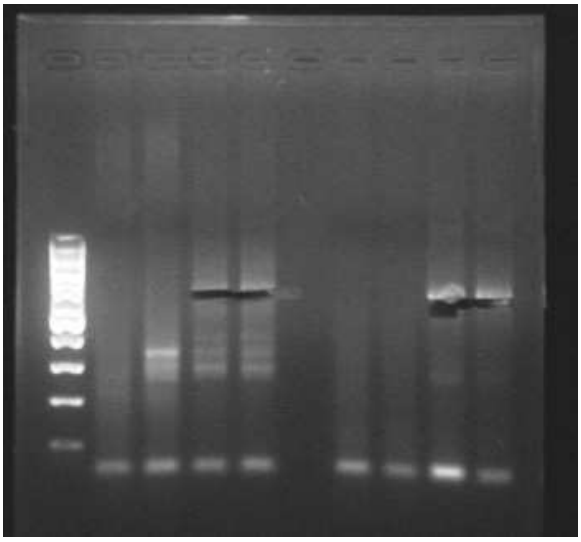

Figure 3.3 – UV picture of agarose gel with cut human EPO insert at approximately 600 bp

3.1.6 Gel extraction of the human EPO insert using E.Z.N.A.® kit:

The E.Z.N.A.® kit was obtained from the Omega Bio-Tek Inc. The 1.5 mL microcentrifuge tube with the gel pieces has been weighted, and the weight of the empty tube was subtracted. Then 4 times the volume of binding buffer compared to the weight of the gel pieces (0.1 g ≈ 0.1 mL) was added and the tube was thoroughly shaken. Incubation for 7 minutes at 55°C to 65°C was conducted. If not all gel pieces were dissolved after this time, the incubation was prolonged until all agarose was dissolved. 750 µL of the solution were added to a 2 mL HiBind® column and centrifuged for 1 minute at 10,000 rcf and room temperature. The flow through was discarded. If the dissolved volume was larger than 750 µL, the loading and centrifugation steps were repeated. Then 300 µL binding buffer were loaded to the HiBind® column, centrifuged for 1 minute at 10,000 rcf and room temperature and the flow through was discarded again. The next step was to add 750 µL DNA wash buffer to the HiBind® column and to wait for 2 to 3 minutes. After conducting another centrifugation for 1 minute at 10,000 rcf and room temperature, the flow through was discarded and the step repeated once. The HiBind® column was dried by centrifuging it again for 1 minute at 10,000 rcf and room temperature.

Elution of the DNA was achieved by first inserting the HiBind® column into a new microcentrifuge tube. Then 20 µL of sterile, distilled water were applied to the middle of the HiBind® column membrane and centrifuged for 1 minute at 10,000 rcf and room temperature. The flow through was reapplied to the HiBind® column and again centrifuged for 1 minute at 10,000 rcf and room temperature. The DNA concentration of the human EPO insert sample was determined using a NanoDrop Technologies™ ND-1000 Spectrophotometer. Afterwards the solution was stored at -20°C.

3.2 Construction of plasmids carrying the human EPO gene

After successful isolation and amplification of the human erythropoietin gene and the chosen restriction sites, i.e., the completion of the insert, the basic plasmids had to be constructed. Only after careful construction and refinement, the vectors and inserts would then turn into active plasmids and would be capable of transporting the gene permanently into mammalian cell cultures (Figure 3.4).

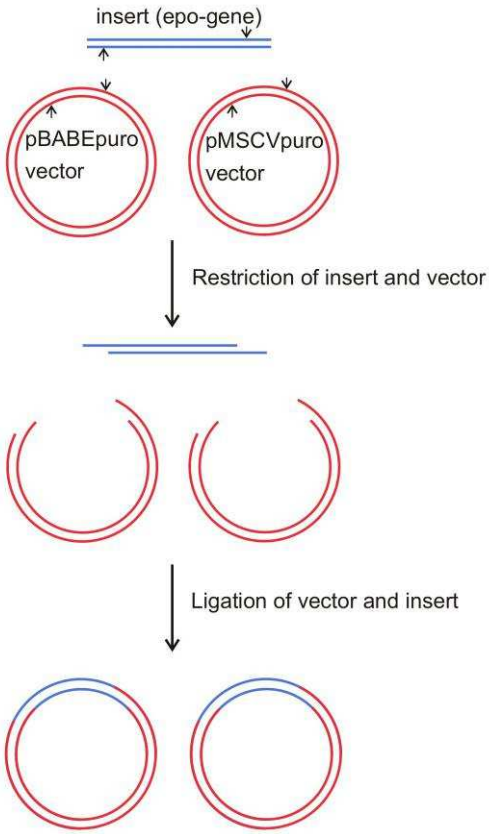

Figure 3.4 – Schematic principle of inserting a gene into a vector

3.2.1 Cutting of insert and vector with the according restriction enzymes

For achieving the correct cut ends of the pBABEpuro vector and the corresponding insert, 9.5 µL of sterile, distilled water were added to a 1.5 mL microcentrifuge tube. Then 5 µL of the vector / insert DNA solution was poured into the tube. After 4 µL 2x Tango buffer (to achieve a 1:10 solution), 1 µL *Bam*HI restriction enzyme solution and 0.5 µL *Eco*RI restriction enzyme solution, both from Fermentas GmbH, were added. The whole mixture was incubated for 1 hour at 37°C.

For the pMSCVpuro vector and the appropriate insert, 10 µL of sterile, distilled water were added to a 1.5 mL microcentrifuge tube. The following ingredients consisted of 5 µL of the vector / insert DNA solution, 4 µL 2x Tango buffer (to achieve a 1:10 solution), 0.5 µL *Xho*I restriction enzyme solution and 0.5 µL *Eco*RI restriction enzyme solution, both from Fermentas GmbH. The tube was then incubated for 1 hour at 37°C.

3.2.2 Purification of vectors and inserts

To purify the inserts, a QIAquick® PCR purification kit from Qiagen™ was used. 100 µL PBI buffer were added to the restriction enzyme cut and mixed. After applying the solution to a QIAquick® column, a centrifugation for 1 minute at 10,000 rcf and room temperature was conducted. The flow through was discarded and 750 µL PE buffer to the QIAquick® column were filled into the QIAquick® column. Another centrifugation for 1 minute at 10,000 rcf and room temperature was done, followed by discarding of the flow through. The QIAquick® column was dried by centrifuging again for 1 minute at 10,000 rcf and room temperature. The DNA insert was eluted by inserting the QIAquick® column into a new microcentrifuge tube. 30 µL of sterile, distilled water were applied to the middle of the QIAquick® column and the tube centrifuged for 1 minute at 10,000 rcf and room temperature. The flow through was reapplied to the QIAquick® column and the centrifugation step for 1 minute at 10,000 rcf and room temperature repeated. The DNA concentration of the cut insert was determined using a NanoDrop Technologies™ ND-1000 Spectrophotometer and the insert solutions were stored at -20°C.

For purification of the vectors, the section “Human EPO insert purification by agarose gel electrophoresis” in chapter 3.1 was performed with the cut vector solutions. Afterwards, the DNA concentration of the cut vector was determined using a NanoDrop Technologies™ ND-1000 Spectrophotometer and the vector solutions were stored at -20°C.

3.2.3 Ligation of the cut vectors and the appropriate cut inserts

To successfully ligate a vector and insert, both have been previously cut with the same restriction enzymes. Afterwards 20 ng of vector DNA and 100 ng of insert DNA were used. They were combined with 4 µL of T4 ligase buffer (to achieve a 1:5 solution) and 2 µL of T4 ligase from Invitrogen™. Sterile, distilled water was added to achieve a total volume of 20 µL. This solution was incubated at room temperature for at least 12 hours (overnight).

3.2.4 Transformation of the construct into chemically competent cells

To transform the vector / insert construct into a functional plasmid, it has to be processed by chemically competent cells. Therefore, the 1.5 mL microcentrifuge tube containing the ligation was briefly centrifuged and put on ice afterwards. 1 vial of 50 µL One Shot® competent cells from Invitrogen™ for each ligation reaction was thawed. 5 µL of the ligation solution was added directly into the vial containing the competent cells and mixed by gentle tapping. The remaining ligation solution was stored at -20°C.

The vial was incubated for 30 minutes on ice, followed by exactly 30 seconds incubation in a 42°C water bath. After placing the vial on ice immediately, 250 µL of pre-warmed S.O.C medium (at 37°C) were poured into each vial under sterile conditions to avoid contamination. A further incubation at 37°C for exactly 1 hour at 225 rpm in a shaking incubator was performed. 200 µL from each transformation vial was spread on separate, labelled lysogeny broth (LB) agar plates with ampicillin (100 µg/mL for the pBABEpuro construct and 50 µg/mL for the pMSCVpuro construct), again applying sterile techniques. The plates were inverted and incubated at 37°C overnight.

3.2.5 Overnight cultures (ONC) from transformation colonies

For each colony, which was picked, 5 mL LB medium were applied to a 15 mL Falcon tube under sterile conditions. 5 µL ampicillin (100 mg/mL in H_2O) were added for pBABE plasmids and 2.5 µL ampicillin (50 mg/mL in H_2O) were added for pMSCV plasmids. Then the colonies were transferred into the tubes. The tubes were incubated at 37°C and 225 rpm in a shaking incubator overnight to receive overnight cultures (ONC).

3.2.6 Plasmid purification

For purification of the plasmids, a QIAprep® spin miniprep kit from Qiagen™ was used. Therefore, an ONC was centrifuged for 3 minutes at 6,800 rcf and room temperature. The medium was discarded and the pellet resuspended in 250 µL P1 buffer and then transfer to a 1.5 mL microcentrifuge tube. 250 µL P2 buffer were added and the tube was mixed thoroughly by inverting the tube 4 to 6 times. After applying 350 µL N3 buffer, another mixture was produced immediately and thoroughly by inverting the tube 4 to 6 times. The 1.5 mL microcentrifuge tube was then centrifuged for 10 minutes at 17,900 rcf and room temperature.

The supernatant was applied to a QIAprep® spin column by either decanting or pipetting. After another centrifugation step for 1 minute at 17,900 rcf and room temperature, the flow through was discarded. 500 µL PB buffer were added to the QIAprep® spin column, centrifuged for 1 minute at 17,900 rcf and room temperature and the flow through was again discarded. Then 750 µL PE buffer were filled into the QIAprep® spin column, centrifuged for 1 minute at 17,900 rcf and room temperature and the flow through was discarded. For drying, the QIAprep® spin column was centrifuged again for 1 minute at 17,900 rcf and room temperature. To elute the plasmid from the QIAprep® spin column, the column was inserted into a new 1.5 mL microcentrifuge tube and 40 µL of sterile, distilled water were applied to the middle of the QIAprep® spin column. After 1 minute of incubation, the tube was centrifuged for 1 minute at 17,900 rcf and room temperature. The flow through was reapplied to the QIAprep® spin column,

followed by again 1 minute of incubation and 1 minute of centrifugation at 17,900 rcf and room temperature. After the DNA concentration was determined using a NanoDrop Technologies™ ND-1000 Spectrophotometer (of a few random samples), the purified plasmid solution was stored at -20°C.

3.2.7 Analyzing the plasmids by cutting with restriction enzymes

"Cutting of insert and vector with the according restriction enzymes" was performed using 5 µL of the plasmid solution (for minipreps with 100 to 500 ng / µL DNA). The enzymes were chosen according to the vector used. The *Bam*HI / *Eco*RI restriction enzymes were used to cut the pBABEpuro vector and the *Xho*I / *Eco*RI restriction enzymes were used to cut the pMSCVpuro vector.

A 1.5% w/v agarose gel with ethidium bromide was prepared, using 1 µL of ethidium bromide stock (5.25 mg/mL in H_2O) per 10 mL gel solution. The gel was covered with 1x TAE buffer solution (Tris base, acetic acid and EDTA) and a 100 bp ladder as well as a 1K bp ladder was applied as standards. The solutions with the plasimds cut by restriction enzymes were mixed with 4 µL loading dye (to achieve a 1:6 solution) and applied to the gel. Current and time were set according to the size of the gel and the current was stopped when the coloured dye reached the end of the gel. The gel was analyzed under ultraviolet light and digital pictures were taken. As a result, 2 distinctive bands of DNA should become visible, one at approximately 5K to 6K bp (the cut vector pBABEpuro or pMSCVpuro) and one at 600 bp (the cut out insert).

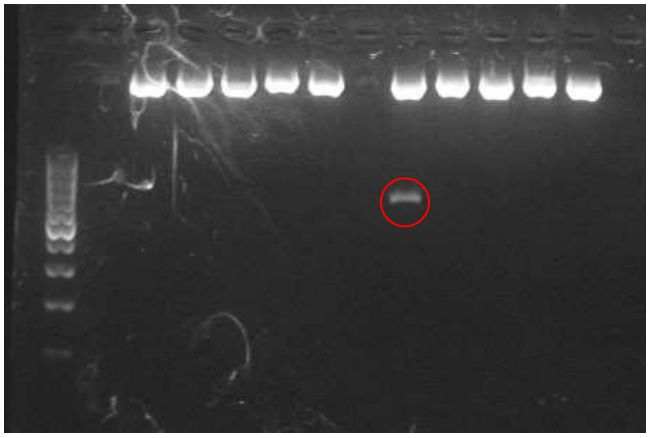

Figure 3.5 – UV picture of agarose gel with cut vectors and inserts

As can be observed in Figure 3.5, one vector / insert construct has been successfully built in 130 attempts. The plasmid consists of a pMSCVpuro vector of 6,295 bp size and the insert (marked by the red circle) with around 600 bp size. All further steps were carried out with this pMSCVpuro plasmid solution.

3.2.8 Analyzing the pMSCVpuro plasmid containing the hEPO gene

To ensure the successful ligation of the pMSCVpuro vector and the hEPO gene insert, shifted cuts with different restriction enzymes were conducted. First, the DNA concentration of the sample was determined using a NanoDrop Technologies™ ND-1000 Spectrophotometer. Since a two way approach was made, two ligations had to be done.

For the first variant, 5 µL plasmid DNA were added to a 1.5 mL microcentrifuge tube containing 2 µL NE 2 Buffer (to achieve a 1:10 solution), 0.2 µL BSA (to achieve a 1:100 solution), 1 µL *Cla*I restriction enzyme solution, 0.5 µL *Bsr*GI restriction enzyme solution and 11.5 µL sterile, distilled water. The mixture was incubated for 1 hour at 37°C.

The second approach also used 5 µL of plasmid DNA. The 1.5 mL microcentrifuge tube was prepared with 4 µL 2x Tango buffer (to achieve a 1:10 solution), 1 µL *Hin*dIII restriction enzyme solution, 0.5 µL *Xho*I restriction enzyme solution and 9.5 µL sterile, distilled water. The restriction cut was also incubated for 1 hour at 37°C.

Afterwards, a 1.5% w/v agarose gel with ethidium bromide was prepared, using 1 µL of ethidium bromide stock (5.25 mg/mL in H_2O) per 10 mL gel solution. The gel was covered with 1x TAE buffer solution (Tris base, acetic acid and EDTA) and a 1K bp ladder was applied as standard. The restriction cut solutions were mixed with 4 µL loading dye (to achieve a 1:6 solution) and applied to the gel. Current and time were set according to the size of the gel and the current was stopped when the coloured dye reached the end of the gel.

The gel was analyzed under ultraviolet light and digital pictures were taken. Approach one should result in 2 distinctive bands at approximately 5,650 bp and 1,200 bp. The second restriction cut should result in one band, which should be at 5,750 bp and one at 1,100 bp (Figure 3.6).

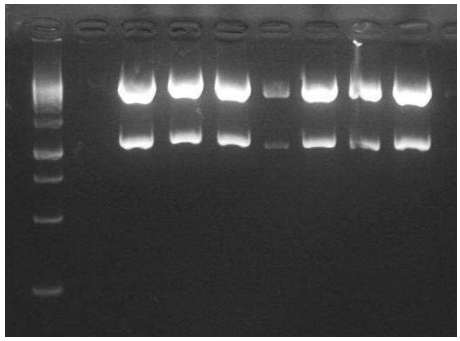

Figure 3.6 – UV picture of agarose gel from the *Hin*dIII and *Xho*I cut

3.3 Construction of retroviral particles

To increase the available amount of plasmids, the sections “Transformation of the construct into chemically competent cells”, “Overnight cultures (ONC) from transformation colonies” and “Plasmid purification” from the previous chapter 3.2 were repeated with the stored ligation solution. To ensure the functionality of the purified plasmid solutions, the section “Analyzing the pMSCVpuro plasmid containing the hEPO gene” was also repeated. The stock of solutions produced was stored at -20°C. All these steps were made for the pMSCVpuro vector including the insert as well as the uncut vector alone.

The next target was to envelope the plasmid into retroviral particles, which would enable the “infection” of mammalian cell lines as well as the permanent addition of the hEPO gene to the DNA of the cells. Therefore, the plasmid had to be transfected into so called packaging cells.

3.3.1 Preparation of packaging cell lines

The cell lines Phoenix™ ampho, Phoenix™ eco (from Allele Biotechnology & Pharmaceuticals Inc.) or RetroPack™ PT67 (from Clontech-Takara Bio Europe) were treated in the same way. The cells were seeded in 75 cm^2 tissue culture flasks with 12 mL medium consisting of DMEM containing 1% v/v Glu, 10% v/v FBS and 1% v/v P/S. They were incubated at 37°C and 5% CO_2 and have been split 1:12 if necessary.

In order to subdivide the cells, the medium was carefully removed under sterile conditions and 10 mL PBS at room temperature were applied, avoiding pouring the PBS directly onto the cells. The tissue culture flask was pivoted to wash the cells and the PBS was carefully removed afterwards. 1 mL trypsin was applied directly onto the cells, and the tissue culture flask was heated to 37°C and taped to detach the cells. The detachment was controlled by microscopy. Afterwards 9 mL of DMEM containing 1% v/v Glu, 10% v/v FBS and 1% v/v P/S were used to take

up the cells and inactivate the trypsin. For the new tissue culture flask, 1 mL of the cell solution were provided and filled up with 11 mL DMEM containing 1% v/v Glu, 10% v/v FBS and 1% v/v P/S. The passage was noted and the tissue culture flask incubated at 37°C and 5% CO_2.

3.3.2 Transfection of pMSCVpuro +/- hEPO insert into packaging cells

To accomplish a metafecten transfection, the Phoenix™ ampho, Phoenix™ eco or RetroPack™ PT67 cells were plated into a 6-well dish with 2 ml DMEM containing 1% v/v Glu, 10% v/v FBS and 1% v/v P/S per well. The cells were used at 70% to 80% confluence for Phoenix™ ampho and Phoenix™ eco cells or 50% confluence for RetroPack™ PT67 cells. Later results presented the particles packed by the Phoenix™ ampho cell line as the best working solution (Chapter 3.4).

1 hour previous to the transfection, the medium was carefully removed and 0.6 mL fresh DMEM containing 1% v/v Glu at 37°C were applied, without pipetting directly onto the cells. 2 1.5 mL microcentrifuge tubes were prepared for each well. Tube one contained 1 µg DNA from the pMSCVpuro plasmid solution with or without the hEPO containing insert, mixed with 50 µL DMEM containing 1% v/v Glu. Tube two was filled with 4.5 µL metafecten per µg DNA mixed with 50 µL DMEM containing 1% v/v Glu. The content of tube one was then applied to tube two, mixed thoroughly by tapping and incubated for 20 minutes at room temperature. Then the solution was applied onto the cells and incubated for 4 hours at 37°C and 5% CO_2.

The solution was carefully removed after the incubation, 2 mL fresh DMEM, containing 1% v/v Glu, 10% v/v FBS and 1% v/v P/S were applied to each well and the wells were incubated at 37°C and 5% CO_2. After 48 to 72 hours, the expression of viral particles should have reached the maximum level. Therefore, the virus particles containing supernatant have been collected in 15 mL Falcon tubes. Cells and cellular debris has been removed by spinning them down via centrifugation for 5 minutes at 1,200 rcf and room temperature. The cleaned supernatant was used immediately for the transduction of the EPO gene into mammalian cells or pipetted into 1.5 mL microcentrifuge tubes. Only 1 mL was

used per tube and then frozen at -80°C. The viral particle solution was thawn only once and heated to 37°C for a minimal period of time before immediate use.

3.4 Transduction of mammalian cell lines

Having successfully completed the preparation of retroviral particles containing the genetic information for the human erythropoietin gene, the choice for the appropriate mammalian cell lines had to be made. The first choice was a Chinese hamster ovary cell line [13], which are the main production hosts for recombinant human EPO in pharmaceutical industry.

However, previous to each transduction, the puromycin effect had to be investigated for each cell line. These experiments had to confirm after which time all cells would be dead without the vector, which includes a resistance against puromycin as selection marker. Therefore, the cells have been cultivated in 75 cm^2 tissue culture flasks with the appropriate medium (see the sections below for further information). Then the cells were transferred to two 6-well dishes with 2 mL medium at 37°C provided per well. Puromycin was added in the range of 1 to 6 µg/mL for the first dish and 0.5 to 2.5 µg/mL for the second dish. The 6-well dishes were incubated at 37°C and 5% CO_2 and examined by microscopy every 24 hours. The experiments were pursued until all cells were dead. The results indicated how long each cell line had to be incubated until only cells carrying the vector should be still alive.

3.4.1 Transduction of CHO-K1 cells by retroviral vector pMSCVpuro

The CHO-K1 cell line available (Chinese hamster ovary cell line - ATCC® Number CCL-61) [14] was cultivated in 75 cm^2 tissue culture flasks with Ham's tissue culture medium, containing 1% v/v Glu and 10% v/v FBS. When necessary the splitting was conducted as already described in the second paragraph of section “Preparation of packaging cell lines”, just with Ham's tissue culture medium instead of DMEM and without P/S. Having achieved the needed confluence

around 40%, the cells were detached again and the suspension was plated into 6-well dishes with 2 mL Ham's tissue culture medium, containing 1% v/v Glu and 10% v/v FBS at 37°C and incubated at 37°C and 5% CO_2 for 24 hours.

After the first unsuccessful transductions because of the ability of CHO cells to block retroviral transmitters [15,16], tunicamycin was applied at this point [17]. For this, the cells were used at 30% to 40% confluence and 0.2 µg/mL tunicamycin were added to each well, 19 hours prior to the transduction.

The medium was carefully removed and 1 mL fresh Ham's tissue culture medium, containing 1% v/v Glu and 10% v/v FBS at 37°C was applied. The control wells were filled with 2 mL of the medium. Polybrene was added to each well, to achieve a final concentration of 6 µg/mL. Then 1 mL of the previously thawed and warmed (at 37°C) viral supernatant was applied and the 6-well dishes were carefully mixed by moving. The incubation was made at 37°C and 5% CO_2.

After 24 hours the cells were split 1:3 by carefully removing the medium and adding 2 mL PBS at room temperature. Pipetting directly onto the cells was avoided and the 6-well dishes were pivoted to wash the cells. The PBS was removed and 200 µL trypsin were applied directly onto the cells. Then the 6-well dishes were heated to 37°C and tapped to detach the cells. After microscopical control for successful detachment, 1 mL Ham's tissue culture medium, containing 1% v/v Glu and 10% v/v FBS at 37°C was added to each well. 3 times 380 µL from each transduction well were transferred into new wells, and 2 mL Ham's tissue culture medium, containing 1% v/v Glu and 10% v/v FBS at 37°C, were added. These wells were incubated at 37°C and 5% CO_2 for 24 hours. Then puromycin was added to each well to reach a final concentration of 4 µg/mL.

The cell line was then further cultivated, using 3 wells for transfer to a 75 cm^2 tissue culture flask or one well for two new wells of a 6-well plate. Incubation was done at 37°C and 5% CO_2 and the Ham's tissue culture medium, containing 1% v/v Glu, 10% v/v FBS and 1% v/v P/S was used as nutrient and selection medium.

3.4.2 Transduction of 3T3-L1 cells by retroviral vector pMSCVpuro

The 3T3-L1 cell line in stock (mouse embryonic fibroblast-like cell line - ATCC® Number CL-173) [18] was cultivated in 75 cm^2 tissue culture flasks with DMEM, containing 1% v/v Glu and 10% v/v FBS. When splitting was necessary, it was conducted as described in the second paragraph of section “Preparation of packaging cell lines”, just without P/S. After achieving 30% to 40% confluence, the cells were detached again and plated into 6-well dishes with 2 mL DMEM, containing 1% v/v Glu and 10% v/v FBS at 37°C. The 6-well dishes were incubated at 37°C and 5% CO_2 for 24 hours.

The medium was removed carefully and 1 mL fresh DMEM, containing 1% v/v Glu and 10% v/v FBS at 37°C was filled into the wells. 2 mL were used for the control wells. Afterwards, polybrene was added to each well to reach a final concentration of 6 µg/mL. Then 1 mL viral supernatant, previously thawed and warmed at 37°C, was applied. The 6-well dishes were carefully mixed by slow movement and incubated at 37°C and 5% CO_2 for 24 hours.

The cells were split 1:5 subsequently by carefully removing the medium and applying 2 mL PBS at room temperature. It was avoided to pipette directly onto the cells and the 6-well dishes were pivoted to wash the cells. The PBS was removed and 200 µL trypsin were delivered directly onto the cells. The dishes were heated to 37°C and tapped to detach the cells. After complete detachment, controlled by microscopy, 1 mL DMEM, containing 1% v/v Glu and 10% v/v FBS at 37°C was added to each well. 5 times 210 µL from each transduction well were transferred into new wells, afterwards filled with 2 mL DMEM, containing 1% v/v Glu and 10% v/v FBS at 37°C. The wells were incubated 24 hours at 37°C and 5% CO_2 and then the necessary amount of puromycin was added to achieve a concentration of 3 µg/mL in each well.

The cell line was cultivated, using either three wells for transfer to a 75 cm^2 tissue culture flask or one well for two new wells of a 6-well plate. Incubation was made at 37°C and 5% CO_2 and DMEM, containing 1% v/v Glu, 10% v/v FBS and 1% v/v P/S was used as nutrient and selection medium.

3.4.3 Transduction of BNL-CL.2 cells by retroviral vector pMSCVpuro

Available BNL-CL.2 cells (mouse liver epithelial cell line - ATCC® Number TIB-73) [19] were cultivated in 75 cm^2 tissue culture flasks with DMEM, containing 1% v/v Glu and 10% v/v FBS. When splitting was necessary, the description in the second paragraph of section “Preparation of packaging cell lines” was followed, just without P/S. After having reached over 80% confluence, the cells were detached and plated into 6-well dishes with 2 mL DMEM, containing 1% v/v Glu and 10% v/v FBS at 37°C. These dishes were incubated at 37°C and 5% CO_2 for 24 hours.

The medium was carefully removed, and the wells were filled with 1 mL fresh DMEM, containing 1% v/v Glu and 10% v/v FBS at 37°C. The control wells were loaded with 2 mL medium. Then polybrene was added to reach a final concentration of 6 µg/mL within each well. Afterwards, 1 mL viral supernatant was applied, previously thawed and warmed at 37°C. The 6-well dishes were carefully mixed by moving and incubated at 37°C and 5% CO_2 for 24 hours.

After the incubation the cells were split 1:3. For this the medium was carefully removed and 2 mL PBS at room temperature were applied, avoiding pipetting on the cells. The 6-well dishes then were pivoted to wash the cells and the PBS was removed. 200 µL trypsin were applied directly on the cells. Afterwards the dishes were heated to 37°C and tapped to detach the cells. After having completed detachment, which was controlled by microscopy, 1 mL DMEM, containing 1% v/v Glu and 10% v/v FBS at 37°C was added to each well. 3 times 380 µL from each transduction well were transferred into new wells and filled with 2 mL DMEM, containing 1% v/v Glu and 10% v/v FBS at 37°C. The dishes were incubated 24 hours at 37°C and 5% CO_2. Then the necessary amount of puromycin was added to achieve a concentration of 0.5 µg/mL in each well.

The cell line was cultivated by using either three wells for transfer to a 75 cm^2 tissue culture flask or one well for two new wells of a 6-well plate. Incubation was done at 37°C and 5% CO_2. DMEM, containing 1% v/v Glu, 10% v/v FBS and 1% v/v P/S was used as nutrient and selection medium.

3.4.4 Verification of rhEPO secretion from the transducted cell lines

To ensure the successful transduction and therefore secretion of recombinant human erythropoietin (rhEPO), supernatants from the cultivated cell lines were taken after 24 hours and measured with an Enzyme ImmunoAssay, the Alpco™ EPO EIA kit [20]. The working principle of an EIA kit and the measurements will be explained in Part B (page 66), without sample concentration. The calibration curve for the measurements of CHO-K1 and 3T3-L1 cell lines after transduction are presented in data and graph in Table 3.4 and Figure 3.7.

Table 3.4 – EPO EIA calibrator and control measurements

calibration curve	EPO value [mU/mL]	absorbance 450 nm	absorbance 405 nm
calibrator A	0.0	0.1988	0.0938
calibrator B	8.6	0.2220	0.1010
calibrator C	23.0	0.2939	0.1216
calibrator D	59.0	0.4841	0.1745
calibrator E	181.0	1.5146	0.4776
calibrator F	554.0	3.3817	1.0712
controls			
EPO control 1 [10.6 – 21.8 mU/mL]	20.5	0.2912	0.1235
EPO control 2 [173 – 266 mU/mL]	239.4	1.7077	0.5327

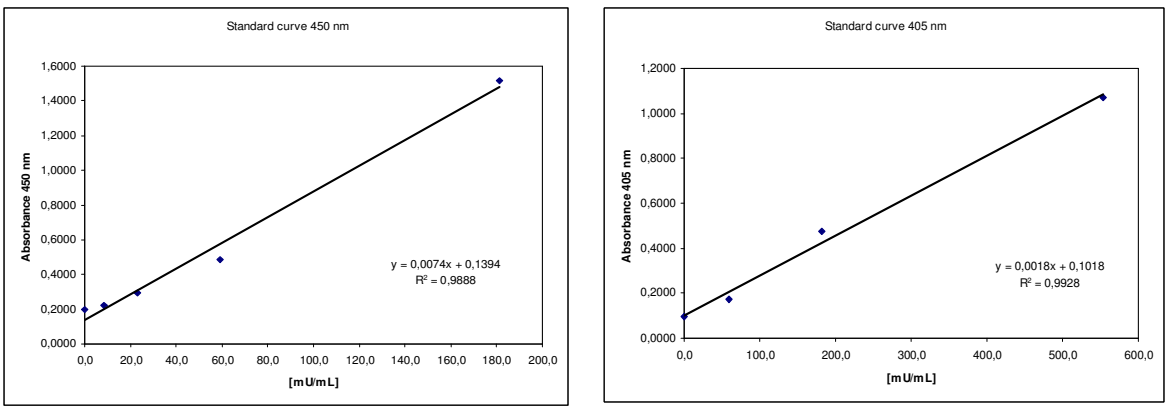

Figure 3.7 – EPO EIA calibration curves for 450 nm and 405 nm including linear fits

Measurements of the supernatant of the CHO-K1 cell line showed no detectable rhEPO secretion. This should occur with the pure vector as negative control (CHO-K1 – pMSCV). However even the cells transducted with the complete construct (CHO-K1 – pEPO) did not show any detectable rhEPO levels (Table 3.5).

Table 3.5 – CHO-K1 supernatant rhEPO EIA measurements

samples	rhEPO value [mU/mL]	absorbance 450 nm	absorbance 405 nm
CHO-K1 – pEPO #1	0.0	0.1185	0.1007
CHO-K1 – pEPO #2	0.0	0.1092	0.0697
CHO-K1 – pEPO #3	0.0	0.0561	0.0473
CHO-K1 – pEPO #4	0.0	0.0948	0.0639
CHO-K1 – pEPO #5	0.0	0.0733	0.0588
CHO-K1 – pEPO #6	0.0	0.0595	0.0525
CHO-K1 – pMSCV #1	0.0	0.0680	0.0564
CHO-K1 – pMSCV #2	0.0	0.0691	0.0589
CHO-K1 – pMSCV #3	0.0	0.0928	0.0631
CHO-K1 – pMSCV #4	0.0	0.1185	0.0719
CHO-K1 – pMSCV #5	0.0	0.0582	0.0507
CHO-K1 – pMSCV #6	0.0	0.0627	0.0565

As a conclusion, no retroviral particles from any of the 3 packaging cell lines (Chapter 3.3) seemed to be appropriate to deliver the hEPO gene into the CHO-K1 cell line, not even with the tunicamycin treatment. However, the same particles showed very different results with the 3T3-L1 cell line (Table 3.6). While the pure construct (3T3-L1 – pMSCV) showed no detectable rhEPO levels, as expected, most of the values for the construct including the hEPO gene (3T3-L1 – pEPO) even exceeded the highest point of the calibration curve and were therefore declared as “high”. Due to the fact that the retroviral particles performed successful with murine (mouse) cell lines, the inability to transduct the hamster cells was assumed to be caused by the murine vector and the retroviral particles. Therefore, all the packaging cell lines were appropriate. The Phoenix^{TM} ampho cells were observed as the fastest and most reliable packaging cells and therefore, they were used further.

Table 3.6 – 3T3-L1 supernatant rhEPO EIA measurements

samples	rhEPO value [mU/mL]	absorbance 450 nm	absorbance 405 nm
3T3-L1 – pEPO #1	high	3.9754	1.2108
3T3-L1 – pEPO #2	high	3.9387	1.1994
3T3-L1 – pEPO #3	489.3	3.1747	0.9825
3T3-L1 – pEPO #4	high	4.0000	2.1658
3T3-L1 – pEPO #5	high	4.0000	2.2029
3T3-L1 – pEPO #6	high	4.0000	2.1177
3T3-L1 – pMSCV #1	0.0	0.0572	0.0485
3T3-L1 – pMSCV #2	0.0	0.0797	0.0666
3T3-L1 – pMSCV #3	0.0	0.0834	0.0664
3T3-L1 – pMSCV #4	0.0	0.0691	0.0591
3T3-L1 – pMSCV #5	0.0	0.0681	0.0580
3T3-L1 – pMSCV #6	0.0	0.0734	0.0655

Since the 3T3-L1 cell line did show secretion of high rhEPO levels, it was used in first preliminary flow experiments. The CHO-K1 cell line was also tested, as described in Part B (page 68), but no further attention was paid due to the lack of rhEPO secretion. Adherence of the 3T3-L1 cell line was very low. Thus another cell line was transducted, and tested for adherence as well as rhEPO secretion – the BNL-CL.2 cell line. The data for the calibration curve of the EPO EIA is shown in Figure 3.8 and Table 3.7.

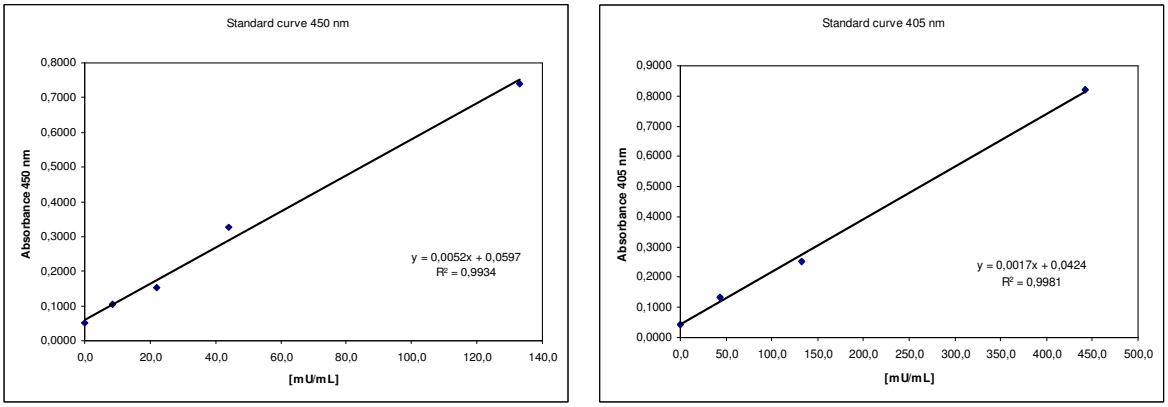

Figure 3.8 – EPO EIA calibration curves for 450 nm and 405 nm including linear fits

Table 3.7 – EPO EIA calibrator and control measurements

calibration curve	EPO value [mU/mL]	absorbance 450 nm	absorbance 405 nm
calibrator A	0.0	0.0504	0.0433
calibrator B	8.5	0.1040	0.0755
calibrator C	22.0	0.1542	0.0559
calibrator D	44.0	0.3269	0.1344
calibrator E	133.0	0.7412	0.2534
calibrator F	443.0	2.6310	0.8192
controls			
EPO control 1 [11.4 – 18.0 mU/mL]	17.0	0.1479	0.0844
EPO control 2 [126 – 200 mU/mL]	195.0	1.1644	0.3739

The BNL-CL.2 cells containing the construct and the hEPO gene (BNL-CL.2 – pEPO) provided secretion of high rhEPO levels, while there was nearly no detectable rhEPO in the supernatant from the cells with only the construct (BNL-CL.2 – pMSCV). The small amounts detected may result from the natural ability of liver cells to produce EPO. The results are shown in Table 3.8. Since the adherence experiments provided good results too, the decision was made to use this cell line as basic rhEPO source. The high output of rhEPO should enable to answer the question, whether hydrodynamic forces have an impact on the protein production or not.

Table 3.8 – BNL-CL.2 supernatant rhEPO EIA measurements

samples	rhEPO value [mU/mL]	absorbance 450 nm	absorbance 405 nm
BNL-CL.2 – pEPO #1	high	4.0000	1.3537
BNL-CL.2 – pEPO #2	432.5	2.4769	0.7777
BNL-CL.2 – pEPO #3	310.8	1.8462	0.5707
BNL-CL.2 – pMSCV #1	2.1	0.0705	0.0704
BNL-CL.2 – pMSCV #2	0.0	0.0646	0.0624
BNL-CL.2 – pMSCV #3	2.3	0.0716	0.0606

3.4.5 Storage of transducted cell lines

The surviving cells of the transductions had to be cultivated to establish a growing cell line. However, samples of each cell line had to be safely stored away by freezing. These frozen stocks are inevitable to access the cell lines again, in case of contamination or other destructive events of the cultivated cells.

To successfully freeze cells without losing too much cell matrial, the medium was carefully removed from a 75 cm^2 tissue culture flask. 10 mL PBS at room temperature were applied while avoiding pipetting onto the cells and the tissue culture flask was pivoted to wash the cells. After removing the PBS 1 mL trypsin was pipetted directly onto the cells. The tissue culture flask was heated to 37°C and tapped to detach the cells. Monitoring was done by microscopy.

After successful detachment, 5 mL of the medium were added. The type of medium was selected according to the requirements of the cell line. The tissue culture flask was thoroughly mixed, and the content was transferred into a 15 mL Falcon tube. The cells were then isolated by spinning down in a centrifuge fur 5 minutes at 1,200 rcf and room temperature.

After carefully removing the supernatant, the pellet was resuspended with previously cooled medium. The medium additionally included 10% dimethyl sulfoxide (DMSO) and 1 mL was used for each vial that should be filled from this tube. The 1 mL was directly transferred to a freezing vial with the cell line, passage and date already noted. The vial was instantly frozen at -20°C for at least 2 hours, to prevent DMSO from damaging cells. Afterwards the vial had to be transferred to -80°C storage for later use. For long term storage, i.e., to build up a cell line stock, the vial had to be further transferred to liquid nitrogen.

3.5 Locations of detectable rhEPO within the BNL-CL.2 cells

After the successful isolation of the hEPO gene, the construction of a working vector and hEPO insert construct, the production of retroviral particles and the transduction into mammalian cells, the first important part was completed. A system of stable, adherent cells was achieved that could be strained while secreting high amounts of detectable protein. However, the question of where those rhEPO proteins reside within the cells had to be answered, to ensure the accuracy of further conclusions.

Therefore, cells had to be fractioned into their sub compartments, namley membrane, cytoplasm and nucleus. To yield comparable results, cells with hEPO gene were cultivated, as well as cells, that contained just the vector For achieving the fractionation, the BNL-CL.2 cells were cultivated as described above, in a 25 cm^2 tissue culture flask with 4 mL DMEM, containing 1% v/v Glu, 10% v/v FBS and 1% v/v P/S for 24 hours at 37°C and 5% CO_2. Samples of the serum were taken and frozen at -20°C. Then the medium was carefully removed and PBS at room temperature was applied, avoiding direct impact on the cells. The tissue culture flask was pivoted to wash the cells and the PBS was removed afterwards. This washing step was repeated once, again with PBS. After having the PBS removed again, PBS was added a third time. This time however, the cells were scratched off the plate into the PBS solution. The solution was thoroughly mixed and collected into a 15 mL Falcon tube.

The cells have been isolated by down spinning in a centrifuge for 5 minutes at 1,200 rcf and room temperature. The supernatant was carefully removed and the pellet resuspended with 1 mL PBS at room temperature. The solution was transferred into a 2 mL microcentrifuge tube and kept on ice since this step. The cells were denaturized by ultrasound in 3 passes, each for the duration of 20 seconds. The nucleus was isolated afterwards by spinning down in a centrifuge for 15 minutes at 1,000 rcf and 4°C. The supernatant was carefully transferred into a 1.5 mL microcentrifuge tube for further separation. The nucleus pellet was resuspended in 1 mL PBS and frozen at -20°C.

The supernatant in the 1.5 mL microcentrifuge tube was used to isolate the membrane by spinning down in an ultracentrifuge for 60 minutes at 100,000 rcf and 4°C. The supernatant consisting of the cytoplasm was carefully removed and transferred to a 1.5 mL microcentrifuge tube, which was frozen at -20°C. The membrane pellet was resuspended with 1 mL PBS and also frozen at -20°C.

All these four samples, namely serum, membrane, cytoplasm and nucleus were analyzed with the Alpco™ EPO EIA kit, the calibration curve is shown in Figure 3.9, the measured calibration values and the controls are displayed in Table 3.9.

Table 3.9 – EPO EIA calibrator and control measurements

calibration curve	EPO value [mU/mL]	absorbance 450 nm	absorbance 405 nm
calibrator A	0.0	0.0613	0.0540
calibrator B	10.3	0.1281	0.0798
calibrator C	25.0	0.2148	0.1060
calibrator D	48.0	0.2954	0.1276
calibrator E	157.0	1.1584	0.3822
calibrator F	544.0	2.6710	1.0768
controls			
EPO control 1 [14.1 – 22.3 mU/mL]	21.4	0.1837	0.1022
EPO control 2 [158 – 250 mU/mL]	173.9	1.1848	0.3871

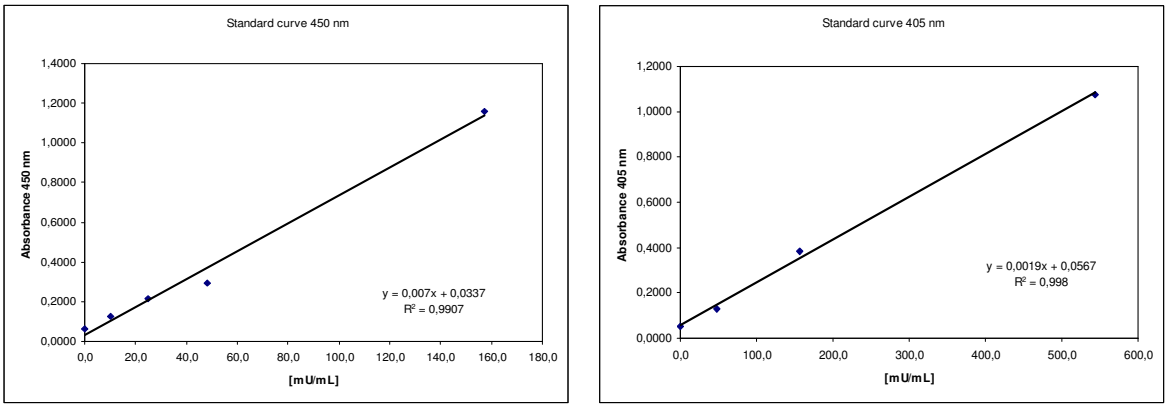

Figure 3.9 – EPO EIA calibration curves for 450 nm and 405 nm including linear fits

The results, displayed in Table 3.10, indicated a high level of rhEPO in the serum and a distinctive amount in the cytoplasm. A small rhEPO value was detectable in the nucleus, which may result from a small contamination during the separation process. The membrane showed nearly no result, compared to the natural low background detection of EPO from the cells with just the vector.

Table 3.10 – BNL-CL.2 rhEPO EIA measurements of different compartments

samples	rhEPO value [mU/mL]	absorbance 450 nm	absorbance 405 nm
BNL-CL.2 – pEPO serum	high	4.0000	2.8433
BNL-CL2 – pMSCV serum	4.8	0.0670	0.0629
BNL-CL.2 – pEPO membrane	4.6	0.0662	0.0574
BNL-CL2 – pMSCV membrane	6.3	0.0780	0.0728
BNL-CL2 – pEPO cytoplasm	29.0	0.2369	0.1157
BNL-CL2 – pMSCV cytoplasm	5.2	0.0702	0.0672
BNL-CL.2 – pEPO nucleus	12.3	0.1200	0.0795
BNL-CL2 – pMSCV nucleus	5.1	0.0696	0.0637

To achieve more distinctive results, another sample preparation method was necessary. The best results yielded the sample preparation described in Part B (page 70), which was done with a Millipore™ Amicon Ultra 0.5 mL Filter 10K [21]. Therefore, the rhEPO samples of membrane, cytoplasm and nucleus were also concentrated with these filters. The measured values are shown in Table 3.11.

Table 3.11 – BNL-CL.2 rhEPO EIA measurements of different compartments with concentration

samples	rhEPO value [mU/mL]	absorbance 450 nm	absorbance 405 nm
BNL-CL.2 – pEPO membrane	7.1	0.0837	0.0669
BNL-CL2 – pMSCV membrane	6.0	0.0756	0.0654
BNL-CL2 – pEPO cytoplasm	153.4	1.1078	0.3635
BNL-CL2 – pMSCV cytoplasm	5.3	0.0708	0.0639
BNL-CL.2 – pEPO nucleus	39.0	0.3068	0.1280
BNL-CL2 – pMSCV nucleus	6.2	0.0768	0.0655

After this measurement, the differences between the cytoplasm, nucleus and membrane were obvious. The EPO levels of the BNL-CL2 – pMSCV samples, the cells with only the vector, are taken as “zero” value, representing the small amount of EPO produced by mammalian liver cells in general. The perceived increased value of the nucleus sample might derive from imprecision of the separation, where a lot of rhEPO proteins still were in the sample solution. Far more important is the difference between the values of the membrane and the cytoplasm samples. While the cytoplasm clearly contains a great amount of rhEPO proteins, there is nearly no detectable level within the membrane fraction. According to these findings, rhEPO is released fast enough not to be trapped in the membrane, and neither is it attaching to it. Therefore, each increasing amount of rhEPO during experiments happened due to a change in the production rate, not because of the release of membrane attached rhEPO proteins. This was another important piece of information to analyze the data as described in Part C, obtained from the experimental process explained in Part B.

4 Summary

To investigate the behaviour of mammalian cells during the production process of recombinant proteins, an appropriate cell line is necessary. The recombinant protein, which should be produced, is another important factor. The decision was made to use recombinant human erythropoietin (rhEPO). It was one of the first therapeutic proteins in industrial production and the well developed methods are available to measure it.

To receive the pure amino acid sequence for the active protein, mRNA has been successfully isolated from a HepG2 cell line. After translating the RNA back into cDNA, constructs composing of two different vectors and the isolated EPO gene have been constructed. After careful purification and testing, a working plasmid was prepared, using the retroviral vector pMSCVpuro. This construct was then enveloped into viral particles, to enable access to mammalian cells and their nucleus. After having infected the cells, the retroviral vector transferred the information for the human EPO protein, as well as antibiotic resistances, into the genome. Under selection pressure from puromycin only cells with the resistance and therefore also the information for hEPO survived.

Three cell lines were transducted, but no rhEPO production was measured from the CHO-K1 cell line. The 3T3-L1 cell line worked well, but had lesser adhesion capabilities as CHO-K1 cells. Finally the BNL-CL.2 cell line combined the working transduction, and therefore rhEPO secretion, with good adherence. This was the appropriate cell line for this thesis.

Not only the rhEPO secretion was measured, but also the content of the membrane, the cytoplasm and the nucleus, ensuring that most rhEPO within the cell resides in the cytoplasm. Furthermore the membrane transfer is acting fast, since the membrane fraction had nearly no detectable amounts of the Protein. Finally, the cell line to investigate the influence of hydrodynamic stress on protein producing mammalian cells was completed.

References

1. Nollert, M.U.; Diamond, S.L.; and Mcintire, L.V.; Hydrodynamic shear-stress and mass-transport modulation of endothelial-cell metabolism; *Biotechnology and Bioengineering* (1991) 38, 588-602.

2. Kurtz, A.; Jelkmann, W.; Sinowatz, F.; and Bauer, C.; Renal Mesangial Cell-Cultures As A Model for Study of Erythropoietin Production; *Proceedings of the National Academy of Sciences of the United States of America-Biological Sciences* (1983) 80, 4008-4011.

3. Jelkmann, W.; Molecular biology of erythropoietin; *Internal Medicine* (2004) 43, 649-659.

4. Jacobs, K.; Shoemaker, C.; Rudersdorf, R.; Neill, S.D.; Kaufman, R.J.; Mufson, A.; Seehra, J.; Jones, S.S.; Hewick, R.; Fritsch, E.F.; Kawakita, M.; Shimizu, T.; and Miyake, T.; Isolation and Characterization of Genomic and Cdna Clones of Human Erythropoietin; *Nature* (1985) 313, 806-810.

5. Lin, F.K.; Suggs, S.; Lin, C.H.; Browne, J.K.; Smalling, R.; Egrie, J.C.; Chen, K.K.; Fox, G.M.; Martin, F.; Stabinsky, Z.; Badrawi, S.M.; Lai, P.H.; and Goldwasser, E.; Cloning and expression of the human erythropoietin gene; *Proceedings of the National Academy of Sciences of the United States of America* (1985) 82, 7580-7584.

6. Jelkmann, W.; Erythropoietin - Structure, Control of Production, and Function; *Physiological Reviews* (1992) 72, 449-489.

7. Fisher, J.W.; Erythropoietin: Physiology and pharmacology update; *Experimental Biology and Medicine* (2003) 228, 1-14.

8. Dingermann, T.; Recombinant therapeutic proteins: Production platforms and challenges; *Biotechnology Journal* (2008) 3, 90-97.

9. Alberts, M.; Bray, D.; Johnson, A.; Lewis, J.; Raff, M.; Roberts, K.; and Walter, P.; Essential Cell Biology - An Introduction to the Molecular Biology of the Cell; (1997)

10. Croughan, M.S.; Hamel, J.F.; and Wang, D.I.C.; Hydrodynamic effects on animal cells grown in microcarrier cultures; *Biotechnology and Bioengineering* (2006) 95, 295-305.

11. Marks, D.M.; Equipment design considerations for large scale cell culture; *Cytotechnology* (2003) 42, 21-33.

12. Goldberg, M.A.; Glass, G.A.; Cunningham, J.M.; and Bunn, H.F.; The regulated expression of erythropoietin by 2 human hepatoma-cell

lines; *Proceedings of the National Academy of Sciences of the United States of America* (1987) 84, 7972-7976.

13. Lattenmayer, C.; Trummer, E.; Schriebl, K.; Vorauer-Uhl, K.; Mueller, D.; Katinger, H.; and Kunert, R.; Characterisation of recombinant CHO cell lines by investigation of protein productivities and genetic parameters; *Journal of Biotechnology* (2007) 128, 716-725.

14. Siess, D.C.; Kozak, S.L.; and Kabat, D.; Exceptional fusogenicity of Chinese hamster ovary cells with murine retroviruses suggests roles for cellular factor(s) and receptor clusters in the membrane fusion process; *Journal of Virology* (1996) 70, 3432-3439.

15. Miller, D.G. and Miller, A.D.; Inhibitors of retrovirus infection are secreted by several hamster-cell lines and are also present in hamster sera; *Journal of Virology* (1993) 67, 5346-5352.

16. Eglitis, M.A.; Kadan, M.J.; Wonilowicz, E.; and Gould, L.; Introduction of human genomic sequences renders CHO-K1 cells susceptible to infection by amphotropic retroviruses; *Journal of Virology* (1993) 67, 1100-1104.

17. Miller, D.G. and Miller, A.D.; Tunicamycin treatment of CHO cells abrogates multiple blocks to retrovirus infection, one of which is due to a secreted inhibitor; *Journal of Virology* (1992) 66, 78-84.

18. Frost, S.C. and Lane, M.D.; Evidence for the Involvement of Vicinal Sulfhydryl-Groups in Insulin-Activated Hexose-Transport by 3T3-L1 Adipocytes; *Journal of Biological Chemistry* (1985) 260, 2646-2652.

19. Patek, P.Q.; Collins, J.L.; and Cohn, M.; Transformed-Cell Lines Susceptible Or Resistant to Invivo Surveillance Against Tumorigenesis; *Nature* (1978) 276, 510-511.

20. ALPCO Diagnostics; Specific quantitative assay for the determination of erythropoietin in serum; (2005)

21. Millipore; Amicon Ultra-0.5 Centrifugal Filter Devices; (2009)

Figures

Tables

Part B

Design and development of an experimental process setup for *in vitro* simulation of hydrodynamic stress

1 Goals and Motivation

After a therapeutic protein was successfully identified, isolated and produced on laboratory scale, the next step was the scale-up to an industrial production level. In pharmaceutical industry, this step is normally performed in batch mode, where each batch is tested to ensure the quality standards. These are very high standards, which are necessary for the safe use of drugs. However, many factors influencing the product quality are not completely understood. Furthermore, a lot of process parameters are determined only empirically, not by scientific approaches. Therefore, it is not possible to predict the outcome of the production.

A lot of variables affect the quality, as well as the quantity, of the products. The most important parameters for bioreactor operations regarding mammalian cells producing proteins are listed below:

- Accumulation of metabolites
- Nutrients
- Oxygen level
- pH-value
- Shear stress (caused by agitation and bursting bubbles)
- Temperature

Most of these single parameters can be controlled in modern bioreactors, but they are all linked to each other through agitation, and thus, hydrodynamic stress. Without sufficient agitation, metabolite accumulation would get too high, oxygen level, nutrients and temperature would not be dispersed enough and the pH-value would not remain constant. Hence, the necessary speed of agitation that does not exceed a level causing damage would be a very promising parameter to be determined in advance.

To measure the influence of this hydrodynamic stress on the production of extracellular proteins by adherent mammalian cell cultures, a quite complex experimental setup had to be designed. First of all, an extensive literature

research was conducted. Since no system was yet described that seemed to satisfy all the needs for this specific experiment, a new measuring process was designed, built up, tested and used that enables the *in vitro* examination of adherent mammalian cell cultures.

The requirements, which deemed necessary for the process setup, are:

- A channel, capable of cell adherence, withstanding a certain flow rate and enabling microscopy during the experiments.
- A pump, controlling and keeping the flow stable.
- A controlling unit for temperature, pH-value and oxygen level.
- A sampling unit, which would allow taking of small sample volumes while keeping the process setup sterile.

This part of the thesis describes the single parts and technical backgrounds of each part as well as the assembly to the complete setup. Additional requirements, identified during the first experiments and the set of possibilities of this unique measuring process are also described. It meets all the requirements mentioned above and also enables new approaches to the examination of adherent cell cultures.

2 Scientific Background

The effect of hydrodynamic stress is described as the significant difference between the growth of microorganisms producing recombinant therapeutic proteins in a laboratory flask or in a stirred tank [1]. Especially mammalian cell cultures are very susceptible to this mechanical stress due to the lack of a cell wall. Simultaneously these cells are of increasing importance for the production of biologically active recombinant therapeutic proteins [2,3]. Nevertheless, the design of a production level bioreactor is still a very complex task, even with increased understanding of the influencing parameters. The distribution of temperature, pH-value and oxygen level in connection to the stirring speed in large scale bioreactors is not a trivial task [4], because of the possible damage of cell cultures. Even the sparging of oxygen could be lethal to cells [5] without a proper protective agent like pluronic F-68 for example [6].

To achieve solutions based on scientific knowledge, the impact of hydrodynamic stress on cell viability and production needs to be certified. Up to now, a lot of the available publications deal with the damage inflicted on cells [7] and / or cell viability [8]. Most of them examine suspended cell cultures in a bioreactor, pumped through a flow device [9] or even through a fluorescence activated cell sorting (FACS) nozzle [10]. Other publications report shear stress analysis performed with high-speed rotating-disc devices [11]. Even a cell-free study of the values or distribution of critical scale-up parameters for large scale bioreactors is available [12]. However in all those publications the determination of the influence of hydrodynamic stress on the production of recombinant proteins was reported either as very difficult or even impossible.

In one of the few studies using adherent cells, the influence of shear stress on the morphology of CHO cells (Chinese hamster ovary cells) was measured [13]. As an outcome of the study, 0.82 [N/m^2] (or [Pa], which equates an energy dissipation rate or EDR of 6.7 x 10^2 [W/m^3]) were determined as “high sheer stress”, already limiting growth, survival and production rates of these cells. Another publication presented an EDR of 10^3 [W/m^3] as lethal shear stress for anchored cells [14].

But not only the results vary extensively in their dimensions (not to mention the technical terms, for example shear rate, shear stress, EDR or Reynolds number), also the experimental setups are quite different in their possibilities and limitations. Taking into account all the possible tanks, stirrers and other parts needed [15], most of the systems are getting too complex to select a single parameter for measurement. Other setups are too simple to transfer the results into a more sophisticated system like a bioreactor.

Therefore, a process setup, which can keep all parameters at a stable state, is necessary. Continuous laminar flow is reported to be very damaging to cells and therefore is a very interesting parameter [16]. The difference between laminar and turbulent flow can be observed in Figure 2.1. The first and foremost decision was that the process should be constructed around a channel, enabling laminar flow even at high throughput rates. This channel should contain adherent cell cultures producing and secreting a defined and measureable recombinant therapeutic protein. These cell cultures should then be exposed to hydrodynamic stress through laminar flow of the medium.

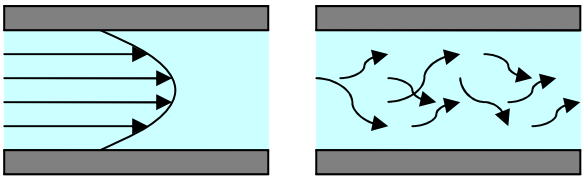

Figure 2.1 – Laminar flow (left) respectively turbulent flow (right)

The temperature, pH-value and oxygen level should be kept at optimal states, while the medium supplies the cells with nutrients while withdrawing metabolites and recombinant human erythropoietin (rhEPO). Samples of the medium should provide information about the changing levels of secreted protein and therefore confirm whether the hydrodynamic forces have an influence on the protein production or not.

3 Experimental Work

3.1 Ibidi™ µ-Slide I

The first step was the choice for the Ibidi™ µ-Slide $I^{0.4}$ [17] (later changed to the advanced Ibidi™ µ-Slide $I^{0.4}$ Luer – Figure 3.1) as channel, were the cells should adhere. These single-use channels provide the same specifications for each experiment, while the cells are also examinable by microscopy.

Figure 3.1 – Ibidi™ µ-Slide $I^{0.4}$ Luer

Given the exact specifications of the channel, the Reynolds number, the maximal EDR at the wall and the shear rate has been provided for tested flow rates (Figure 3.3 to Figure 3.4). Lethal damage to anchored cells occurs already at EDR 10^3 [W/m^3] and the maximum EDR in a 22,000 L mixing vessel is reported as 10^5 [W/m^3] [18]. With 80 mL/min flow rate the forces in the channel would result in the mentioned EDR of 10^5 [W/m^3], higher rates could even surpass this strain.

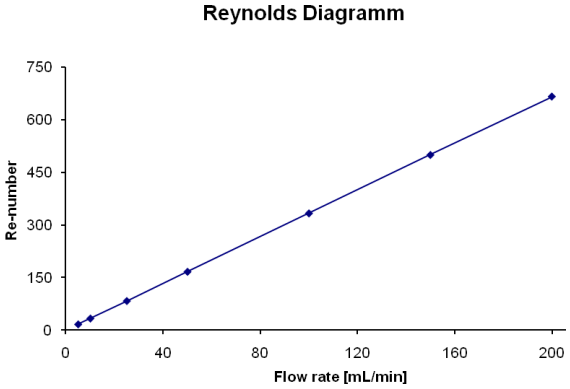

Figure 3.3 – Reynolds number *vs* Flow rate [mL/min]

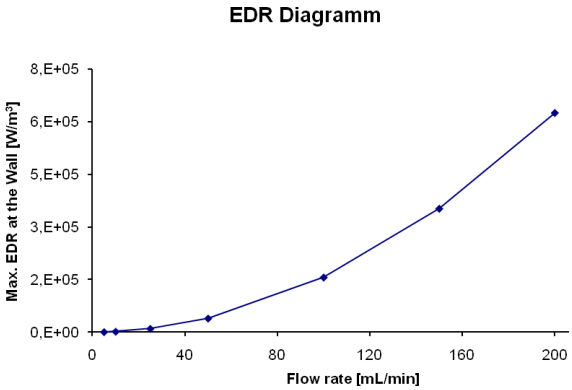

Figure 3.2 – EDR [W/m^3] *vs* Flow rate [mL/min]

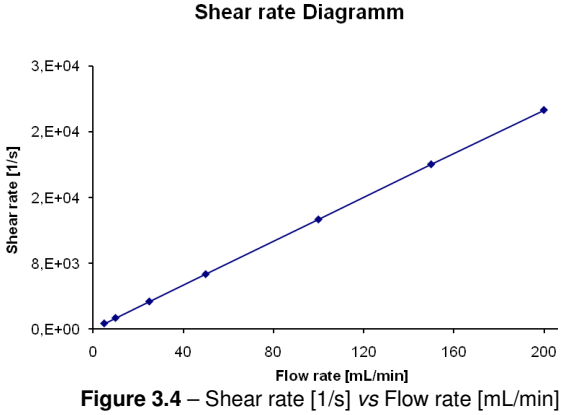

Figure 3.4 – Shear rate [1/s] *vs* Flow rate [mL/min]

3.2 Microscope

The second step was the integration of a microscope (Figure 3.5) into the process setup. This enables to survey the cells and their behaviour, as well as cell counting or area detection. Digital imaging is favourable for data acquisition and storage. Having the opportunity to analyze the digital images at a later time considerably shortens the time consumed for the examination itself. In addition, a computer aided automatic evaluation of the cell covered area is possible. A java utility, with an adjusting programme, will be described later.

Figure 3.5 – Leica™ 400M microscope with Leica™ DFC320 digital camera

3.3 Peristaltic pump

Figure 3.6 – Ismatec™ MCP-Process IP 65 peristaltic pump

The third critical part for completion of the first rough setup was an item to control and to keep the flow stable. After acquiring technical data for different possible solutions, the choice was made for an Ismatec™ MCP-Process IP 65 peristaltic pump with a SB-3V multichannel-pump head (Figure 3.6). This peristaltic pump is sealed against dust and splash water. It can be controlled and programmed by a computer via an EIA-232 (RS-232) port. Furthermore, the pump is capable of changing the direction of the flow, making even pulsating movement possible.

3.4 First experiments

These three parts were tested in a first simple setup (Figure 3.7), using a heating plate and a water bath to control the temperature. A 250 mL flask filled with medium (DMEM, 1% v/v Glu, 10% v/v FBS and 1% v/v P/S) was placed in the water bath at 37°C. The tubing (Ismaprene™ Pharmed 3.2 mm) connected the medium flask to the peristaltic pump and via the µ-Slide I back to the flask. The slide itself was placed on the heating plate and only for a short time removed for microscopy.

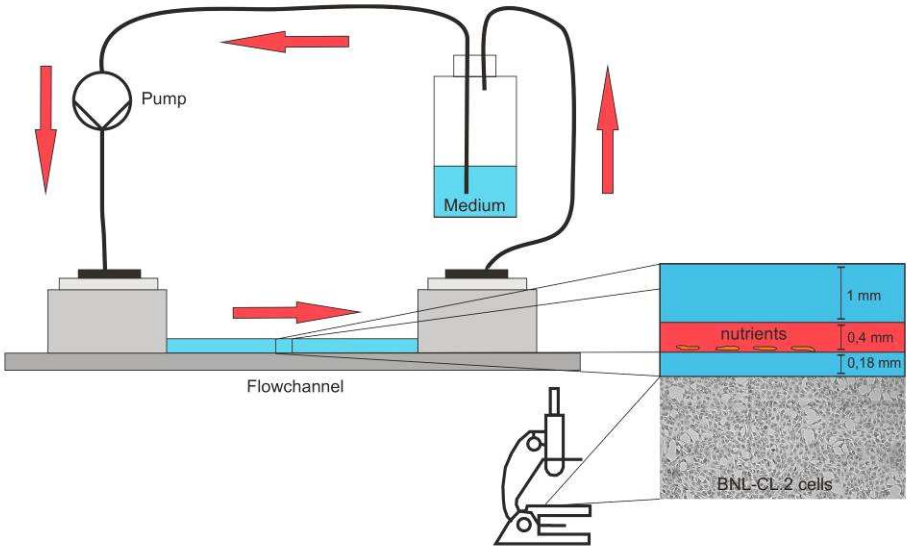

Figure 3.7 – First setup with slide, microscope and peristaltic pump

This setup was helpful to determine the most useable cell line to start with and also showed the limitations of this first process design. This important information was used to redesign and refine the process. First and foremost, the need for unit keeping the medium at a defined temperature and pH-value as well as supplying it with oxygen was evident.

3.5 Bioreactor

The most appropriate unit for controlling temperature, pH-value and oxygen level was a laboratory scale bioreactor. To keep the level of secreted proteins detectable, it should have a preferably low working volume and it should be capable of heating as well as cooling. In the designed process of course, the cells must not enter the bioreactor, to prevent falsifications of the measured data. A bio-t® mini laboratory scale bioreactor from Zeta™ Holding GmbH was available for this thesis (Figure 3.8).

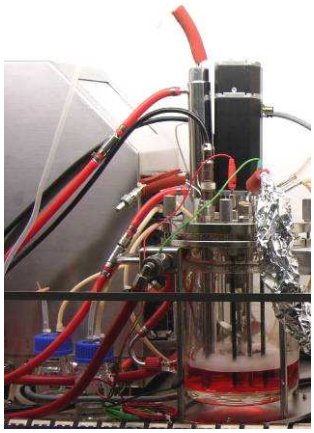

Figure 3.8 – Zeta™ bio-t® mini laboratory scale bioreactor

This bioreactor is capable of keeping the temperature, pH-value and oxygen level stable, providing digital readouts of the data and works already with a minimum volume of 400 mL. For temperature control, the agitator vessel is equipped with a jacket, enabling cooling as well as heating. This comes especially handy, when temperature experiments should be conducted or the pasteurized content of the agitator vessel should be cooled down.

Figure 3.9 – Pressure less ion exchanger DI 425

For optimal utilization of the bioreactor, a clean compressed air supply was needed, which was also at disposal, not only filtering dust and oil, but even microbes. In addition, to preserve the heating and cooling system of the bioreactor from damage, a water softener system, the pressure less ion exchanger DI 425, was implemented into the supply line (Figure 3.9). To control the pH-value, 0.5 molar solutions of HCl and NaOH were prepared for the automated system. Furthermore, a computer was also connected via an EIA-232 (RS-232) port and using the corresponding software from Zeta™, the data from temperature sensor, oxygen sensor, pH sensor and stirrer were recorded.

3.6 Laminar flow clean bench

Introducing a bioreactor into the process was necessary, but made the setup quite complex. Further additions to the system will also be necessary, for example to allow sterile sampling. However, everything should stay sterile inside and a certain amount of handling needs to be possible. Therefore, the decision was made to build the process setup within a laminar flow clean bench, biosafety level 2 approved.

To contain the whole process setup, including bioreactor and control unit, peristaltic pump, slide and the necessary tubing, as well as a water and a compressed air supply, power supply, computer connections and a water outlet, the clean bench needed a lot of workspace. The selected Clean Air™ EF 6 biological safety cabinet class II (Figure 3.10) therefore has a large work area of 1719 x 440 mm.

Figure 3.10 – Clean Air™ EF 6 biological safety cabinet class II

3.7 Sampling system

Up to now, most of the systems provided by manufacturers of lab scale bioreactors are not suitable to take small samples. This reduces the amount of medium dramatically, especially if one intends to take samples continuously in long time fermentations. E.g., one sample of 10 mL every two hours for 48 hours would be 240 mL. Therefore, a lab scale bioreactor with a working volume of 400 mL medium would be drained too fast from sampling. The other possibility is to draw samples with a sterile syringe through a self-sealing membrane. However this kind of sampling will keep sterile or leak proof only for a limited number of samples.

Therefore, a sampling system was designed and built that can be incorporated into a sterile external circuit. This circuit draws medium via the peristaltic pump, passes it through the sampling system and returns it to the bioreactor vessel. The sampling system enables not only temperature readouts but also the taking of sterile small samples (from 1 to 0.1 mL) during running experiments [18].

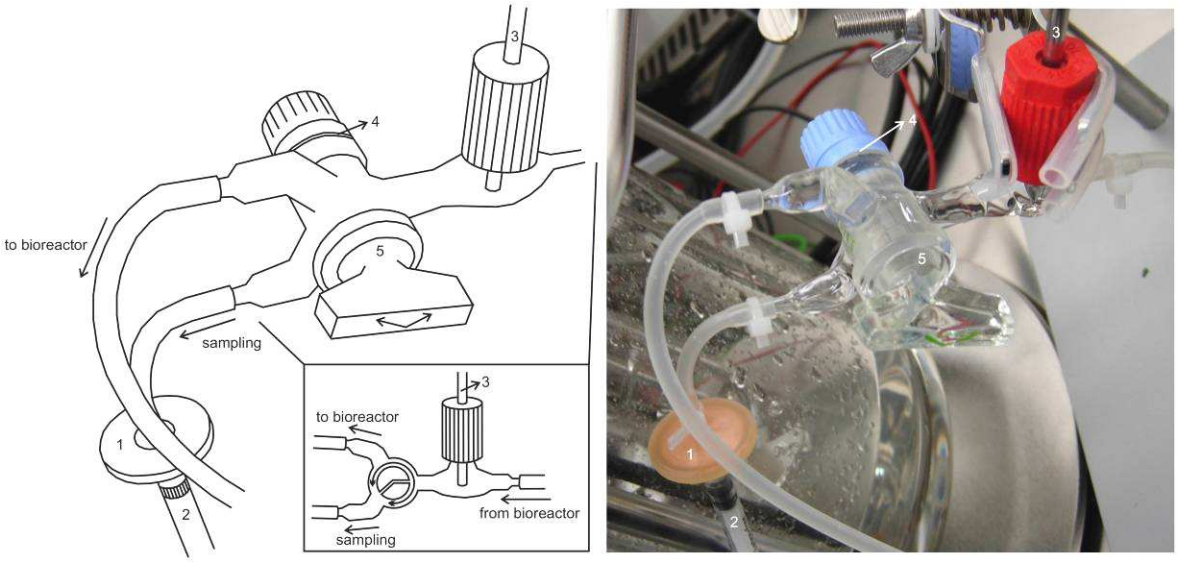

Figure 3.11 – Scheme and picture of the sampling system included in a external circuit[18]

The prototype is shown in Figure 3.11. The main part is a three-way stop cock consisting of a ground-in stopper with a small channel inside (5). To prevent leaking, a seal (4) is mounted onto the ground-in stopper and the glass grinding prevents free movement. This setup enables to switch between two outlets, one leading back to the bioreactor vessel, the other to a sterile sampling unit with a Luer adapter. E.g. sterile one way syringes (BD Plastipak™, 1 m – 2) can be used to draw the samples while a sterile filter (Whatman™ Spartan 13, 0.2 µm – 1) that prevents any contamination of the remaining system. The system also includes the possibility to add a temperature sensor (Testo™ 110 – 3), which allows measuring the temperature at the point of sampling under sterile conditions.

3.8 Extension of a microscope stage

The position of the slide is an important part of the whole external circuit. Since the sampling should occur after the slide, it needs to be placed between the peristaltic pump and the sampling system. However, another crucial component is needed to fixate the Ibidi™ µ-Slide $I^{0.4}$ Luer under flow conditions. This should prevent movements of the slide at higher flow rates. Furthermore, an option to attach the slide to a microscope stage, enabling positioning of the slide using the coordinate grid of the stage, would be very useful. During all this operations, the slide must keep connected to the circuit, in order to maintain sterile conditions.

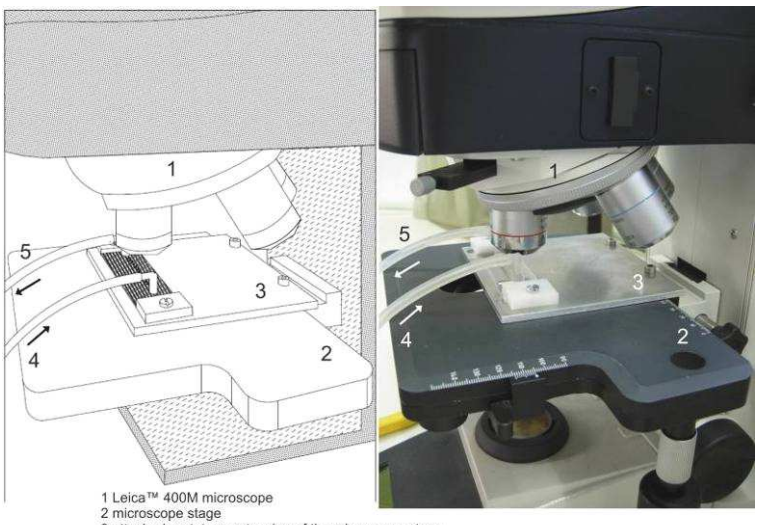

Figure 3.12 – Scheme and picture of the connected microscope stage extension[19]

Since a commercially available option was designed as described above, which fulfilled all needs, another prototype has been built and incorporated into the experimental process setup (Figure 3.12) [19].

As displayed in Figure 3.13, the extension consists of a metal main rack (1), with two plastic clamps (2) siding a depression, where an object slide with an engraved grid (5) could be inserted and the Ibidi™ µ-Slide $I^{0.4}$ Luer (3) can be mounted. Afterwards, the whole unit can be fixed with standard screws (8) to any microscope stage. Therefore, the fine mechanical movement of the microscope stage remains possible, for example while keeping the slide attached by the Luer

connections (6 and 7) to a flow system. With the extension microscopy can be done without detaching the slide from the circuit. The use of the coordinate grid of the microscope stage also remains possible. This allows exact repositioning of already examined fields of vision.

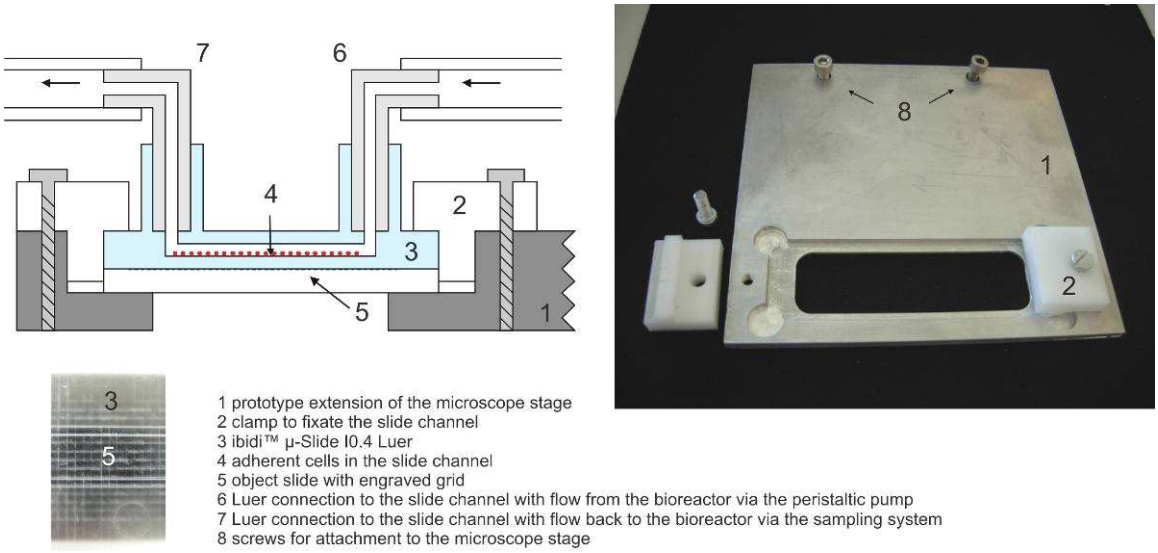

Figure 3.13 – Scheme and picture of the extension of a microscope stage[19]

3.9 Filter system

As final step before the circuit reconnects to the bioreactor, a filter system should be incorporated, to prevent cells and cell artefacts from entering the bioreactor, respectively moving through the whole circuit. After literature research, information search from the manufacturers and some experimental tests, the decision was made for Pall™ Mini-Kleenpak, Supor EKV, 0.2 µm sterile filters (Figure 3.14). These filters are able to endure flow rates up to 200 mL/min, are equipped with a gas valve and can be heat-sterilized in autoclaves. The last point is especially important, since the bioreactor and the whole closed external circuit have to be autoclaved prior to an experiment in order to keep the equipment sterile.

Figure 3.14 – Pall™ Mini-Kleenpak sterile filters with three-way stop cock

To ensure functionality in case of a clogged filter, two filters have been embedded into the circuit. A three-way stop cock enables switching between the two filters. While the filters are built for a wide range of fluids, including buffers, biological fluids, tissue culture media and ophthalmic products, the minimal hold-up volume is less than 6 mL and does not expend too much of the total medium volume. The filter membrane itself is low protein and preservative binding, which ensures maximum transmission of active ingredients. In case of this work it was Erythropoietin.

3.10 Bubble trap

Figure 3.15 – Bubble trap working in a running experiment

During the first experiments with medium and cells at low flow rates, bubble swarms swept through the setup. When they passed the slide, the bubbles detached many of the adherent cells, often rendering further measurements useless. To cope with this problem, a T-piece was integrated in front of the slide. This so called “bubble trap” was able to collect the bypassing bubbles and kept them out of the circuit (Figure 3.15). In later experiments, the upright part was enlarged to increase the trap volume.

3.11 Complete experimental process setup

The complete process setup was constructed by assembling the introduced parts in the paragraphs 3.1 to 3.3 and 3.5 to 3.10. Afterwards, experiments with deionised water were conducted, to define the needed temperatures at the zeta™ bio-t® mini bioreactor. In order to achieve 37°C within the Ibidi™ µ-Slide $I^{0.4}$ Luer, the temperature at the bioreactor has to be set at a higher level (Table 3.1). The whole setup with the flow from the bioreactor via the process pump to the slide and further through the sampling system, the filters and finally back into to bioreactor works as a cooling circuit.

Table 3.1 – Flow rates with corresponding set and measured temperatures

flow rate	temperature set at the bioreactor	temperature measured at bioreactor	temperature measured at sampling system
15 mL/min	51.5 °C ± 0.5 °C	50.8 °C	33.3 °C
25 mL/min	44.0 °C ± 0.5 °C	43.6 °C	34.5 °C
50 mL/min	40.5 °C ± 0.5 °C	40.0 °C	35.0 °C
75 mL/min	39.0 °C ± 0.5 °C	38.7 °C	35.6 °C
100 mL/min	38.5 °C ± 0.5 °C	38.1 °C	35.7 °C
150 mL/min	38.0 °C ± 0.5 °C	37.5 °C	35.8 °C
200 mL/min	38.0 °C ± 0.5 °C	37.5 °C	35.9 °C

While EPO proteins are reported as temperature stable [20], settings above 47 °C were not used, to prevent the proteins from degrading while they were cycling through the whole process. Visual examination during the experiments with lower temperature showed no negative influence of the lower temperature to cell viability.

The whole setup is presented in Figure 3.16. All the relevant parts described above are shown and numbered. The flow in the external circuit starts with the “Bioreactor” (1), moving in the direction of the “Peristaltic pump” (6), further through the “Bubble trap” (7), the “Ibidi™ µ-Slide I” fixated by the “Extension of a microscope stage” (8) and the “Sampling system” with temperature sensor (9) before passing the “Filter system” (5) and re-entering the bioreactor. The three most important sensors within the bioreactor are also marked, namely the temperature (2), pH-value (3) and oxygen (4) sensors. All these parts are settled within the “Laminar flow clean bench”, while the “Microscope” is outside of the clean bench, due to space and operational capability.

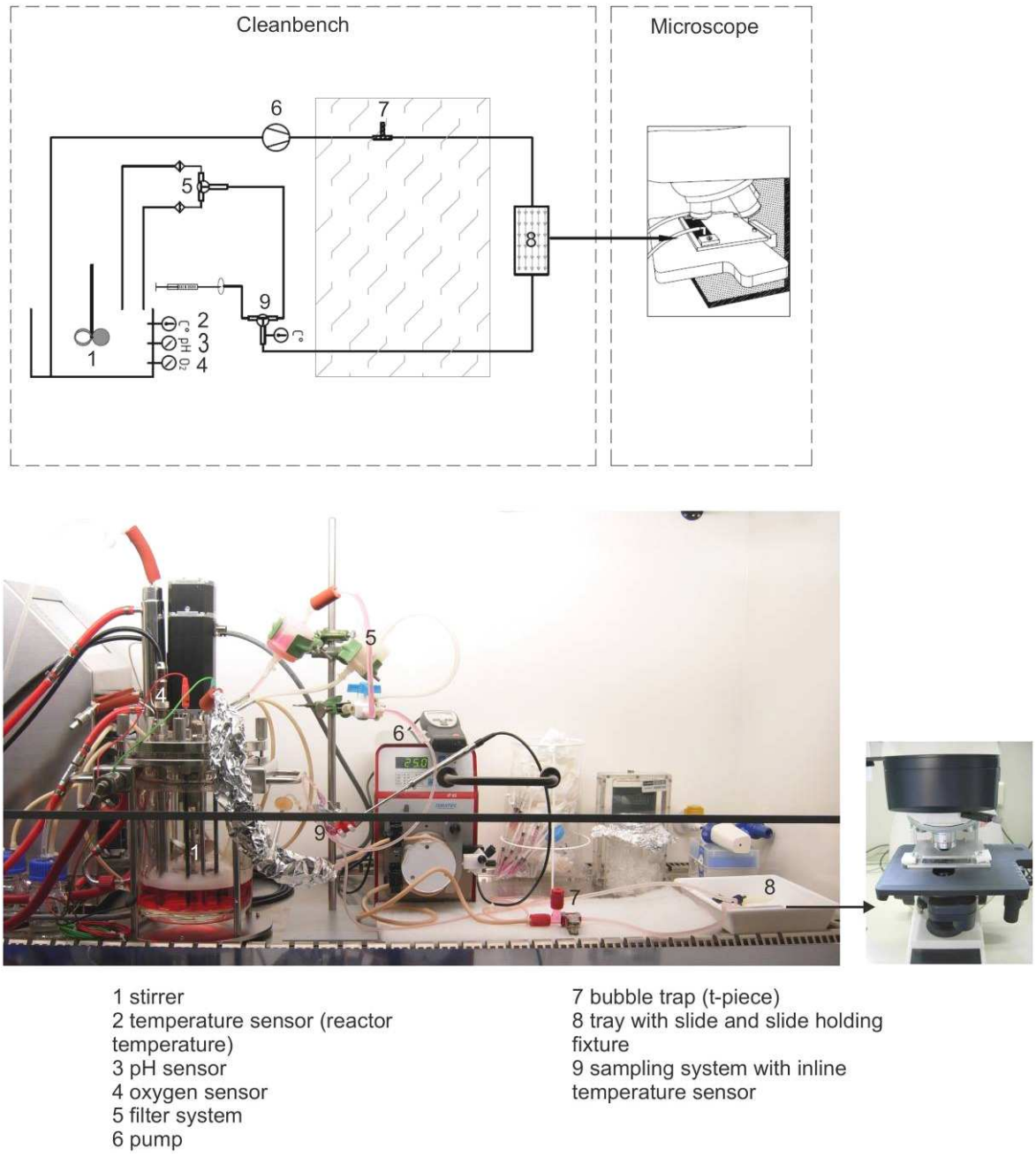

Figure 3.16 – Scheme and picture of the complete experimental process setup

To achieve a better overview, the detailed connections to the bioreactor are shown in Figure 3.17. The scheme and picture present the already mentioned pH sensor (1), temperature sensor (2) and oxygen sensor (11) as well as the stirrer (14). Further data links to the bioreactor control unit are the level sensor (8) and the foam sensor (10). The compressed air adapter (3) and the water connections to the reflux condenser (13) are also operated by the control unit. Acid (5) and base (4) supplies for the pH-value control are connected to the corresponding inlets and

are activated by small peristaltic pumps at the control unit. The feeding tube (12) is used to fill the bioreactor via a connection valve with medium after having been autoclaved. Finally the circular flow starts at the harvest tube (9) and, after completing the whole circuit, re-enters the bioreactor through one of the refeeding junctions (6 and 7), depending on the preset filter.

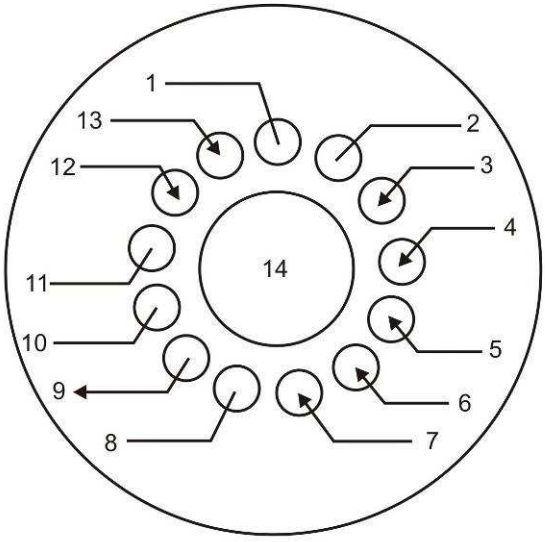

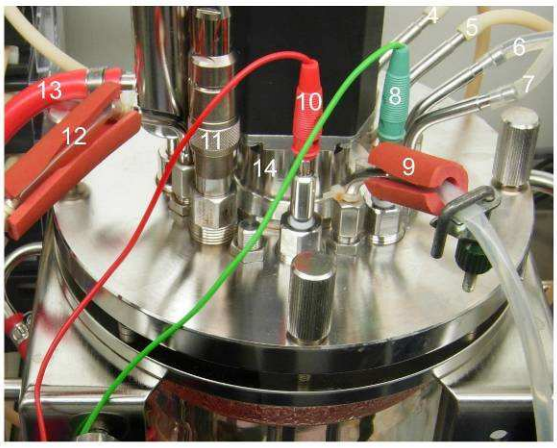

1 pH sensor
2 temperature sensor
3 supply air
4 base addition
5 acid addition
6 refeeding junction
7 refeeding junction
8 level sensor
9 harvest or draft tube
10 foam sensor
11 oxygen sensor
12 feeding tube
13 reflux condenser
14 stirrer

Figure 3.17 – Scheme and picture of the bioreactor cover plate and circuit points

3.12 Cell experiments – surface matters

Having finished preliminary testing and setup, 17 experiments with cells have been conducted. Of course the need for some changes or better solutions was encountered during these experiments. The “Bubble trap” was one of the necessary improvements to keep the cells adherent and alive. It was incorporated after a bubble swarm emptied the channel during microscopy at experiment number 7. After successfully completing experiment 17 (50 hours), the influence of these bubble swarms was tested. First, as displayed in Figure 3.18, bubble swarms were intentionally purged through the system with a flow rate of 10 mL/min. There were some stressed cells to be noticed, but only a few cells detached.

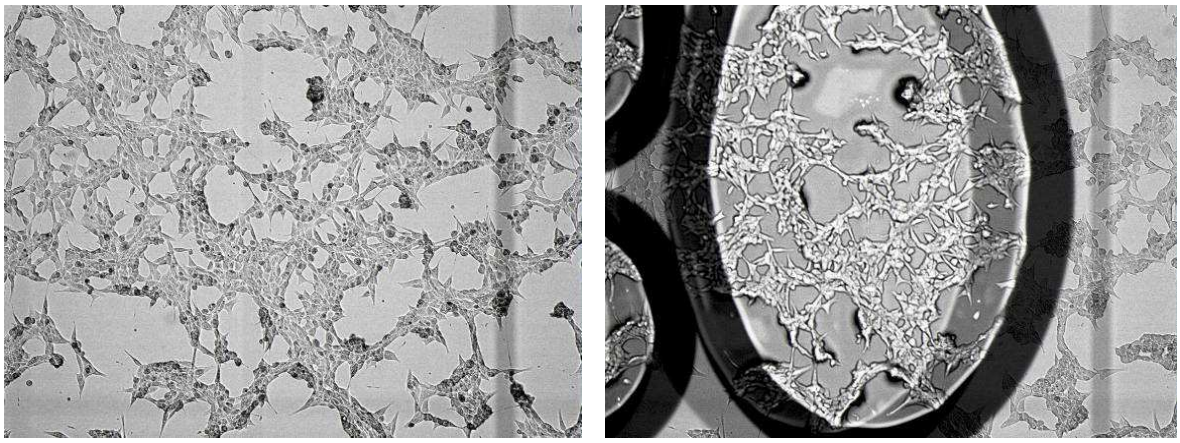

Figure 3.18 – Pictures from BNL-CL.2 cells on Ibidi™ µ-Slide I Collagen IV at 10 mL/min

Figure 3.19 – Pictures from BNL-CL.2 cells on Ibidi™ µ-Slide I Collagen IV at 25 mL/min

Directly after taking these pictures by digital microscopy, the cells were stressed with bubble swarms at a flow rate of 25 mL/min. As can be observed in Figure 3.19, the remaining cells were still adherent after 50 hours of experimental stress. The induced bubble swarm almost completely wiped the channel empty at this velocity. Acknowledging these facts, the prevention of such swarms passing the channel and therefore the adherent cells, was a very important factor. Without these interferences, experiments with the duration of 48 hours could be done.

Another important factor affecting the adherence is the number of cells seeded into the slide channel overnight (ON – around 14 hours). The cell number of 6 x 10^5 was specified by the Ibidi™ µ-Slide I manual for slides with 0.4 mm channel height (100 µL volume) and was used for the starting experiments [21]. A basic overview of the first 17 experiments is given in Table 3.2.

Table 3.2 – Experiments 1 to 17 with surface, cell number, flow rate and duration

experiment number	surface	cell number seeded (ON)	flow rate	duration
1	ibiTreat	6 x 10^5	50 mL/min	12 h
2	ibiTreat	6 x 10^5	50 mL/min	1 h
3	ibiTreat	6 x 10^5	50 mL/min	2 h
4	ibiTreat	6 x 10^5	25 mL/min	8 h
5	ibiTreat	6 x 10^5	25 mL/min	7 h
6	ibiTreat	6 x 10^5	25 mL/min	23 h
7	ibiTreat	6 x 10^5	25 mL/min	4 h
8	Fibronectin	6 x 10^5	25 mL/min	50 h
9	Fibronectin	3 x 10^5	25 mL/min	48 h
10	Collagen IV	3 x 10^5	25 mL/min	48 h
11	Fibronectin	1.4 x 10^6	25 mL/min	12 h
12	Fibronectin	6 x 10^5	25 mL/min	8 h
13	Collagen IV	5.8 x 10^5	25 mL/min	1 h
14	Collagen IV	5.8 x 10^5	25 mL/min	47 h
15	Collagen IV	6 x 10^5	25 mL/min	2 h
16	Collagen IV	10^5	25 mL/min	48 h
17	Collagen IV	3 x 10^5	25 mL/min	50 h

BNL-CL.2 cells on ibidi™ µ-Slide I ibiTreat after 1 hour

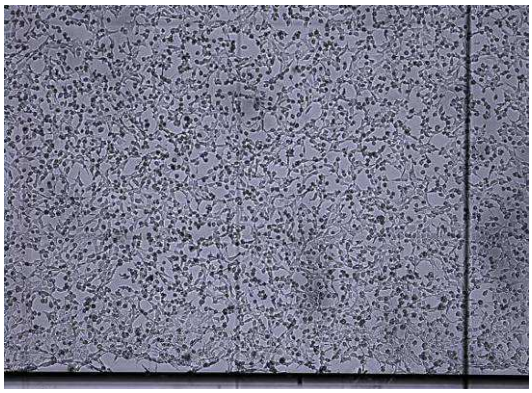

BNL-CL.2 cells on ibidi™ µ-Slide I ibiTreat after 2 hours

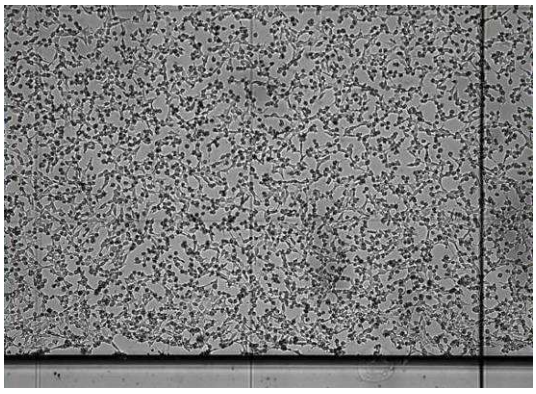

BNL-CL.2 cells on ibidi™ µ-Slide I ibiTreat after 3 hours

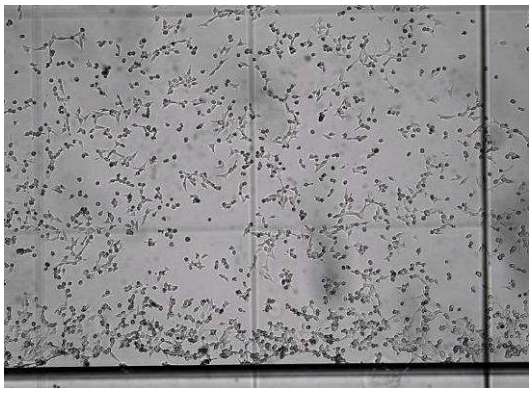

BNL-CL.2 cells on ibidi™ µ-Slide I ibiTreat after 4 hours

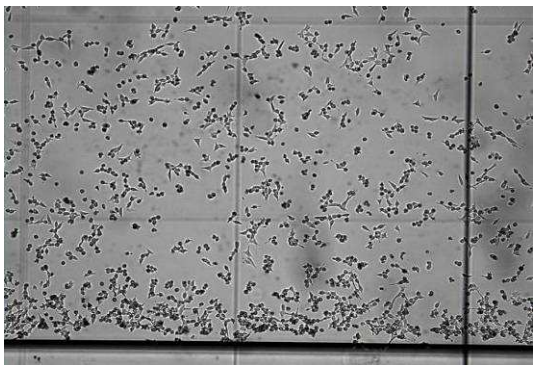

BNL-CL.2 cells on ibidi™ µ-Slide I ibiTreat after 5 hours

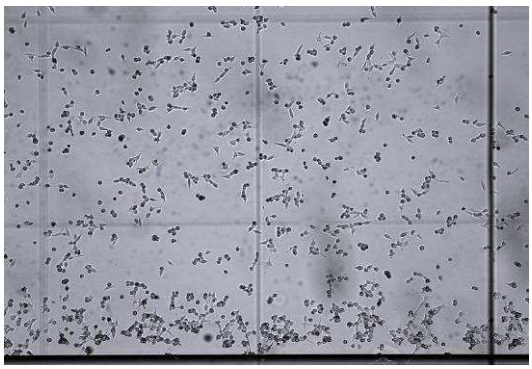

BNL-CL.2 cells on ibidi™ µ-Slide I ibiTreat after 6 hours

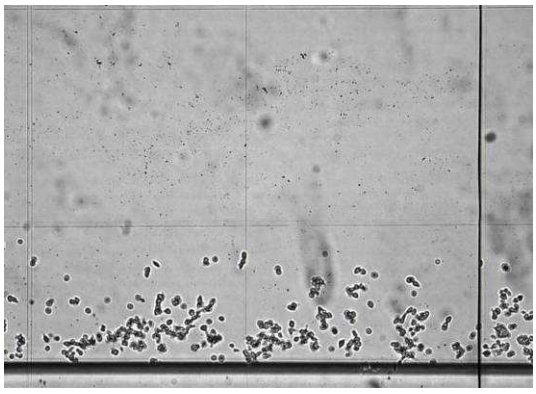

BNL-CL.2 cells on ibidi™ µ-Slide I ibiTreat after 7 hours

BNL-CL.2 cells on ibidi™ µ-Slide I ibiTreat after 8 hours

Figure 3.20 – Pictures from BNL-CL.2 cells on Ibidi™ µ-Slide I ibiTreat surface

Especially the slide surface and its conditions for the adherence of cell cultures was in need of improvement. As an example, Figure 3.20 shows the digital microscope pictures from experiment number 4 with 25 mL/min flow from 1 hour to 8 hours, with 6 x 10^5 rhEPO-producing BNL-CL.2 cells seeded overnight on an Ibidi™ µ-Slide $I^{0.4}$ with ibiTreat surface.

At this mean flow rate of 25 mL/min (EDR 9.77 x 10^3), the cells are already continuously detaching, leaving virtually no measureable cell mass after a few hours. Obviously ibiTreat, a physical modification of the polyethylene derivative surface of the Ibidi™ µ-Slide I channel, offers not enough adhesion strength for the experiments. Of course, these conditions are inappropriate for long term experiments, so the adherence had to be improved drastically.

Taking reproducibility into consideration, the set of manufactured surface coatings provided by Ibidi™ were tested if they provide better adherence under flow conditions. Besides the ibiTreat surface, coatings with collagen IV, Fibronectin and Poly-L-Lysine are available for the Ibidi™ µ-Slide $I^{0.4}$ and the µ-Slide $I^{0.4}$ Luer. The most useful number of cells to be seeded into the slide for overnight adherence was tested simultaneously.

3.12.1 Collagen IV

Collagens comprise a large family of insoluble extracellular glycoproteins that are essential components of connective tissues such as tendons, ligaments, cartilage, bone and skin. The mature polypeptides are secreted as coiled, left-handed helices that subsequently assemble into rope-like collagen fibres. Collagen IV is a network forming triple-helix collagen whose C-terminus is forming dimers while the N-terminus forms tetramers [(22)]. It is a main component of basal laminae, layers of an extracellular matrix which are a structural base for specialised mammalian cells, e.g. epithelial cells [(23)]. Thus, collagen IV used as coating forms a natural base for adherent mammalian cells. Since BNL-CL.2 cells are liver epithelial cells, this was considered a very adequate surface.

The digital microscopy pictures of 4 measurement points of experiment number 17 are shown exemplary in Figure 3.21. The basic setting of the experiment was a flow rate of 25 mL/min for up to 50 hours, with 3 x 10^5 rhEPO-producing BNL-CL.2 cells seeded overnight on an Ibidi™ µ-Slide $I^{0.4}$ Luer with collagen IV coated surface. This was the best achieved result so far and therefore served as basis for further experiments. Of course detachment of cells occurred, but in small quantities compared to all other experiments. The channel was not emptied that fast and easy as with the ibiTreat surface and the cells detached either in very small groups or as single units. All experiments conducted with collagen IV coating also proved that the cell number of 3 x 10^5 was most effective for this kind of surfaces and overnight adherence. This amount of cells provided a nearly confluent monolayer with strong attachment of the cells to the collagen fibrils. Later experiments certified these assumptions and proofed the eligibility of collagen IV coated surfaces for the adherence of BNL-CL.2 cells.

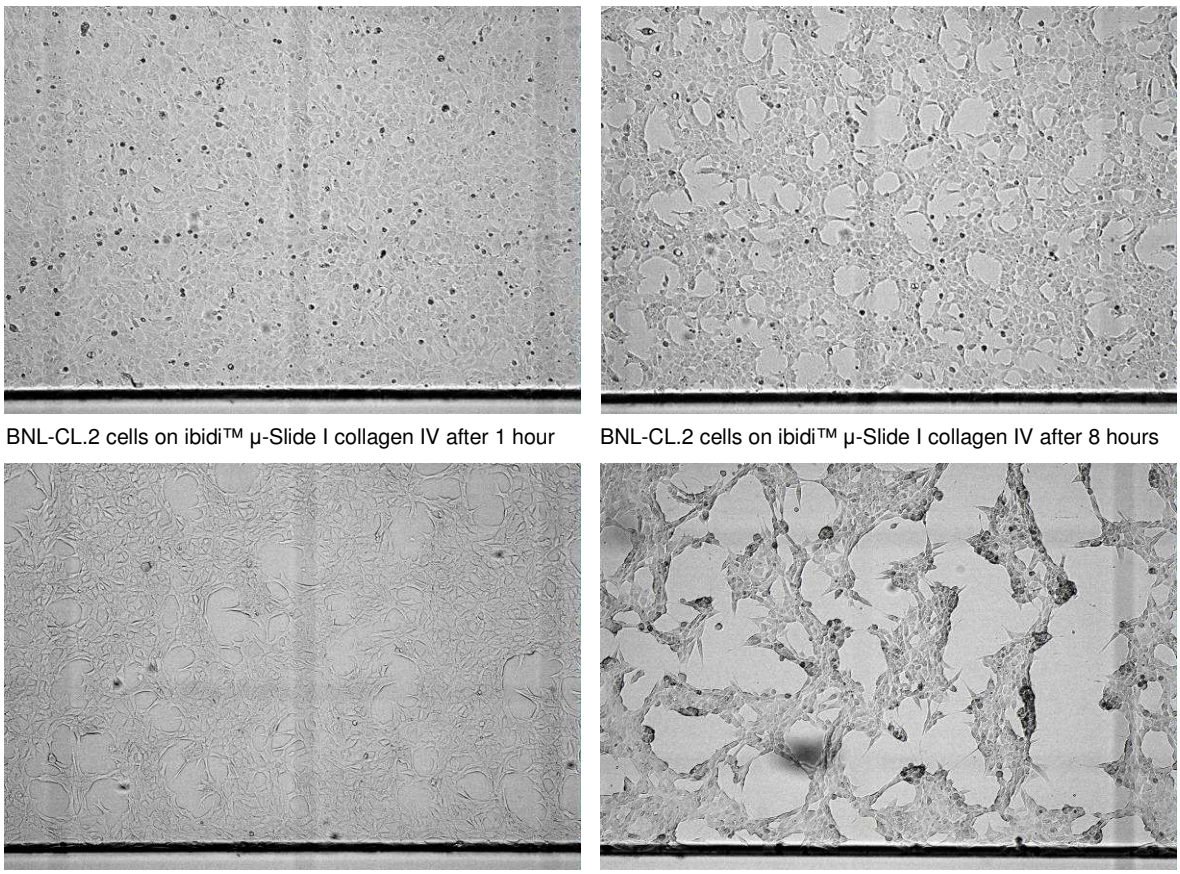

BNL-CL.2 cells on ibidi™ µ-Slide I collagen IV after 1 hour

BNL-CL.2 cells on ibidi™ µ-Slide I collagen IV after 8 hours

BNL-CL.2 cells on ibidi™ µ-Slide I collagen IV after 24 hours

BNL-CL.2 cells on ibidi™ µ-Slide I collagen IV after 48 hours

Figure 3.21 – Pictures from BNL-CL.2 cells on Ibidi™ µ-Slide I Luer collagen IV surface

3.12.2 Fibronectin

The complex molecule Fibronectin is generally an important factor in cell adhesion, migration, growth and differentiation. It is usually a dimer composed of two nearly identical subunits with a molecular mass of around 250 kDa. Despite being the product of a single gene, there are over 20 variants in human Fibronectin due to alternative splicing of the mRNA. Furthermore, the protein is an abundant soluble constituent of plasma and also part of the insoluble extracellular matrix. Therefore, Fibronectin can be subdivided into two forms, the soluble plasma form and the less-soluble cellular form.

Its function as ligand for a dozen of integrin receptors enables the connection between the extracellular matrix and the intracellular cytoskeleton in mammalians. But Fibronectin also has a wide range of other functional activities. Utilising a lot of distinctive binding domains, it can attach to a number of biologically important molecules that include heparin, collagen/gelatin and fibrin [(24)]. Therefore, it is a highly suitable protein for coating surfaces and improving adherence, since it can act as matrix connecting to the intracellular cytoskeleton.

Described as the strongest adherence improving factor, Fibronectin was the first tested surface coating in the experiments 8, 9, 11 and 10. The adherence was strongly improved by the use of Fibronectin coated slides as shown on the pictures in Figure 3.22 from experiment number 8. The conditions of this experiment were 25 mL/min flow for up to 50 hours, with 6 x 10^5 rhEPO-producing BNL-CL.2 cells seeded overnight on an Ibidi™ µ-Slide $I^{0.4}$ with Fibronectin coated surface.

The observations indicate that the Fibronectin matrix not only improves adhesion to the channel wall, but seems also to enhance the interaction and connection between the cells. This was concluded due to the observed cell detachment in big units, when enough stress was endured. Therefore, the use of the Fibronectin coating was not advisable for the BNL-CL.2 cells, since the duration of cell adherence was too arbitrary. Nevertheless, the experiments with Fibronectin provided the first breakthrough towards the desired duration of 48 hours for an experiment.

BNL-CL.2 cells on ibidi™ µ-Slide I Fibronectin after 1 hour

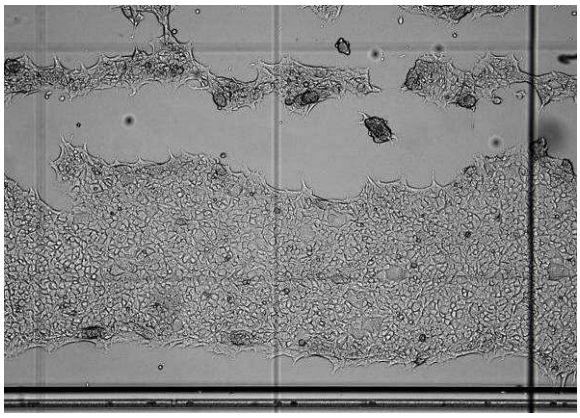

BNL-CL.2 cells on ibidi™ µ-Slide I Fibronectin after 24 hours

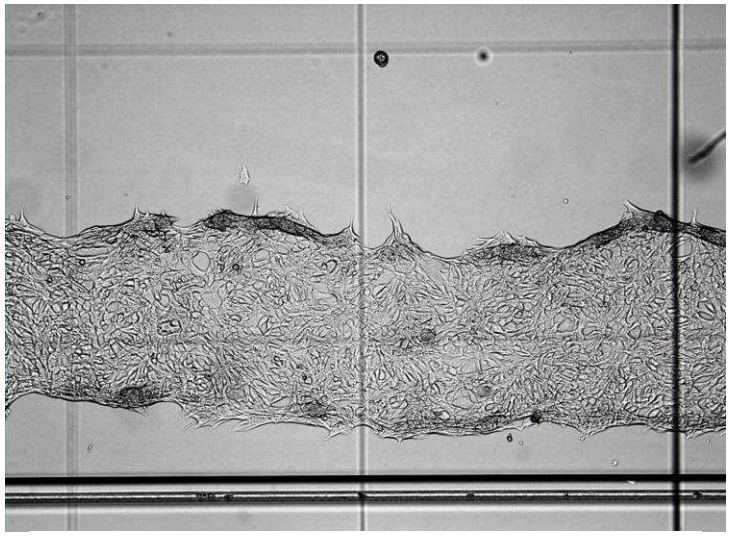

BNL-CL.2 cells on ibidi™ µ-Slide I Fibronectin after 48 hours

Figure 3.22 – Pictures from BNL-CL.2 cells on Ibidi™ µ-Slide I Luer Fibronectin surface

3.12.3 Poly-L-Lysine

The multiply charged polypeptide Poly-L-Lysine exists as a random coil in its polycationic form. This carrier molecule interacts with negatively charged molecules at the surface of a cell, and therefore, binding itself by electrostatic force to the cell membrane. It is also known to bind to tumour cells with high affinity both *in vivo* and *in vitro*, due to the stronger negative charge of tumour cell membranes. Poly-L-Lysine is even capable of being cytotoxic by penetrating the membrane and inhibiting cell growth [(25)]. The later facts are not of any concern when Poly-L-Lysine is used as a coating. Poly-L-Lysine just provides a positively charged surface, were cell adherence is improved without any interaction of receptors, just electrostatic binding.

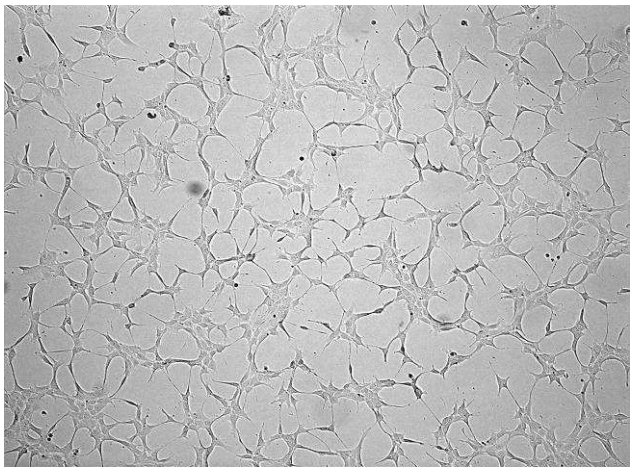

Figure 3.23 – BNL-CL.2 cells on Ibidi™ µ-Slide I Luer Poly-L-Lysine surface

Poly-L-Lysine coating was not thoroughly tested any more under experimental conditions, since the successful breakthrough with Collagen IV. However, Figure 3.23 as an example from the pretesting displays 4.5 x 10^4 BNL-CL.2 cells after ON adhesion.

3.13 Erythropoietin levels – refining measurement issues

Selecting the method to be used for the qualification and quantification of the produced amount of rhEPO, enzymatic detection by an ELISA/EIA kit [26] was chosen. These methods are well established, good to handle and kits for rhEPO detection are available from different manufactures with different sensitivity.

3.13.1 ELISA/EIA principles

The Enzyme-Linked Immuno Sorbent Assay method itself was developed from the radioimmunoassay in the 1970's. Simultaneously, the Enzyme ImmunoAssay (EIA) was developed, which is based on the same principle as the ELISA [27,28]. All these assays use antigen-antibody linkage for the capture of specific proteins. But ELISA and EIA use enzymatic reactions which lead to a coloured product instead of the radioactive labelled antibodies used for the RIA method. Therefore, measurements with ELISA/EIA kits can be easily analyzed with a photometer and the handling does not require special workplaces for radioactive material.

In case of the experimental process setup, the choice was made for the Alpco™ EPO EIA kit, a so called "sandwich" or two-side EIA, capable of detecting very low quantities of EPO. The kit contains 12 strips with 8 wells each, already coated with

streptavidin. Streptavidin has four domains, each forming a strong, non covalent and specific complex with biotin. To enable the antigen-antibody linkage, the calibrator, control and sample solutions are filled into the wells of the plate. Then a second solution with a mouse monoclonal antibody linked to a detection enzyme and third a solution of a biotinylated mouse monoclonal antibody is added. While the mixture is incubated, the biotin-linked antibody attaches to the streptavidin on the wall of the wells (as mentioned above). Furthermore, the antigen, in this case the rhEPO, attaches to both antibodies. Therefore, a tripartite complex bound to the walls of the well is formed (Figure 3.24).

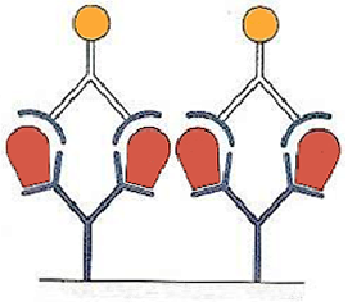

Figure 3.24 – Streptavidin (wall) bound biotin reacts with antibody (+ enzyme) and antigen ©[29]

The complex consisting of the two antibodies and the antigen is reminiscent of a sandwich and therefore, responsible for the name. The mouse monoclonal antibodies are specific for well defined regions in the amino acid chain of human erythropoietin. As the glycosylation is not necessary for detection also non-glycosylated EPO proteins can be measured and are used as calibrators in this kit.

After the incubation the wells are washed several times to remove the unbound antibodies and substances. Only the wall-bound components stay in the well. Horseradish peroxidase (HRP) is used as detection enzyme for the colour reaction. HRP reacts in presence of H_2O_2 with substrate molecules which are oxidised according to this reaction [30]. In the Alpco™ EPO EIA kit the substrate tetramethylbenzidine (TMB) is used, causing a blue coloured solution. After a defined incubation time, an acidic stopping solution is added to stop the enzymatic reaction and to turn the colour to yellow (Figure 3.25). The intensity of this colour, measured with a spectrophotometer, is directly proportional to the concentration of

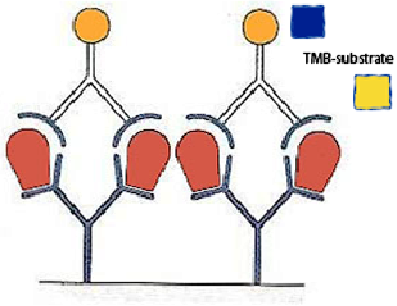

Figure 3.25 – Detection enzyme reacts with substrate to blue, yellow with stopping solution ©[29]

the enzyme and therefore, to the concentration of the antigen. This enables the quantification of protein in the calibrators, controls and samples.

3.13.2 EIA measurements

To correlate the measured values with the concentration the results obtained from the calibrators are used to generate a calibration diagram, absorbance *vs.* concentration, with a linear slope. This enables the quantitative interpretation of the values obtained from the samples [30].

For the measurement of the first experiments, the calibrators were applied two times into the wells of the EIA kit and their values and averaged, while the controls were measured only once. For each sample, 200 µL were taken directly into a well without dilution or concentration. The values [mU/mL] for the calibrators are defined and Table 3.3 shows the corresponding absorbance readings.

Table 3.3 – EPO EIA calibrator measurements form experiment 8

calibration curve	EPO value [mU/mL]	absorbance 450 nm	absorbance 405 nm
calibrator A	0.0	0.0641	0.0539
calibrator B	10.3	0.1528	0.1144
calibrator C	25.7	0.2069	0.1039
calibrator D	50.0	0.3292	0.1368
calibrator E	154.0	0.9415	0.3163
calibrator F	480.0	3.2779	1.0589

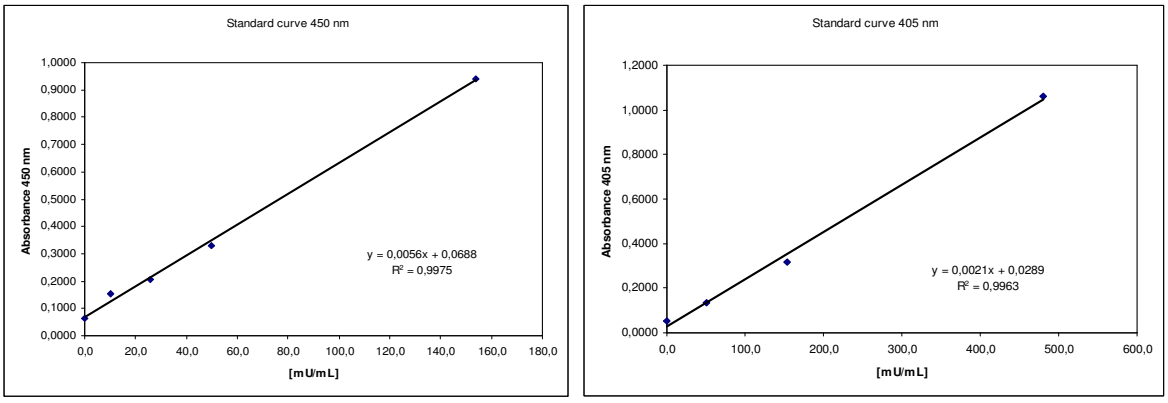

Figure 3.26 – EPO EIA calibration curves for 450 nm and 405 nm including linear equations

With these values, two calibration curves were constructed, one for λ = 450 nm values and one for λ = 405 nm values (Figure 3.26). The achieved linear equations with coefficients of determination were used first to calculate the controls and estimate the reliability of the calibration curves (Table 3.4).

Table 3.4 – EPO controls 1 and 2 from experiment 8

controls	EPO value [mU/mL]	absorbance 450 nm	absorbance 405 nm
EPO control 1 [14.2 – 23.5 mU/mL]	14.5	0.1498	0.0826
EPO control 2 [152 – 240 mU/mL]	180.0	1.2561	0.4070

While control 1 was calculated with the equation for λ = 450 nm, control 2 has been calculated with the equation for λ = 405 nm, since the absorbance at 450 nm surpasses the calibration value E. The values met the described range, therefore proving the suitability of the calibration curves.

Table 3.5 – Measured and calculated rhEPO values from experiment 8

samples	rhEPO value [mU/mL]	absorbance 450 nm	absorbance 405 nm
BNL-CL2 - pEPO 08.01 1h	0.0	0.0636	0.0538
BNL-CL2 - pEPO 08.02 2h	0.0	0.0736	0.0622
BNL-CL2 - pEPO 08.03 3h	3.5	0.0886	0.0692
BNL-CL2 - pEPO 08.04 4h	2.3	0.0817	0.0683
BNL-CL2 - pEPO 08.05 5h	2.1	0.0806	0.0655
BNL-CL2 - pEPO 08.06 6h	3.7	0.0893	0.0689
BNL-CL2 - pEPO 08.07 7h	1.5	0.0770	0.0637
BNL-CL2 - pEPO 08.08 8h	0.0	0.0711	0.0584
BNL-CL2 - pEPO 08.09 24h	6.3	0.1039	0.0935
BNL-CL2 - pEPO 08.10 26h	0.0	0.0741	0.0839
BNL-CL2 - pEPO 08.11 28h	1.4	0.0768	0.0627
BNL-CL2 - pEPO 08.12 30h	2.3	0.0816	0.0714
BNL-CL2 - pEPO 08.13 32h	2.1	0.0804	0.0652
BNL-CL2 - pEPO 08.14 48h	1.4	0.0767	0.0630
BNL-CL2 - pEPO 08.15 50h	1.7	0.0782	0.0646

Table 3.5 lists the measured sample values from experiment number 8, the first experiment to endure over a longer period of time. Most calculated rhEPO level values are above zero (zero is equal to below 1.2 mU/mL, which is the detection limit of the Alpco™ EPO EIA kit), but none of them extends calibrator B, which is the first designated value of rhEPO concentration. In order to prove rhEPO levels and even more changes within these levels, the absorbance had to be drastically increased.

To improve to measurable protein levels, the amount of each sample was set to 1 mL. With this volume, concentration of the EPO protein level should be possible. Trials utilizing a available Speed-Vac system to reduce the volume without losing proteins proved that vacuum drying is not suitable for rhEPO sample preparation. The measured protein levels were even lower than without additional treatment. The next step was a trial measurement with ultracentrifugation. A set of different volumes and sizes of Amicon Ultra Centrifugal Filters from Millipore™ was tested (Figure 3.27). The system consists of three parts: a filtrate collection tube, a low protein binding ultra filtration membrane filter and a concentrate collection tube. After evaluation of the results, the filter units with 0.5 mL volume and 10 kDa pore size were most suitable [31]. After making a passage with two times 0.5 mL for each sample, it is necessary to replenish the remaining 40 µL with 160 µL sterile, deionised water, since the sample volume for the Alpco™ EPO EIA kit is 200 µL. Despite this dilution, the protein concentration of EPO is increased fivefold.

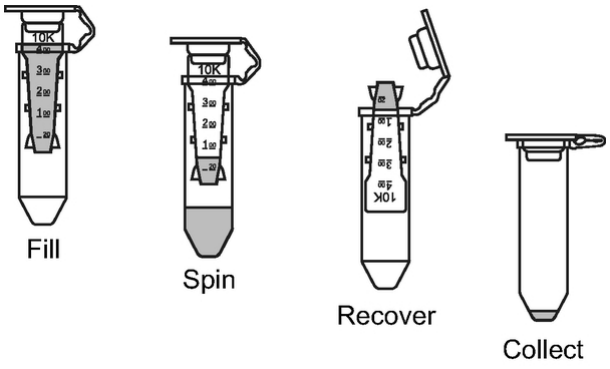

Figure 3.27 – Scheme of Amicon Ultra Centrifugal Filters

Table 3.6 – 3 Measured samples from experiment 19 without and with ultracentrifugation

samples	rhEPO value [mU/mL] without ultracentrifugation	rhEPO value [mU/mL] with ultracentrifugation
BNL-CL2 - pEPO 19.09 26h	0.0	7.9
BNL-CL2 - pEPO 19.13 32h	0.0	8.6
BNL-CL2 - pEPO 19.14 48h	0.0	10.0

As shown in Table 3.6, the comparison of some results from experiment 19 indicate the differences between samples with and without prior preparation. This was the evidence that concentrating the samples was moving the value levels into a reasonable range. Having verified these findings, all further samples have been concentrated utilizing Amicon Ultra-0.5 Centrifugal Filters before the rhEPO measurement to enable successful determination of level differences.

3.14 Well-established experimental standard operation procedures

Having ascertained and tested all necessary parts and optimised the order of the experimental setup, the coating for the slide channel, the number of BNL-CL.2 cells for ON adhesion and the procedure of the measurements, the next step was to establish standard operation procedures, to ensure comparable results. These procedures were a combination of well established cell biological and biotechnical methods and the necessary operations of the experimental setup.

3.14.1 Preparing a Ibidi™ µ-Slide $I^{0.4}$ Luer with adherent BNL-CL.2 cells

First the cell culture needed to be cultivated towards at least 80% confluence in a 75 cm^2 tissue culture flask. Having achieved the necessary density, the medium (DMEM containing 1% v/v Glu, 10% v/v FBS and 1% v/v P/S) was carefully removed from the tissue culture flask. 10 mL PBS (phosphate buffered saline – at room temperature) were applied and the tissue culture flask was pivoted to wash the cells (it had to be avoided to pipette the PBS directly onto the cells). Afterwards the PBS was also carefully removed and 1 mL trypsin was applied directly onto the cells. The tissue culture flask was then heated to 37°C and carefully tapped to detach the cells. The progress was controlled by phase-contrast microscopy. Having detached the cells, 5 mL of medium were applied, mixed with the cells and transferred into a 15 mL Falcon tube. For isolation of the cells, the Falcon tube was centrifuged for 5 minutes and 1,200 rcf at room temperature. Afterwards, the supernatant was carefully removed and 1 mL of medium at 37°C was used to suspend the cells again.

The cells had to be counted, to achieve the correct cell number of 3 x10^5 in 100 µL. Therefore, a 15 µL sample was taken from the suspended cell culture and the necessary volume to cover one side of a Neubauer counting chamber was applied. The consistent dispersion of the cells was controlled and the cells in the four large corner quadrants (4x4 smaller quadrates) were counted using a phase-contrast microscope. If the cell mass was too dense to be counted, the suspended cells were diluted 1:10 before applying them to the Neubauer counting chamber. The counted numbers of the four quadrants were summarized, divided by the factor 4 and multiplied by 10 to receive the number of cells per µL. After another multiplication by 100 the cell number per 100 µL was the result. Previous dilutions into account had to be taken into account.

The cell suspension was diluted to the concentration of 3 x 10^5 cells / 100 µL. Then 100 µL of the diluted suspension were carefully pipetted into the µ-Slide channel, avoiding bubbles. Afterwards each reservoir was filled with 60 µL of the medium and incubated overnight at 37°C and 5 % CO_2. The slide with attached cells was ready to be used for experiments in the next morning, after the cell condition was controlled by phase contrast microscope.

3.14.2 Starting an experiment

Assuming that the bioreactor was sterilized, it had to be placed within the laminar flow clean bench. Therefore, the whole front of the clean bench was opened, influencing the sterile interior. The tubing was set into position as described in Figure 3.16. All the sensor, water and air connections mentioned in Figure 3.17 were attached and the reservoirs for acid (0.5 M HCl) and base (0.5 M NaOH) control were checked, if they still contain enough solution. Afterwards the clean bench was closed and all surfaces are sterilized by UV radiation.

Having finished the sterilization, the temperature sensor was attached to the sampling system (Figure 3.11) under normal working conditions of the laminar flow clean bench. All remaining coverage was removed and the bioreactor control unit was connected to the water drain and the recording computer. Acid and base

supplies were connected and the exhaust air tube was submerged into disinfectant solution. The hose clamp was removed from the harvest tube and computer and control unit were activated.

The bioreactor jacket was filled with deionised water utilising manual controls of the circulation pump and the cooler at the bioreactor control unit. Sterile medium (DMEM containing 10% v/v FBS and 1% v/v P/S) was filled into a specially prepared tissue culture flask and loaded via the peristaltic pump, the connection valve and the feeding tube into the bioreactor. The sterile connection module at the feeding tube was closed, after having added 350 mL of medium to the 100 mL of deionised water already in the bioreactor. Next the fermentation was started with the necessary temperature (depending on the flow rate – see Table 3.1), a pH value of 7.2 ± 0.4 and the stirrer was set to 100 rpm. Next the water tap was opened carefully, achieving enough but not too much water pressure for deionised water supply. The compressed air flow was manually set to 20 mm at the bioreactor control unit and the peristaltic pump was started with the desired flow rate. This has to be done at least 6 hours in advance of an experiment, to polarize the oxygen sensor and temperate the medium and its surroundings.

To insert the Ibidi™ µ-Slide $I^{0.4}$ Luer (Figure 3.1), the flow was stopped and the connection tubes to the slide, right now directly joined by a small piece of tubing, were blocked by clamps in the direction of the flow. After removing the tube, the Luer connectors were inserted into the slide openings. The clamps were removed, again in order of the flow direction and the peristaltic pump was started again. First 5 minutes with a flow rate of 5 mL/min, followed by 5 minutes with 10 mL/min and then the flow rate was set to the desired intense. This “slow start” should prevent eventually present bubbles from damaging the cells right at the start.

3.14.3 Running an experiment

For sampling and taking digital microscope pictures, the peristaltic pump first had to be stopped. Then the three-way stop cock was set to connect from the bioreactor to the sampling tube (Figure 3.11). The first 0.5 µL were taken with the

still connected sterile one way syringe and were discarded. Having removed the holdup volume of the sampling system, the next 1 mL were taken with a new sterile one way syringe and filled into 1.5 mL microcentrifuge tube, which was labelled and frozen at -20°C. The syringe was again placed at the sampling system sterile filter to prevent dripping and the three-way stop cock was set back to the normal circuit.

Afterwards the extension of a microscope stage (Figure 3.12) was attached to the microscope. Digital pictures were taken from 3 positions of the slide channel (Figure 3.13). The positions should be the same during every measurement point using the engraved grid as help, as well as the basic settings for the microscope and the software.

Having finished the sampling, the extension was again placed within the laminar flow clean bench. The peristaltic pump was started for 1 minute at a flow rate of 5 mL/min, followed by 1 minute at 10 mL/min and finally the flow rate was set to the chosen value for the experiment.

3.14.4 Terminating an experiment

After finishing an experiment, the bioreactor and all parts that were in contact with the medium have to be autoclaved. The preparation for this sterilization started with rinsing the tubing with deionised water and closing the harvest tube with a clamp afterwards. Then the temperature of the bioreactor was set to 75°C for 3 hours, to pasteurize the contents of the reactor.

After the temperature was cooled down below 30°C, the calibration of the pH and oxygen sensor was necessary. For the pH sensor, standard calibration solutions for pH 7.00 and pH 4.01 were used. The oxygen sensor was calibrated utilizing 80 mL deionised water with roughly a teaspoonful of sodium sulfite (Na_2SO_3) to simulate an oxygen free environment (Na_2SO_3 binds the dissolved oxygen in the water). Afterwards the sensor was just put into the air for 100% oxygen level, as

suggested in the manual. When all calibrations were done, the bioreactor control unit and the recording computer were turned off.

The sterile filter of the sampling system was replaced and the temperature sensor was removed. The Luer connectors were disconnected from the slide and were joined again by the short piece of tubing. The tubes from the acid and base supplies were removed and the connectors were closed by linking them with another short tube. Then all connections between the control unit and the bioreactor were removed and the reactor with the external circuit was taken out of the laminar flow clean bench. Afterwards the clean bench was closed and all surfaces are sterilized by UV radiation.

The reactor was opened and the reactor vessel was first emptied, subsequently cleaned with disinfectant solution and deionised water. 100 mL deionised water were filled into the vessel, then the reactor was closed again. The water in the reactor jacket was reduced below the upper water connection and the sensor adapters as well as the temperature sensor opening and the sterile filter of the sampling system were covered with aluminium foil. Then the temperature sensor connector to the bioreactor control unit was first isolated with cotton and then also covered by aluminium foil. The same procedure applied to the whole harvest tube, while the air supply tube was closed with a clamp and the opening for the motor unit of the agitator was closed with the provided sealing. After having finished all preparations, the external circuit, the air supply tube and the temperature sensor connector cable were carefully wrapped around the bioreactor without making bends. Finally, some deionised water was added to the Pall™ Mini-Kleenpak filters (Figure 3.14). Just before autoclaving, the upper water connection was opened as well as the Mini-Kleenpak filter, which was not in line of the circuit. The whole setup was autoclaved for 20 minutes at 121°C and could be used for “Starting an experiment” again after having cooled down.

3.14.5 Erythropoietin measurement

The sample preparation for using the Amicon Ultra-0.5 Centrifugal Filter Devices increased the protein levels fivefold and eased the use of the Alpco™ EPO EIA kit. Therefore, all necessary filtrate collection tubes and filters devices were prepared and the samples were thawed. 0.5 mL of each sample was added to a filter and centrifuged for 20 minutes at 14,000 rcf (relative centrifugation force) and room temperature. The filtrate collection tubes were emptied and the filter devices were inserted upside down in the concentrate collection tubes. Next a centrifugation step for 2 minutes at 1,000 rcf was done and the filter devices were reinserted into the filtrate collection tubes. Another 0.5 mL of the same sample was added to each corresponding filter and centrifuged for 20 minutes at 14,000 rcf and room temperature. The step of emptying of the filtrate collection tubes was repeated. The filter devices were inserted upside down in the same concentrate collection tubes were the concentrate from the first run still remained. The samples were centrifuged again for 2 minutes at 1,000 rcf. Then 160 µL sterile distilled water was added to each sample to achieve 200 µL volume needed for an ELISA test.

The ELISA measurements were done with an Alpco™ EPO EIA kit. The procedure was performed as it is described in the enclosed instruction. The first steps were the preparation of the kit itself, therefore the non-zero calibrators and the controls were reconstituted with 2 mL deionised water, the zero calibrator was filled with 4 mL deionised water. Finally the 30 mL washing concentrate was diluted with 570 mL deionised water.

For the measurement itself, a sufficient number of strips with streptavidin coated wells were placed in the holder. 200 µL of calibrators, controls and samples were pipetted into the wells. The calibrators were assayed twice to ensure a reliable calibration curve for calculating the EPO values. Of course the content of each well needed to be noted thoroughly. Then 25 µL of reagent 1, the biotinylated antibody, was added to each well, followed by 25 µL of reagent 2, the enzyme labelled antibody. All four sides of the holder were taped against a rigid object (e.g., a pen) to mix the reagents and the sample, calibrator or control. Spillage needed to be avoided. The plate was placed on an orbital shaker and covered with

aluminium foil to prevent light exposure. The shaker was set to 170 rpm and the plate was shaken for two hours at room temperature.

Then the washing step was carried out, were the fluid was removed, and each well was washed by adding and removing of 350 µL washing puffer for five times. 150 µL of reagent B, the TMB substrate solution, were added and the tapping was repeated as already described. The plate was again covered with aluminium foil to avoid light exposure and placed on an orbital shaker with 170 rpm. This time the plate was shaken for 30 minutes at room temperature. Afterwards, 100 µL stopping solution was transferred into each well and the tapping was repeated. The absorption measurement at 450 nm and 405 nm with a micro plate reader had to be conducted within ten minutes after addition of the stopping solution. The wave length of 405 nm enabled the quantification higher concentrations of rhEPO [32].

3.15 Cell numbers – digital area calculation

The experimental setup was working well, allowing experiments for over 48 hours with continuous sampling and digital microscopy survey. The protein levels of rhEPO were detectable in nearly all samples. However, to make these values comparable, the number of cells or at least the areas still covered had to be analyzed and included. Due to the large number of digital pictures, a fairly automated system would be advisable.

The first decision was to use the analyzing software ImageJ (http://rsbweb.nih.gov/ij/). This public domain program version 1.42q is based on java and enables detailed picture analysis. To calculate the cell covered area, a 32-bit greyscale digital microscope picture was converted in an 8-bit greyscale image. Then the background was “subtracted” resulting in elimination of bright areas, sharpening of edges and cleaning up of single pixels. Enhancing the contrast and normalizing the pixels further prepared the image, followed by a conversion into a binary black and white picture. Two times dilating the result fitted the cell covered areas (black) to the same actual size as observed in the

unmodified picture. Then a rectangle was drawn to avoid the edges of the channel within the analyzed area (Figure 3.28). The value represented the percentage of covered areas compared to the whole area (black and white within the rectangle).

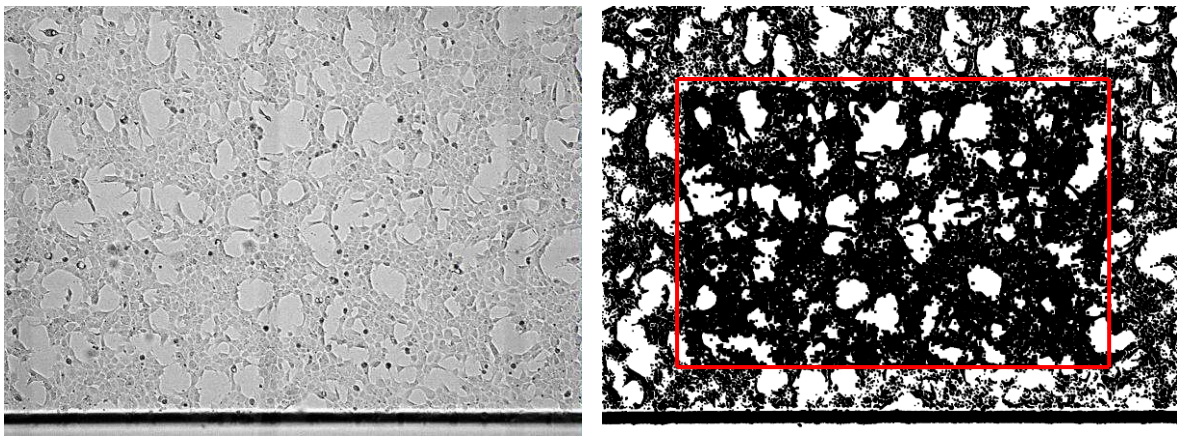

Figure 3.28 – Digital and analyzed image (area with red perimeter) from experiment 17 (5 h)

To ease the use and velocity of analyzing the microscope pictures, a small script for ImageJ was made. Since one experiment on average consisted of around 15 samples with 3 digital images for each sample, a large quantity of photographic data had to be examined. Using this script provided the covered area data in minutes for a whole experiment, compared to hours of work, if this was done manually. Furthermore, by exactly assigning the rectangle through pixel coordinates, all measurements were based upon exactly the same area.

4 Summary

The first consideration for developing a process that enables the determination of the influence of hydrodynamical forces on mammalian cell cultures is the identification of those parameters influencing the desired results. In such cases, where of a single force interaction should be measured, all other common parameters like temperature, pH-value, oxygen level, nutrients, metabolites, etc., are strongly influencing the viability and production rate of the mammalian cells. In order to maintain this complex behaviour of mammalian cell lines, while exposing the cells to hydrodynamical forces, the solutions available on the market are limited.

Complex systems for example lack the possibility to continuously take small samples (without losing monoseptical conditions) and to examine the morphology of the cells (by microscopy), because they are closed in order to avoid microbial contamination. Simple systems on the other hand are not feasible to keep parameters like pH-value, temperature or oxygen level stable, especially not for extended time periods. A process combining all features and therefore allowing experiments with exactly defined parameters over a longer period of time, while keeping sterile and allowing sampling and microscopy is not yet available.

Therefore, a measuring process was designed, built up, tested and used that enables the *in vitro* examination of adherent mammalian cell cultures. The complete process setup consists of the following important parts to achieve all desired features:

- The process setup is constructed around a channel in a microscope slide, where adherent cells could be seed and examined under a microscope.
- A microscope, preferably with digital imaging for storage and processing of the cell images, enables visual control of cell morphology.
- A peristaltic pump agitates the medium at an exactly defined flow rate through the whole circuit.

- A bioreactor, providing control of temperature, pH-value, oxygen level, nutrients and mixing is included. It needs at least three external circuit points available, two for inserting / recycling the medium and one with a feeding tube to draw medium out of the reactor.
- The whole setup fits into a sterile workbench, improving sterility while handling the process setup during experiments.
- Due to the need for a system to draw small samples anytime, without endangering the sterility of the whole process setup, a prototype was designed and built. It includes a temperature sensor, to ensure cell viability and protein stability outside the bioreactor.
- The slide channel needs a fixation, avoiding instability through movement from tubes and flow, while allowing the exact use of a microscope. Also an object slide with an engraved grid, to be placed beneath the slide of interest, is advisable. This enables the counting of cells or measurement of free and cell covered areas. For this another prototype was designed and built.
- A so called "bubble trap" is incorporated, removing bubbles from the circuit, which would interfere with the adherent cells.
- A two way filter system is included, which is necessary to prevent detached cells from re-entering the circuit and interfering with the whole experiment.

Several single parts or features of this measuring process are quite common. For example bioreactors or digital microscopy, even microscope slide with channels. However, only the unique combination of all these parts provides a process setup, where a single parameter can be measured, while all other influences are kept at a needed or pre-defined state.

After extended testing of single parts, the whole system and measurements of the cell secreted rhEPO, standard operation procedures for the experimental process have been defined, to ensure comparability of conducted experiments. The ELISA kit procedure was also adapted, increasing the concentration of rhEPO utilizing ultracentrifugation filters. Finally digital image processing was refined, automated and therefore accelerated.

This experimental process is now capable of examining a designated parameter (physical, chemical or pharmacological) and its influence on cell growth, morphology, protein production etc., while all other influencing parameters are kept at a stable state. It provides this stable environment and sterility, while enabling sampling and (digital) microscopy at the same time and desired frequency. For example changes on protein secretion and morphology of an adherent cell culture can be examined under low temperature, while pH-value, oxygen level, nutrient supply and metabolite removal are maintained by the measuring process.

This developed process permits a new approach to the examination of adherent cell cultures. The possible scope of application is wider than that of any other system. Additionally new examinations can be made, like continuous live imaging of cell cultures under varying temperatures for extended time periods [(33)].

References

1. Croughan, M.S. and Hu, W.S.; From microcarriers to hydrodynamics: Introducing engineering science into animal cell culture; *Biotechnology and Bioengineering* (2006) 95, 220-225.

2. Mohan, C.; Kim, Y.G.; Koo, J.; and Lee, G.M.; Assessment of cell engineering strategies for improved therapeutic protein production in CHO cells; *Biotechnol. J.* (2008) 3, 624-630.

3. Sethuraman, N. and Stadheim, T.A.; Challenges in therapeutic glycoprotein production; *Current Opinion in Biotechnology* (2006) 17, 341-346.

4. Nienow, A.W.; Reactor engineering in large scale animal cell culture; *Cytotechnology* (2006) 50, 9-33.

5. Meier, S.J.; Hatton, T.A.; and Wang, D.I.C.; Cell death from bursting bubbles: Role of cell attachment to rising bubbles in sparged reactors; *Biotechnology and Bioengineering* (1999) 62, 468-478.

6. Murhammer, D.W. and Goochee, C.F.; Sparged animal-cell bioreactors - Mechanism of cell-damage and pluronic F-68 protection; *Biotechnology Progress* (1990) 6, 391-397.

7. Mollet, M.; Ma, N.N.; Zhao, Y.; Brodkey, R.; Taticek, R.; and Chalmers, J.J.; Bioprocess equipment: Characterization of energy dissipation rate and its potential to damage cells; *Biotechnology Progress* (2004) 20, 1437-1448.

8. Senger, R.S. and Karim, M.N.; Effect of shear stress on intrinsic CHO culture state and glycosylation of recombinant tissue-type plasminogen activator protein; *Biotechnology Progress* (2003) 19, 1199-1209.

9. Godoy-Silva, R.; Mollet, M.; and Chalmers, J.J.; Evaluation of the Effect of Chronic Hydrodynamical Stresses on Cultures of Suspensed CHO-6E6 Cells; *Biotechnology and Bioengineering* (2009) 102, 1119-1130.

10. Mollet, M.; Godoy-Silva, R.; Berdugo, C.; and Chalmers, J.J.; Computer Simulations of the energy dissipation rate in a fluorescence-activated cell sorter: Implications to cells; *Biotechnology and Bioengineering* (2008) 100, 260-272.

11. Hutchinson, N.; Bingham, N.; Murrell, N.; Farid, S.; and Hoare, M.; Shear stress analysis of mammalian cell suspensions for prediction of industrial centrifugation and its verification; *Biotechnology and Bioengineering* (2006) 95, 483-491.

12. Xing, Z.Z.; Kenty, B.N.; Li, Z.J.; and Lee, S.S.; Scale-Up Analysis for a CHO Cell Culture Process in Large-Scale Bioreactors; *Biotechnology and Bioengineering* (2009) 103, 733-746.

13. Motobu, M.; Wang, P.C.; and Matsumura, M.; Effect of shear stress on recombinant Chinese hamster ovary cells; *Journal of Fermentation and Bioengineering* (1998) 85, 190-195.

14. Mollet, M.; Godoy-Silva, R.; Berdugo, C.; and Chalmers, J.J.; Acute hydrodynamic forces and apoptosis: A complex question; *Biotechnology and Bioengineering* (2007) 98, 772-788.

15. Schumann, W.; Henzler, H.-J.; Yim, S.S.; Shamlou, P.A.; Kretzmer, G.; Kieran, P.M.; Malone, D.M.; and MacLoughlin, P.F.; Influence of Stress on Cell Growth and Product Formation; (2003)

16. Tanzeglock, T.; Soos, M.; Stephanopoulos, G.; and Morbidelli, M.; Induction of Mammalian Cell Death by Simple Shear and Extensional Flows; *Biotechnology and Bioengineering* (2009) 104, 360-370.

17. ibidi GmbH; Flow Chamber; (2003) PCT/EP02/10770,

18. Kutschera, C.; Muhr, A.; and Khinast, J.; Vorrichtung zur Entnahme von Proben aus einem Reaktor- oder Kesselsystem, insbesondere Bioreaktoren oder Rührkessel; (2010) CH 29.12.09, 01988/09.

19. Muhr, A.; Richter, U.; Kutschera, C.; and Khinast, J.; Objekthalterung für Lichtmikroskop; (2010) DE G02B 21/26 (2006.01), DE 20 2009 017 583 U1.

20. Narhi, L.O.; Arakawa, T.; Aoki, K.H.; Elmore, R.; Rohde, M.F.; Boone, T.; and Strickland, T.W.; The Effect of Carbohydrate on the Structure and Stability of Erythropoietin; *Journal of Biological Chemistry* (1991) 266, 23022-23026.

21. ibidi GmbH; micro-Slides I Luer; (2008)

22. Mochizuki, T.; Lemmink, H.H.; Mariyama, M.; Antignac, C.; Gubler, M.C.; Pirson, Y.; Verellendumoulin, C.; Chan, B.; Schroder, C.H.; Smeets, H.J.; and Reeders, S.T.; Identification of Mutations in the Alpha-3(Iv) and Alpha-4(Iv) Collagen Genes in Autosomal Recessive Alport Syndrome; *Nature Genetics* (1994) 8, 77-82.

23. Petitclerc, E.; Boutaud, A.; Prestayko, A.; Xu, J.S.; Sado, Y.; Ninomiya, Y.; Sarras, M.P.; Hudson, B.G.; and Brooks, P.C.; New functions for non-collagenous domains of human collagen type IV - Novel integrin ligands inhibiting angiogenesis and tumor growth in vivo; *Journal of Biological Chemistry* (2000) 275, 8051-8061.

24. Pankov, R. and Yamada, K.M.; Fibronectin at a glance; *Journal of Cell Science* (2002) 115, 3861-3863.

25. Arnold, L.J.; Dagan, A.; Gutheil, J.; and Kaplan, N.O.; Antineoplastic activity of poly(L-lysine) with some ascites tumor cells; *Proceedings of the National Academy of Sciences of the United States of America* (1979) 76, 3246-3250.

26. Goto, M.; Murakami, A.; Akai, K.; Kawanishi, G.; Ueda, M.; Chiba, H.; and Sasaki, R.; Characterization and use of monoclonal-antibodies directed against human erythropoietin that recognize different antigenic determinants; *Blood* (1989) 74, 1415-1423.

27. van Weemen, B.K.; The Rise of Eia/Elisa; *Clinical Chemistry* (2005) 51, 2226-2226.

28. Lequin, R.M.; Enzyme Immunoassay (EIA)/Enzyme-Linked Immunosorbent Assay (ELISA); *Clinical Chemistry* (2005) 51, 2415-2418.

29. Kaldenhoff, R. and Richter, G.; Praktische Biochemie; (2003)

30. Muhr, A.; Humane mesenchymale Stammzellen in der Frakturheilung - Eine Materialfrage?; (2006)

31. Millipore; Amicon Ultra-0.5 Centrifugal Filter Devices; (2009)

32. ALPCO Diagnostics; Specific quantitative assay for the determination of erythropoietin in serum; (2005)

33. Muhr, A.; Kutschera, C.; and Khinast, J.; Steriles invitro Messverfahren für adhärente Säugetierzellen; (2011) A 266/2011, pending.

Figures

Tables

Part C

Impact of hydrodynamic stress on the protein production of an adherent mammalian cell line

1 Goals and Motivation

To improve the large scale production of recombinant proteins such as erythropoietin (EPO) or monoclonal antibodies, a significant body of work has already been done. However, there are still a lot of parameters to be identified, especially concerning mammalian cells. The understanding of influences on mammalian cells in stirred large scale bioreactors would moreover enable process design prior to the production instead of trial and error during the process. This could further explain differences in yield on the laboratory scale and on the production scale and lead to amendments in scale-up processes. Only this knowledge would allow “quality by design” in biopharmaceutical production processes.

For this an eligible cell line, determined as BNL-CL.2 cells secreting recombinant human EPO, has been successfully constructed in Part A of this thesis. This cell line was applied as the basis of the experimental work. In principle, mammalian cells are necessary for correct glycosylation of the EPO protein, therefore ensuring its activity as well as stability [(1)]. The chosen mouse liver epithelial cells seemed especially appropriate, since the liver is the main source of EPO during mammalian fetal stage, [(2)] and contain all necessary mechanisms for full bioactivity (glycosylation). The general detection of rhEPO was also found to be very easy, utilizing an Enzyme ImmunoAssay (EIA).

In Part B of the thesis, a suitable experimental process setup was designed, capable of keeping temperature, pH-value and oxygen level at optimal values while enabling constant medium flow rate over the adherent cells, continuous sampling of low volumes of the medium, digital microscopy of the cells and sterility of the whole system over an adequate period of time. To cope with all these demands, commercially available parts of the complete setup (bioreactor, laminar flow clean bench, process pump and others) had to be combined with self designed and assembled prototypes (sampling system [(2)] and microscope dish extension [(3)]) in a new and unique way, not yet reported in literature. Extensive test

runs ensured that the process setup facilitated experiments within the required ranges and limits.

After thorough testing and analysis of the first experiments, a set of working protocols has been established and some methods have been refined to suit the demands. This was enabling the investigation, whether hydrodynamic forces have an impact on the protein production of attached cells. And, if there is an impact, which is expected, what would be the level of force that stops this production? Answers to this question would lead to profound knowledge about avoiding certain EDR levels for the future development of scale-up processes.

With the experience obtained from the first experiments, the aim was set for EDR ranges from 1.56×10^3 (10 mL/min flow rate) up to 1.41×10^4 (30 mL/min flow rate). These EDR ranges are common as average forces in typical large-scale bioreactors with volumes of 20,000 L [(4)]. However the change of production of recombinant proteins has also been reported to be very difficult to measure in experimental setups [(5)] due to the low concentration. But, as already stated in Part B, the specified experimental process setup is capable of detecting very low amounts of rhEPO.

This final part of the thesis deals with experiments using all designed parts and obtained knowledge from the previous chapters. The full capabilities of the setup and measurement methods were used to create unique data about the production behaviour of adherent mammalian cells under hydrodynamic stress. These data have been thoroughly analyzed and provided new insights regarding the influencing factors and their impact on large scale protein production. Furthermore, previously publicized EDR limits of 6.4×10^2 [W/m^3] already drastically reducing productivity of adherent mammalian cells [(6)] have been surpassed.

2 Scientific Background

Mammalian cells are necessary for the production of biologically active recombinant proteins. The whole biopharmaceutical sector is one of the fastest developing and growing industrial fields [7]. The production methods however are still the same as for fermentations – large scale bioreactors, where the settings from the laboratory scale are applied and then fitted to meet the requirements [6]. One factor is agitation, either by stirrers or bubble columns, which has to be done with higher forces in large scale reactors. Bubbles are known for quite some time to attract cells at the gas / liquid interface [8] and disrupt them, when the bubbles are bursting [9,10]. While investigations have been conducted regarding general particle stress in reactors [8] or short time stress exposure [11], the influence of continuous hydrodynamic forces towards cells, especially mammalian cells, lacks profound scientific knowledge [12].

The reasons for mechanical damage of cells in a reactor are the shear forces, the collision of microcarriers with themselves and with turbulent micro eddies [13], as well as the already mentioned bubble bursts. While collisions and bursts are well explained and understood, hydrodynamic long-term influence needs to be investigated. Starting with a basic introduction, a simple shear force causes thin parallel plates to slide over each other, as for example in a pack of cards. Shear can also occur in other geometries, e.g., in planar and rotational systems (Figure 2.1).

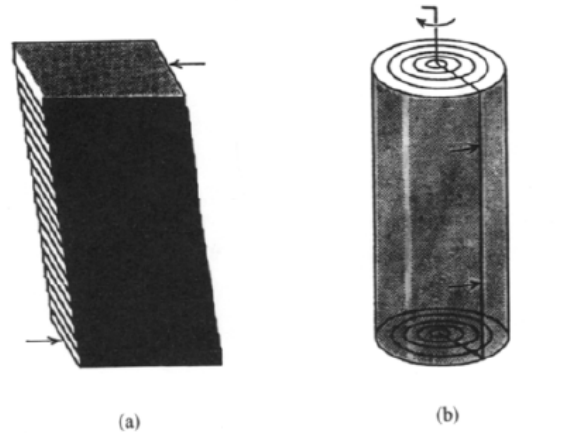

Figure 2.1 – Schema of planar (a) and rotational (b) systems containing shear forces

The shear force causes deformation, which is essentially a change of the relative position of neighbouring elements. In a bioreactor, shear force must be applied via impellers or sparging to produce fluid flow, which is necessary for sufficient distribution of nutrients, temperature and oxygen.

The mixing of liquids is the result of velocity gradients (shear rates) within the agitated system. The velocity gradients existing between the two material streams of fluid are defined as the shear rate γ [1/s] and is expressed as (1)

$$\gamma = \frac{d\upsilon_x}{dy} \quad (1)$$

where υ_x is the velocity in the x-direction and γ is perpendicular to x. The shear rate is directly proportional to the shear stress τ [Pa] and is given by (2)

$$\tau = -\mu\gamma \quad (2)$$

where μ is the viscosity of the fluid. These equations are applicable for Newtonian fluids, such as water (main component of cell culture media) with constant μ. For non-Newtonian fluids, such as suspensions and dispersions, μ depends on the shear rate [17].

An alternative to the shear stress term is the use of the local energy dissipation rate (EDR), first suggested by Bluestein and Mockros in 1969 [14]. This energy dissipation rate is a scalar value with units of power per unit of volume, [W/m^3], which represents the rate of work that is done on a fluid element. It has been successfully used as parameter to characterize and predict cell damage to some extent [15]. The range of shear forces found in various bioprocess environments deviate between an EDR of 10^1 to 10^5 W/m^3 [12]. EDR has been used extensively in literature during the last years. Due to comparability, it was also used to describe the force upon the cells in this thesis.

With the geometry of the Ibidi™ µ-Slide I$^{0.4}$ Luer described in Part B (page 47) and a laminar flow of a Newtonian fluid (which cell culture media are regarded to be), EDR ranges from approximately 1.5 x 10^3 up to 3.5 x 10^5 could be used to stress cells with the experimental setup.

3 Experimental Work

3.1 Data analysis and processing

Prior to the description of the different sets of experiments and their results, the question how to process the acquired data had to be resolved. As described in Part B of this thesis, the experimental process setup allowed us to obtain the following information for each measurement point:

- The concentration of rhEPO in milli units per millilitre [mU/mL], measured by ELISA tests.
- The settings of the bioprocess equipment, logged by a computer.
- The set flow rate within the Ibidi™ µ-Slide $I^{0.4}$ Luer.
- 3 digital microscopy pictures from the same 3 locations in the slide as the measurement points before and afterwards.

The settings for the equipment already had been tested and the logs were a control to prevent unexpected behaviour due to wrong temperature, pH-value or a stuck stirrer. The flow rate itself was used to classify the experiments and calculate the corresponding EDR values. The concentration was mathematically processed as well as the digital microscopy pictures had to be analyzed and taken into account.

3.1.1 Recombinant human erythropoietin concentration

The concentration of rhEPO was converted into [pg/mL] to enable further calculations and comparison of the acquired data. In order to enable this conversion, information from literature was used, reporting the activity of rhEPO with approximately 200,000 units per milligram [U/mg] [16,17]. This would result in 1 mU being equivalent to 5×10^{-9} mg or simplified in 1 mU/mL equivalent to 5 pg/mL. Therefore, the first step for data calculations was to multiply the values obtained

from the ELISA measurements by 5. However, since most of the values were also divided by 5, because of the concentration with the Amicon Ultra Centrifugal Filters from Millipore™, the numbers remained the same as in mU/mL.

3.1.2 Recombinant human erythropoietin half-life

The results from the previous paragraph were the concentrations of rhEPO in the medium at the measurement points. Since the enzyme rhEPO has a rather short half-life, the protein production must have been higher to compensate this loss. With additional information from literature about the half-life of EPO from mammalians [17], the half-life of EPO was averaged to 2.2 hours.

After transforming the equation $half-life = \frac{\ln 2}{k}$, the elimination constant k was calculated (0.32 [h^{-1}]). Having determined k and knowing and the concentration at point zero (c_0), the half-life reduction could be calculated for every measurement point (c_t) at the corresponding time (t) (3):

$$c_{(t)} = c_0 * e^{-kt} \qquad (3)$$

This calculation has been done and added to the measured value for every measurement point (except the starting measurement of each experiment), resulting in increased values but taking rhEPO degradation into account. The calculations were always done with from the concentration of the previous measurement point as c_0.

3.1.3 Recombinant human erythropoietin release from burst cells

After the analysis of the digital microscope pictures was performed as described in Part B (page 77), information about the reduction of cell covered area and therefore the loss of cells was obtained. But since the production was measured in overall concentration, this information could not be used directly. Having measured

the amount of rhEPO in the cytoplasm fraction of the BNL-CL.2 cells in Part A (page 35), the average protein level in a cell was determined. The mean value of rhEPO in the cytoplasm of 5 x 10^6 cells was ~ 29.9 mU/mL or 149.5 pg/mL, so a single cell contains 3 x 10^{-5} pg/mL.

This information combined with the change of the cell covered area from measurement point to measurement point and the value of 3 x 10^5 BNL-CL.2 cells as confluent layer in the Ibidi™ µ-Slide $I^{0.4}$ Luer (Part B) allowed to take the amount of rhEPO released from burst cells into account.

First of all, apoptosis is frequent in detached cells [18]. Here, these cells would not proliferate or produce proteins elsewhere in the experimental system. The filters, which were implemented in the system, contained low protein binding membranes with 0.2 µm pore size. This should enable the rhEPO proteins to pass the filter, while preventing detached cells from circulating the whole system. To ensure the assumption that these cells would burst at the filter membrane, the membranes were removed, possible cells were lysed and the solution was analyzed for rhEPO. The results showed no detectable amounts of rhEPO.

To assure a realistic trend of the rhEPO concentration graphs, the rhEPO from burst cells was removed from each measurement point. In order to do so, the percentage of remaining cells was removed from 100%. Assuming that 100% were approximately 3 x 10^5 cells and a single cell contained about 3 x 10^{-5} pg/mL rhEPO, it was possible to calculate the amount of rhEPO contained in the detached cells. This calculation was done from each measurement point to measurement point and the conclusion was subtracted from the calculated rhEPO values. By this step, the influence of bursting BNL-CL.2 cells releasing rhEPO on the progression of the protein production was removed from the final data.

3.1.4 Exemplary calculation

To illustrate the paragraphs above, an exemplary calculation for experiment 32 will be shown. The BNL-CL.2 cells after 24 hours had an average density of 65.53% according to the automatic determination explained in Part B (page 77). The measured rhEPO value was 3.41 mU/mL, already divided by 5 to remove the concentration increase from the Amicon Ultra-0.5 Centrifugal Filters from Millipore™.

First the concentration of the rhEPO was converted to [pg/mL], resulting in 17.05 pg/mL. The half-life degradation was calculated, referring to the concentration from the measurement point after 22 hours (12.95 pg/mL):

$$x = 12.95\ [c_0] - \underbrace{(12.95\ [c_0] * 2.71828182845904\ [e]^{-0.315\ [k]\ *\ 2\ [t]})}_{[c_t]}$$

Having combined the calculation of c_t and the deduction from c_0, the value of rhEPO degrading in these 2 hours was the result x or 6.05 pg/mL in numbers. This value was added to the converted concentration, representing the real production, being far grater than the half-life. So far, a result of 23.1 pg/mL rhEPO has been obtained.

However, to take the rhEPO from burst cells into account, the difference of the cell density was used. Therefore the percentage remaining after 24 hours was subtracted from the cell covered area at the measurement at 22 hours. With this percentage of detached cells, the number of cells which would cover 100% of the area and the cytoplasm content of rhEPO in a single cell, the following calculation was made:

$$x = \overbrace{((67.53 - 65.53) / 100)}^{\text{[area percentage of detached cells]}} * 300{,}000\ \text{[cell number at 100\% cell density]} * 2.9858 \times 10^{-5}\ \text{[pg/mL rhEPO within a single cell]}$$

For this measurement point, x equals 0.18 pg/mL rhEPO wich had to be subtracted from 23.1 pg/mL rhEPO. The step was included, because this circulating rhEPO was not secreted from living cells but the content of burst cells, which were not be productive anymore. Therefore this would create a logical error in the analysis of the calculated data. The final result for the production of rhEPO at experiment 32 after 24 hours was a concentration of 22.92 pg/mL rhEPO.

These calculations were conducted for every measurement, except the start points of the experiments. The starting measurements lacked concentrations and density changes from previous points and were therefore taken “as measured”. For better comparison each calculated graph is displayed in comparison with the measured values. The standard deviations for those graphs are depicted and were calculated using the "biased" or "n" method with the formula (4):

$$\sqrt{\frac{\sum (x-\bar{x})^2}{n}} \tag{4}$$

3.1.5 Production rate of recombinant human erythropoietin

The achieved results so far depict the concentration of rhEPO from measurements and the mathematically obtained amounts that “should have been” measured, if no half-life degradation or cell burst would occur. A further step was the calculation of the production rate of rhEPO. The assumption was to integrate the half-life and the loss of cell material, therefore resulting in a production rate for a fully cell covered slide channel with no rhEPO loss due to degradation. The calculations were based on measured mean values of the rhEPO concentration [pg/mL] and mean values of cell coverage [%]. The production rate was derived from the following formula (5):

$$V * \frac{dc}{dt} = r * A_{(t)} - k * c_{(t)} * V \tag{5}$$

The working volume (V) of 450 mL was the same for all experiments, as mentioned in Part B (page 73). The concentration of rhEPO $c_{(t)}$ was measured and the half-life elimination constant (k) has already been explained in chapter 3.1.2 above. The cell covered area $A_{(t)}$ consisted of the 250 mm^2 area (A) of the slide channel and the percentage of cell covered area (f): $A_{(t)} = A * f$ The graphs in Figure 3.1 shows a brief summary of the available cell density data. All data are provided in chapter 5.

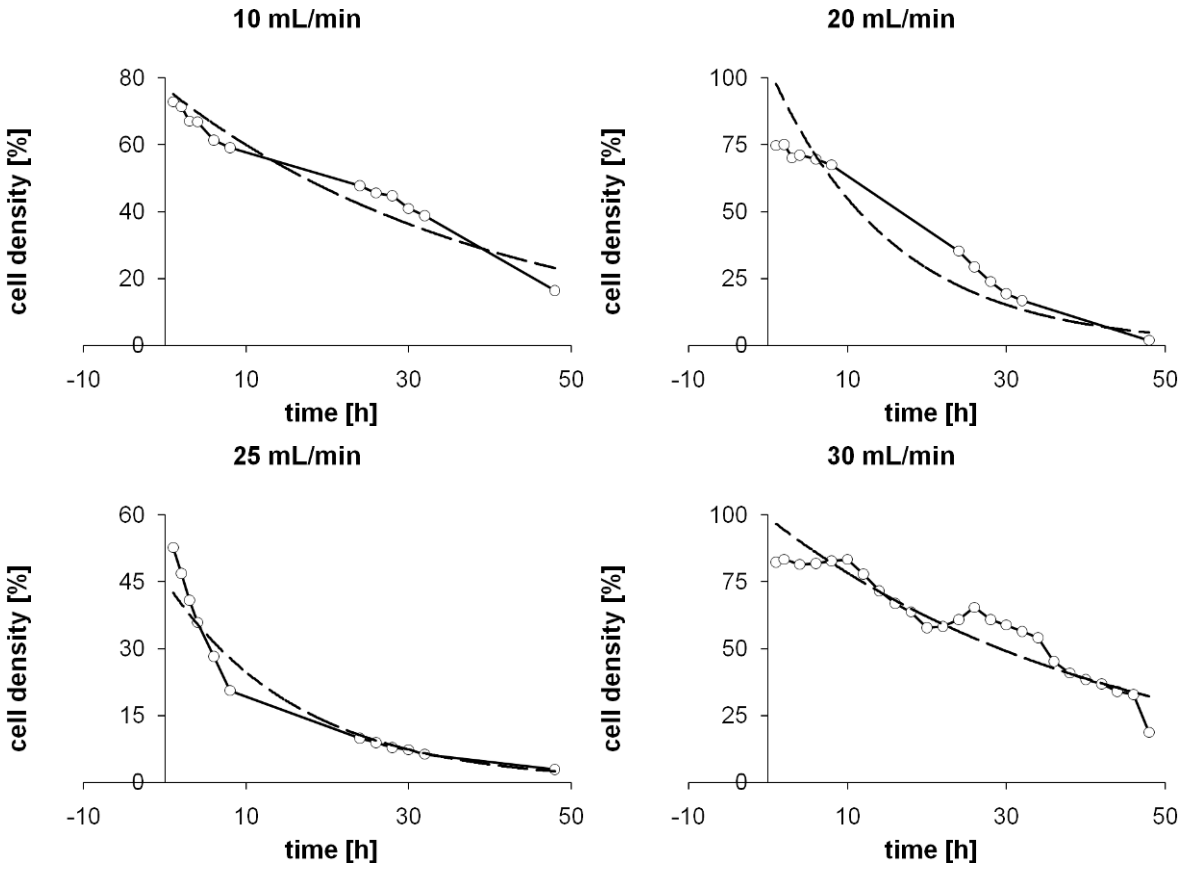

Figure 3.1 – cell density [%] *vs* time [h] for each flow rate

The last missing term to express the production rate (r) was $(\frac{dc}{dt})$. Since the time steps were not equal, the slope had to be calculated as a parabola. Three equations were derived from the basic formula (6):

$$y = a * x^2 + b * x + c \qquad (6)$$

where x is the time of the measurement [h] and y is the concentration [pg/mL].

$$y_{i-1} = a * x_{i-1}^2 + b * x_{i-1} + c \quad (7)$$

$$y_i = a * x_i^2 + b * x_i + c \quad (8)$$

$$y_{i+1} = a * x_{i+1}^2 + b * x_{i+1} + c \quad (9)$$

Equation (7) defines the measurement point prior to the calculation point, while equation (9) describes the measurement point after this point. The equation (8) describes the time x_i, where the slope is calculated. Equation (10) was derived from combining the three previous equations into a function, which could be used for each measured value:

$$\int_{x_i} \frac{dy}{dx} = 2 * a * x_i + b \quad (10)$$

With $a = \frac{\frac{y_{i+1} - y_i}{x_{i+1} - x_i} - \frac{y_i - y_{i-1}}{x_i - x_{i-1}}}{x_{i+1} - x_{i-1}}$ and $b = \frac{y_i - y_{i-1}}{x_i - x_{i-1}} - \frac{x_i + x_{i-1}}{x_{i+1} - x_{i-1}} * (\frac{y_{i+1} - y_i}{x_{i+1} - x_i} - \frac{y_i - y_{i-1}}{x_i - x_{i-1}})$.

The mathematical exceptions were the first and the last calculation points of an experiment. In these cases a and b were both used either from the following measurement point or from the prior measurement point.

Through the expression and calculation of the necessary variables, the production rate r [pg/mm^{2}h] can be calculated with equation (11):

$$r = \frac{V * \frac{dc}{dt} + k * c_{(t)} * V}{A_{(t)}} \quad (11)$$

3.2 Flow of 10 mL/min respectively EDR 1.56 x 10^3 [W/m^3] for 48 h

The experimental runs following the experiments described in Part B were continuously numbered. Therefore, the first experiment including a full working process setup as well as defined operational and measurement procedures was experiment 18. The raw data were achieved with the experiments 18, 19, 20, 21, 22, 29 and 30. While 18, 19, 20, 21 and 22 were done in a row, the experiments 29 and 30 followed later and were used to fill some data gaps resulting from different sampling times and a mechanical stirrer failure resulting in a stop of mixing after 28 hours at experiment 29. The flow rate was set to examine the influence of a rather slow flow of 10 mL/min or in other terms, an EDR of 1.56 x 10^3 W/m^3. All experiments were conducted with BNL-CL.2 cells secreting rhEPO. These cells were seeded overnight in a collagen IV coated Ibidi™ µ-Slide $I^{0.4}$ Luer. Moreover, the process parameters at the bioreactor for all these experiments were set to a temperature of 47°C ± 0.5°C, a pH-value of 7.4 ± 0.4 and 100 rpm (rotations per minute) for the stirrer.

Since the whole external circuit in the working setup acts as cooler, the temperature in the bioreactor has to be higher than 37°C. For the flow rate of 10 mL/min, the temperature should be set above 51°C, as was ascertained by previous tests without cells. However, it was not set that high in order to prevent the EPO proteins from degradation, even though they are reported to be temperature-stable up to at least 55°C with the correct glycosylation [19]. The loss of functional rhEPO deemed a more serious risk then a marginal lower temperature. Especially since 35°C are not as low as a mild hypothermia and lower temperatures are even reported to possibly increase protein production for certain cell lines these experiments were conducted at this temperature [20]. The tolerance had to be set to 0.5°C in order to prevent continuous alternation of heating and cooling. The same applies to the tolerance of the physiological pH-value and the addition of acid or base droplets. The rpm setting of the stirrer is an empirical value from the preliminary experiments, composed of sufficient mixing and reduced foaming of the medium.

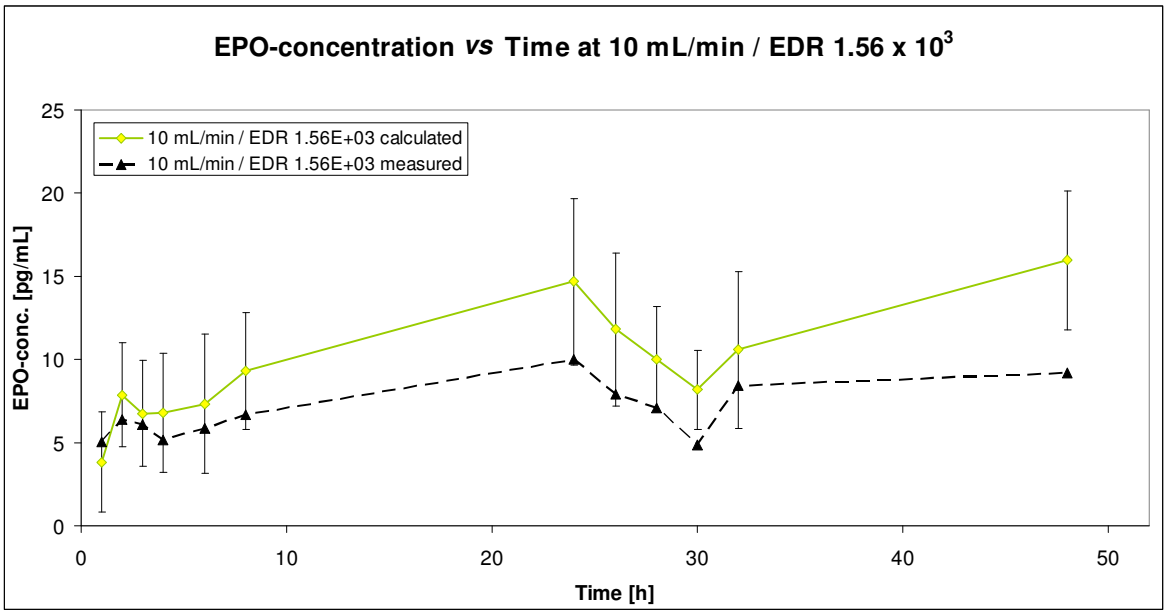

Figure 3.2 – rhEPO concentration [pg/mL] *vs* time at a flow rate of 10 mL/min

The results are displayed in Figure 3.2, comparing the measured mean values versus the calculated mean values. The concentration of the measured mean values was only converted to [pg/mL], to keep the graphs comparable. The graph consisting of the calculated values was generally at a higher level, taking the half-life of rhEPO into account. The burst of detached BNL-CL.2 cells and the release of the intracellular rhEPO levels were also included into the values. However, due to the small number of detached cells, these values had only a small influence at this flow rate. The comparable graphs show a slow but steady increase of the rhEPO levels after some time to accommodate to the surroundings. The reduction after 24 hours fits with the generation time of the BNL-CL.2 cells [21], followed by a recovery of the production until reaching 48 hours. The stress at this flow rate of 10 mL/min did not induce to an increased loss of cell mass at the point of generation time. Not even the fact, that mammalian cells turn to a round shape could be easily detached during mitosis [22] increased the cell loss. However the protein production and secretion of mammalian cells is reported to be dependent on the cell cycle [23] and is partially stopped during mitosis [24]. This would explain the reduced rhEPO concentration. Apart from the generation time, no severe loss of production was induced by an EDR of 1.56 x 10^3 W/m^3. Additionally, the level reported to seriously hamper productivity of adherent mammalian cells [25] had

been definitely surpassed, as well as the successful detection of changing product levels [5].

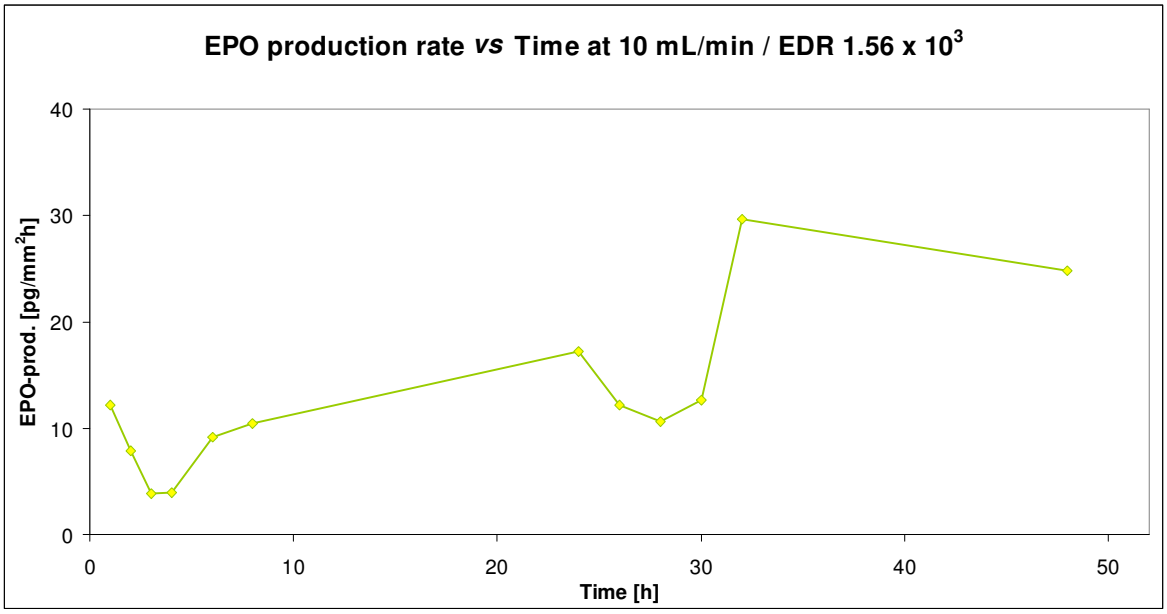

Figure 3.3 – rhEPO production rate [pg/mm^{2}h] *vs* time at a flow rate of 10 mL/min

The production rate depicted in Figure 3.3 resembled the concentration depended graphs in the most important characteristics, namely the adaption at the start of an experiment and the reduction during the generation time (mitoses phase) at around 24 hours. Interestingly the production rate decreased towards 48 hours, when obviously not only the loss of cell material was the reason for a reduced rhEPO concentration.

3.3 Flow of 20 mL/min respectively EDR 6.25 x 10^3 [W/m^3] for 48 h

The experiments used to obtain data were numbered 23, 25 and 27. All these experiments have been made with BNL-CL.2 cells secreting rhEPO and seeded overnight in a collagen IV coated Ibidi™ µ-Slide I$^{0.4}$ Luer. The settings for this flow rate of 20 mL/min or EDR 6.25 x 10^3 W/m^3, were similar to those for 10 mL/min. The temperature was set to 47°C ± 0.5°C, the pH-value to 7.4 ± 0.4 and the stirrer to 100 rpm at the bioreactor control unit.

The data are shown in Figure 3.4, again comparing the measured mean values against the calculated mean values. The measured graph displays the start, a small change at 24 hours but else keeps at the same level. The calculated graph however, displays a steeper slope within the first hours, which flattens towards the measurement after 24 hours. After the already encountered sudden reduction around the generation time of the BNL-CL.2 cells, the rhEPO levels increased again. Since cell proliferation is quite difficult under constant flow with a random chance of success, the cell morphology as well as density already varied more between the experiments than with 10 mL/min. This resulted in the increased standard deviations afterwards.

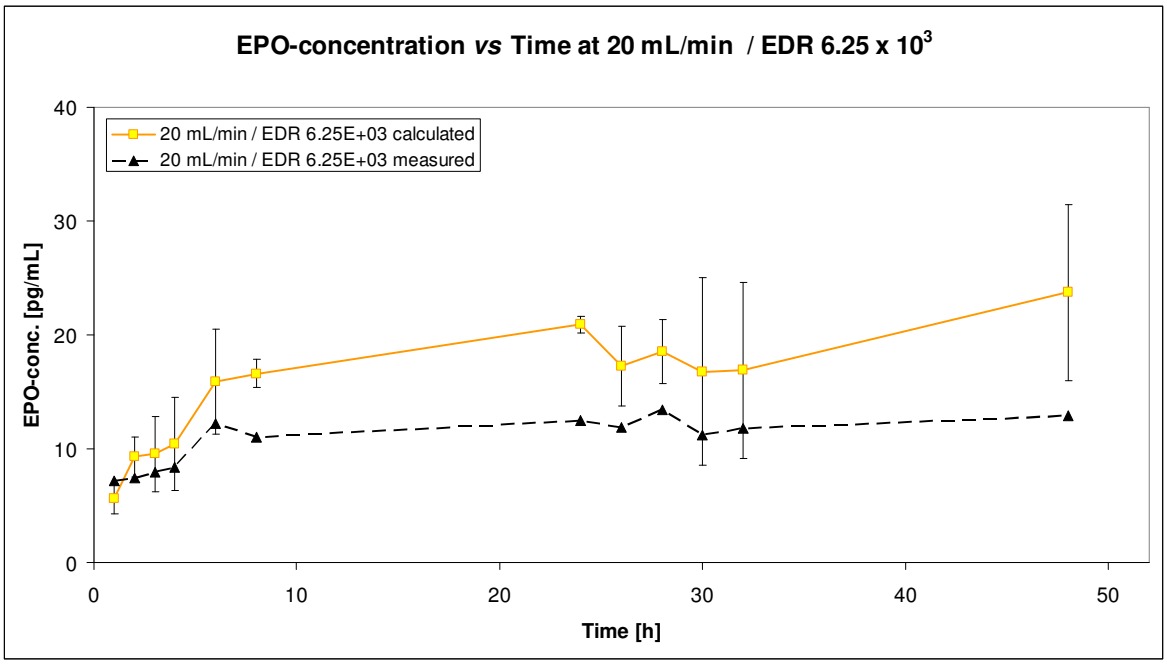

Figure 3.4 – rhEPO concentration [pg/mL] *vs* time at a flow rate of 20 mL/min

In summary, the EDR of 6.25 x 10^3 W/m^3 still did not seriously impact the production of rhEPO. The measured protein levels were even higher than before, possibly due to the fact of better nutrient supply and a more accommodating temperature. On the contrary, the generation time had a more varying effect on the further development of the production, as cell detachment sometimes increased during mitosis.

The production rate in Figure 3.5 illustrated a nearly continuous increase except for the adaption at the start of the experiments, not indicating the mitosis phase. This increase resembles the concentration graphs with a steeper slope. The value at 48 hours was not included as a very low remaining area of cell mass interfered with the mathematical calculations. If the area percentage inserted into the function (11) is very low, the result is a much too high production rate.

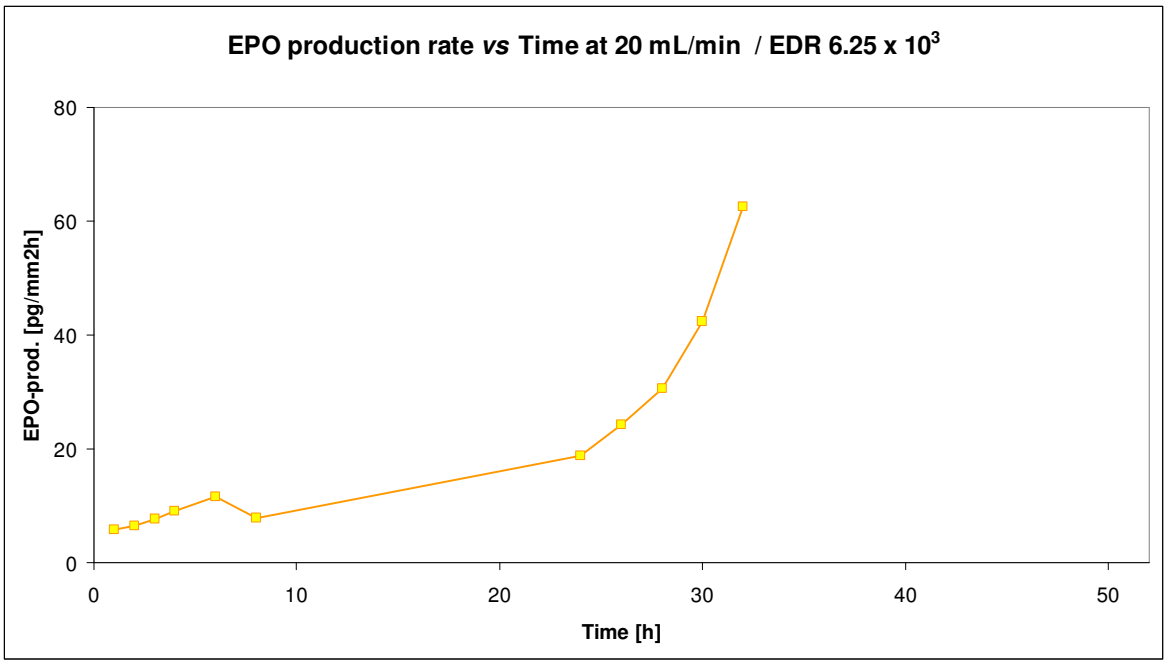

Figure 3.5 – rhEPO production rate [pg/mm²h] *vs* time at a flow rate of 20 mL/min

3.4 Flow of 25 mL/min respectively EDR 9.77 x 10^3 [W/m^3] for 48 h

The experiments used to obtain data for this flow rate were numbered 24, 26 and 28. All experiments have been made with BNL-CL.2 cells secreting rhEPO, which were seeded overnight in a collagen IV coated Ibidi™ µ-Slide $I^{0.4}$ Luer. The settings for this flow rate of 25 mL/min (EDR 9.77 x 10^3 W/m^3) at the bioreactor control unit were temperature to 44°C ± 0.5°C, pH-value to 7.4 ± 0.4 and the stirrer to 100 rpm. This should result in a stable temperature of 37°C within the slide channel at this flow rate.

The measured and calculated graphs compared in Figure 3.6 display that the cells needed a longer period of time to adapt to the conditions within the channel. However, these hydrodynamic force conditions already resemble a 20,000 L mixing vessel. The graphs are similar again, with a generally higher level and more distinctive changes for the calculated values. The slope is steep at the first measurement points forming a peak. This possibly results from a burst of production before the first wave of detaching cells, not able to withstand this hydrodynamic force. The digital microscope pictures approved this suggestion.

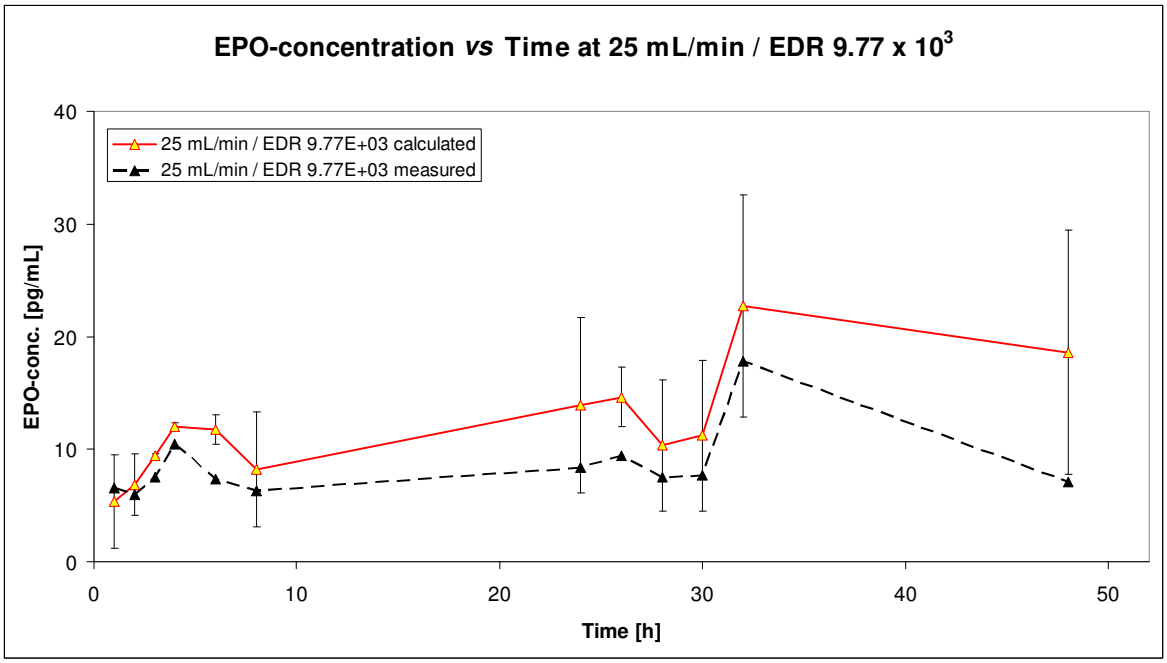

Figure 3.6 – rhEPO concentration [pg/mL] *vs* time at a flow rate of 25 mL/min

Following this peak is a slower slope, because of the reduced cell number. The next sudden reduction of the concentration occurred the same way like in the experiments with 10 and 20 mL/min but at 26 hours instead of 24 hours, possibly slightly shifting the generation time. After a short time of regeneration, another definite peak is encountered at 30 hours. This peak again indicated a drastic increased level of rhEPO. This may result from an increased output of the adherent BNL-CL.2 cells before they get detached, faster than in the previous experiments. This detachment possibly results from continuous cell death (apoptosis) after having endured too much hydrodynamic stress. If the adherent cells are not yet apoptotic, they start the programmed cell death after having lost

their anchorage and stop producing proteins [18]. Another fact strengthening this assumption is the continual decrease of the protein production afterwards. These results indicated that at a stress level around EDR 10^4 W/m^3, the cells reacted to the stress with bursts of production followed by a flush of detaching cells.

In Figure 3.7 the production rate depicted a similar behaviour like the concentration, with an adaption phase at the beginning and the reduction during the generation time. This time, the last two measurement points had to be skipped, due to very large respectively low and unlikely values. They would, however show an increase of the production rate towards 32 hours and a reduction afterwards. Since the production rate is derived from the concentration values but integrating the cell mass, the graphs tended to increase towards the last measurement points. There was still measurable rhEPO concentration but the remaining cell mass was very low.

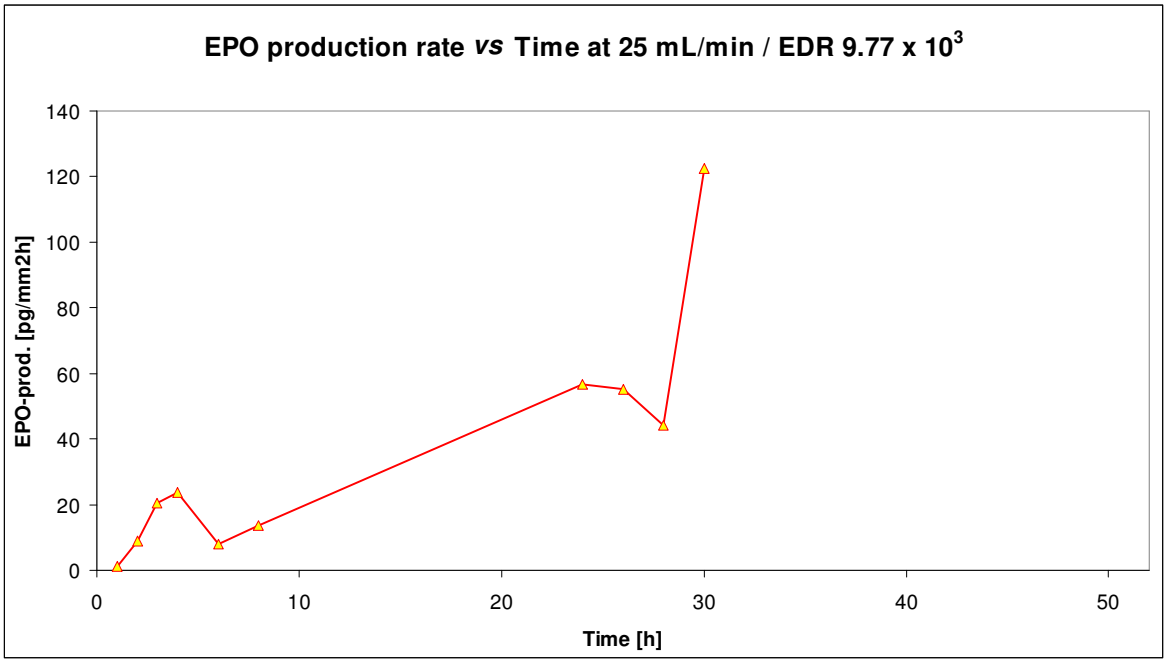

Figure 3.7 – rhEPO production rate [pg/mm^{2}h] *vs* time at a flow rate of 25 mL/min

3.5 Flow of 30 mL/min respectively EDR 1.41 x 10^4 [W/m^3] for 48 h

The numbers of the experiments conducted for this flow rate were 31, 32, 33, 34 and 35. These experiments have been planned interleaving, in an attempt to cover the whole experimental time of 48 hours with measurement points. All experiments have been done with BNL-CL.2 cells secreting rhEPO. They have been seeded overnight in a collagen IV coated Ibidi™ µ-Slide $I^{0.4}$ Luer. The bioreactor control unit was set to a temperature of 42°C ± 0.5°C, a pH-value to 7.4 ± 0.4 and the stirrer to 100 rpm for the flow rate of 30 mL/min or EDR 1.41 x 10^4 W/m^3.

The two graphs of the calculated and the measured mean rhEPO levels in Figure 3.8 are similar again, differing only in the increased levels of rhEPO for the calculated mean values. The graphs generally look less stable and continuous, despite increasing levels of rhEPO until a first peak at 26 hours like before with the experiments at 25 mL/min. However, this peak is mostly defined by the sudden drop of the protein concentration afterwards, referring again to the generation time of the BNL-CL.2 cells.

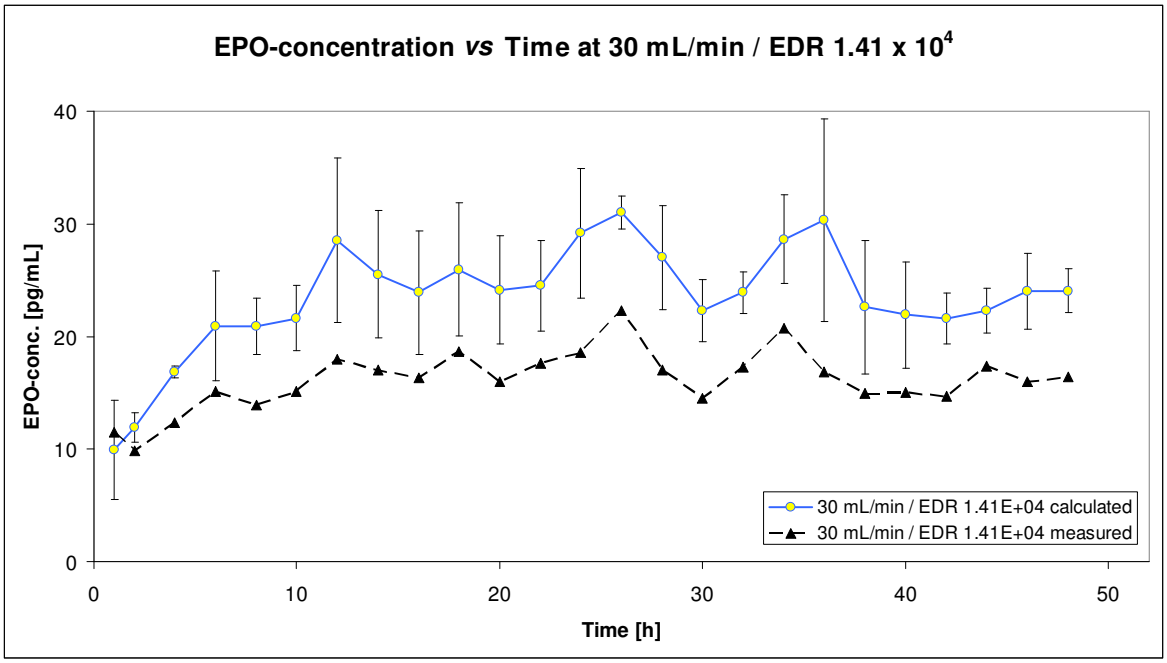

Figure 3.8 – rhEPO concentration [pg/mL] *vs* time at a flow rate of 30 mL/min

A second peak appeared shortly afterwards, again resembling increased output prior to detachment and cell flushing. In this set of experiments the amount of rhEPO remained at a stable level for the rest of the measurement points. For this time period, the decay of rhEPO, the production and secretion from the cells were in equilibrium. The cells surviving the hydrodynamic stress up to this moment remained alive and lost only small numbers for the rest of the experiment, as proven by the digital pictures of the microscope (Figure 3.9).

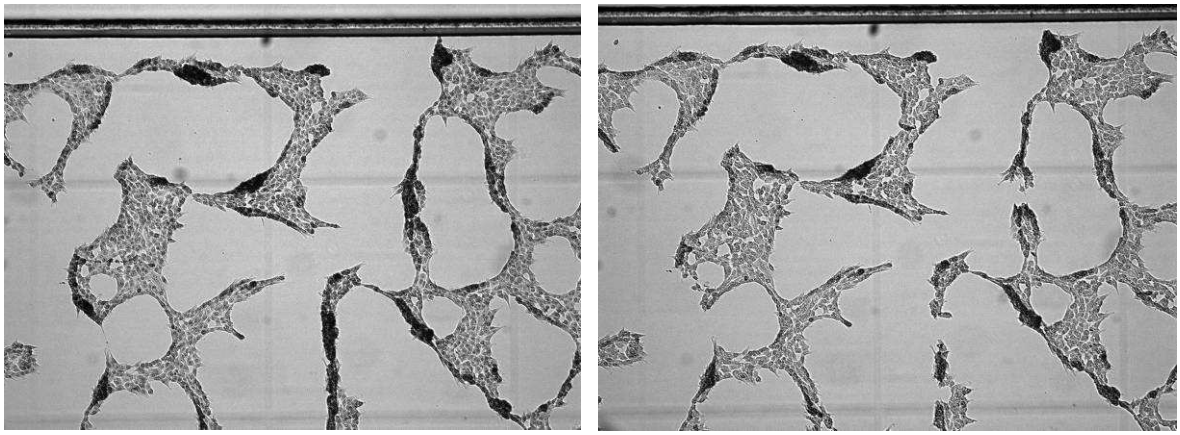

Figure 3.9 – BNL-CL.2 cells from experiment 35 after 36 hours (left) and 48 hours (right)

Having achieved the highest levels of rhEPO in these experiments, the limiting factors up to now were the speed of the nutrient supply and the stability of temperature – at least until the generation time of the BNL-CL.2 cells. In summary, this set of experiments showed a clear impact of the hydrodynamics on the cell's productivity. Furthermore, the previous sets of experimental data were proven to be valid by these combined experiments. The peaks and drops of the rhEPO concentration are well within the measurement points of the experiments.

The production rate in Figure 3.10 reconfirms the concentration graphs, depicting a continuous increase except during the mitosis phase. The smaller reductions contribute to lower concentrations while the amount of lost cell material was not increasing to this extend. At the last measurement points, the production rate had to increase mathematically, since the concentrations of rhEPO remained at a stable level but the cell mass was still decreasing. This was of course valid for all production rates.

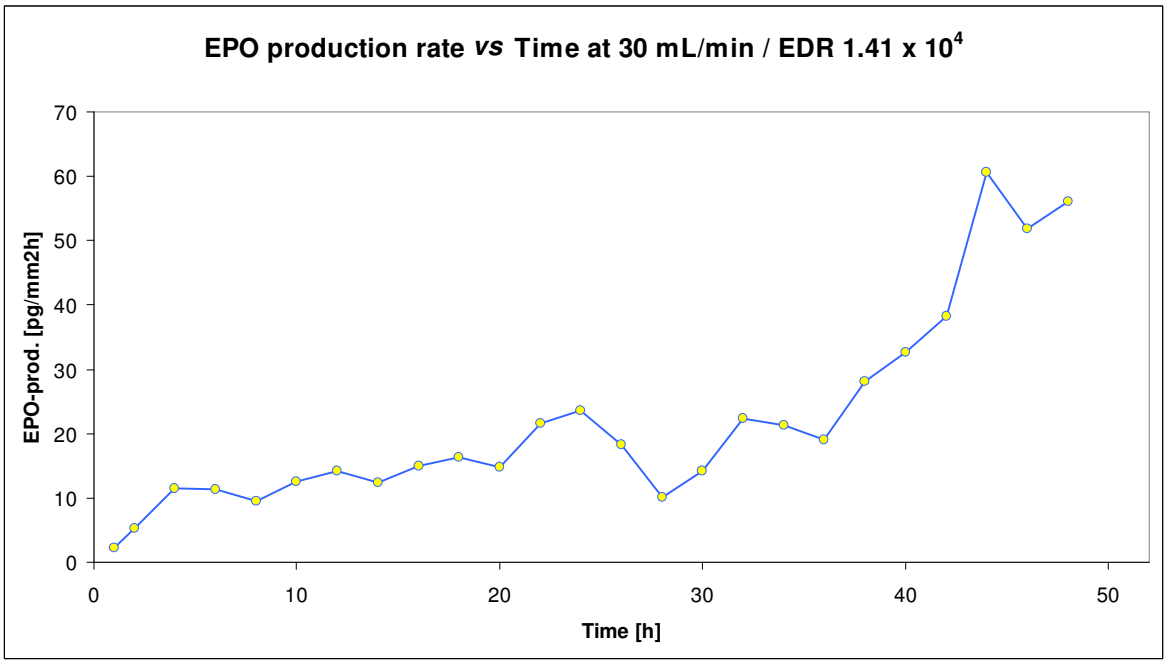

Figure 3.10 – rhEPO production rate [pg/mm^{2}h] *vs* time at a flow rate of 30 mL/min

3.6 Comparison of the calculated values

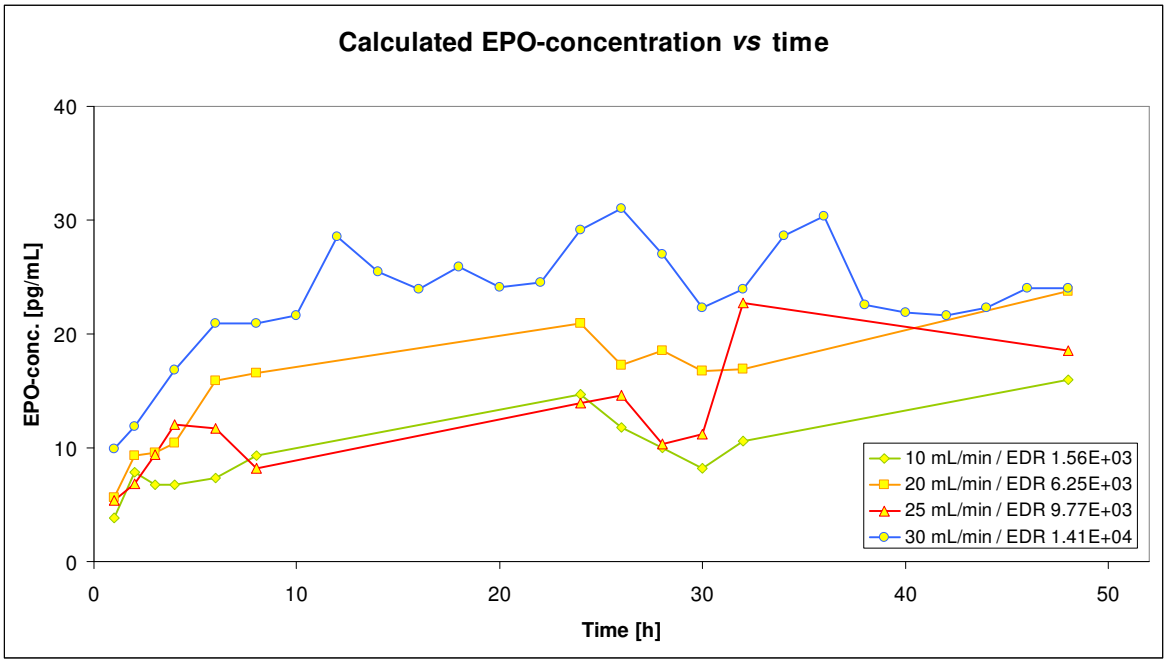

Figure 3.11 – rhEPO concentrations [pg/mL] *vs* time at 10, 20, 25 and 30 mL/min

A comparison of the four graphs, using the calculated mean values, is displayed in Figure 3.11. What can be clearly seen is a general trend of increasing rhEPO levels towards 24 respectively 26 hours of continuous impact of hydrodynamic stress. As observed from the microscopic images (Figure 3.12), a first wave of detachment occurred already at the start of each experiment. After that, the cells stayed at the surface until the generation time. The numbers of detached cells at this point were quite different with 25 mL/min, being the most selective flow rate at the beginning of the experiments. However, the sudden drop after approximately 24 to 26 hours of continuous impact of stress is again common to all four graphs.

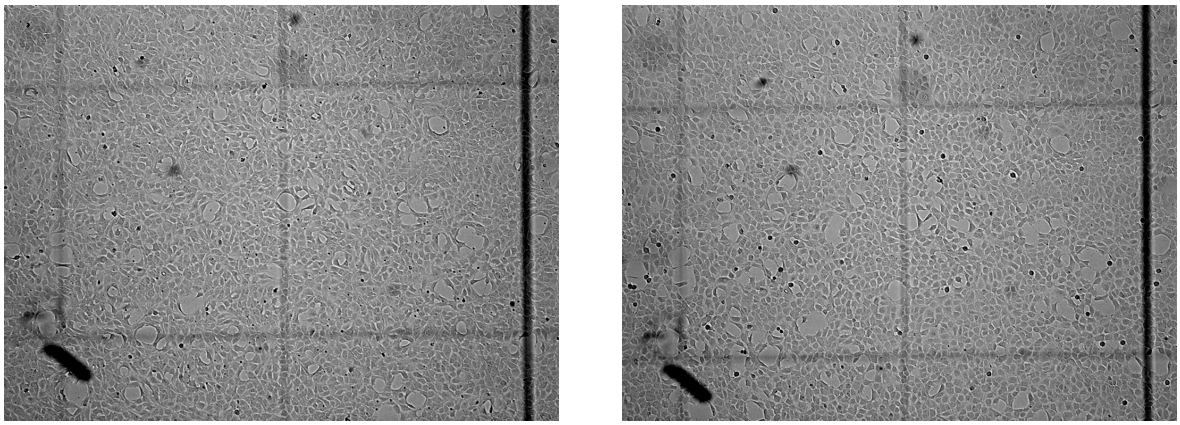

Figure 3.12 – BNL-CL.2 cells on Ibidi™ µ-Slide I Luer collagen IV at the start and after 1 h

Around the generation time, the behavior of the rhEPO graphs at 10 mL/min and 20 mL/min was similar, while the higher flow rates produced quite different results. The calculated mean values for 25 mL/min, as well as for 30 mL/min, indicated a decrease of the rhEPO level or at best a balance between production and half-life. Obviously, increased hydrodynamic forces have a stronger impact on cells conducting mitoses, as mentioned before [22]. Stronger hydrodynamic forces seemed to enforce the ups and downs of rhEPO levels during these phases, as increased cell detachment was reflected by impaired rhEPO production. The strong difference from the flow rate 25 mL/min to the other 3 graphs was assumed to result from the stress level. An EDR of 10^4 W/m^3 seemed to be the threshold, were cells could keep attached but reduce protein production to survive. With higher flow rates, the cells either kept attached and producing or were removed quite fast.

The comparison of measurement points in Figure 3.13 reflected these results. At a flow rate of 10 mL/min, a peak occurred at 24 hours, while the other measurement points at 8, 32 and 48 hours remained approximately at the same level of rhEPO. The flow rate 20 mL/min displayed a similar behavior, except for the higher levels and a slight increase of rhEPO after 36 hours. The columns for 25 mL/min and 30 mL/min showed a stronger increase in the amount of produced rhEPO. However, a reduction of the rhEPO levels towards the last measurement points at 48 hours was also encountered. Moreover, the flow rate of 25 mL/min displayed the most variable values right after the start of the experiments. This resulted in measurement of the lowest amount of rhEPO after 8 hours and the second lowest level after 48 hours. As already mentioned, these results contributed to the assumption that EDR 10^4 W/m^3 was starting to hinder protein production as a consequence of surviving strategies of the BNL-CL.2 cells.

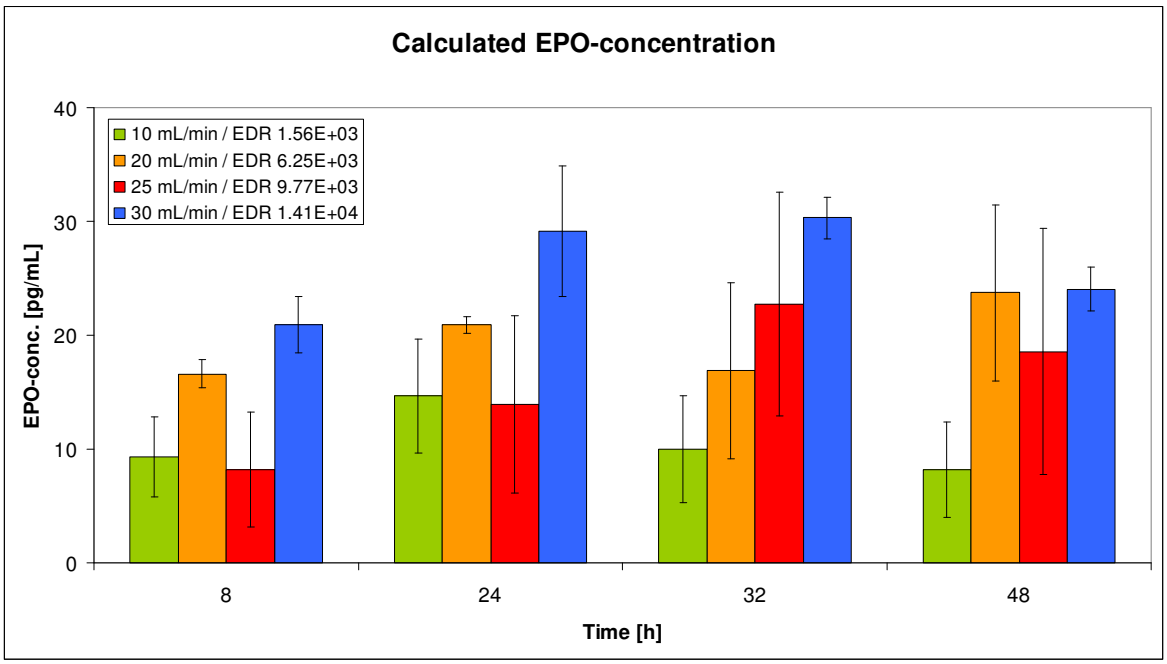

Figure 3.13 – rhEPO concentrations [pg/mL] compared at 8, 24, 32 and 48 hours

4 Summary

After successful preparation of a suitable mammalian cell line (Part A) and a complex experimental setup (Part B), the impact of hydrodynamic stress on the protein production was examined for the following flow rates, respectively energy dissipation rates (EDR):

Table 4.1 – Summary of the general settings for the conducted experiments

flow rate (adjusted at peristaltic pump)	EDR (calculated for µ-Slide $I^{0.4}$)	temperature (adjusted at bioreactor)	pH-value (adjusted at bioreactor)	agitation (adjusted at bioreactor)
10 mL/min	1.56 x 10^3 W/m^3	47 °C ± 0.5 °C	7.2 ± 0.4	100 rpm
20 mL/min	6.25 x 10^3 W/m^3	47 °C ± 0.5 °C	7.2 ± 0.4	100 rpm
25 mL/min	9.77 x 10^3 W/m^3	44 °C ± 0.5 °C	7.2 ± 0.4	100 rpm
30 mL/min	1.41 x 10^4 W/m^3	42 °C ± 0.5 °C	7.2 ± 0.4	100 rpm

The results from the experiments were analyzed and compared with the measured values. It was recognized that the graphs of direct and calculated values were quite similar, except the slightly higher levels and better developed peaks of the processed results. This was of course due to considering the rhEPO half-life, as well as the content of BNL-CL.2 cells bursting at the filters after detachment. Finally, these extended results from all four stress levels were compared.

The first conclusion was the sudden reduction of the rhEPO levels after 24 to 26 hours at all flow rates. Since this was also approximately the generation time of the BNL-CL.2 cells, the mitosis led to the strongest changes under permanent hydrodynamic stress. While the protein production is generally decreased during cell division, the cells formed round shapes and were easily detached. Especially under constant flow, the daughter cells were probably not adhering. The mother cells could lose adhesion at higher flow rates, and therefore, detach from the channel base. Taking this finding into account, not only hydrodynamic forces alone could influence adherent or microcarrier bound cell cultures [26].

After this event, the difference between the flow rates was clearly visible. At 10 and 20 mL/min the remaining cells recovered and started producing slightly more rhEPO than was lost due to half-life. At flow rates of 25 and 30 mL/min the changes after the generation time were much more severe, probably resulting from greater random effects on the cells during and after the mitosis. The cells stressed with 1.41 x 10^4 EDR W/m^3 (30 mL/min) recovered and remained approximately at the same numbers and level of rhEPO. At an EDR of 9.77 x 10^3 W/m^3 (25 mL/min) on the contrary the loss of cells after the generation time was higher and the production did not recover to equilibrium with the rhEPO half-life. An EDR around 10^4 W/m^3 was assumed to stress the BNL-CL.2 cells to some extent were they manage to survive for some time at the expense of reduced protein production. Higher EDR levels were either endured or removed the cells very fast, resulting in more constant results to the end of the experiments.

In order to resolve these results from another point of view, the production rate was calculated, utilizing the mean values of measured concentration and cell covered area. These graphs resembled the concentration graphs, especially in the adaption phase at the beginning and the mitosis phase around 24 to 26 hours. While the production rates at 20 and 25 mL/min flow rate increased at the later time points due to the effect of low cell covered areas, the graphs regarding 10 and 30 mL/min flow rates even showed a production rate decrease towards the last measurement points.

This new findings and results contribute to the growing knowledge about the influence of hydrodynamic stress on adherent mammalian cell cultures and their production of recombinant proteins. As already mentioned, the EDR of 10^4 W/m^3 seems to be an interesting level for examination of intracellular reactions to mechanical stress [(27)], for example the production of heat shock proteins (HSP) [(28)]. Furthermore, the influence of continuous stress during the mitosis was also identified as a major topic. The results further clearly display that there is still a lot of work that has to be done. With a good understanding of the important parameters, the common trial and error production could be changed. It would become possible to design ahead to the production process [(29)].

5 Raw and calculated data

The following chapter offers the sample names, time and measured rhEPO concentrations in [mU/mL] from all experiments. The calculated values for rhEPO in [pg/mL], half-life and release from burst cells are displayed (if available) as well as the measured cell covered area.

5.1 Experiments 1 to 17

These samples were not concentrated and no calculations were done.

Table 5.1 – rhEPO concentration. cell area and time values from experiments 1 to 5

sample:	real [mU/mL] EPO value:	real [pg/mL] EPO concentration:	cell covered area [%]:	time elapsed [h]:
50 mL/min				
BNL-CL2 - pEPO 01.01 0h	0.00	0.00	83.17	0
BNL-CL2 - pEPO 01.01 12h	0.00	0.00	2.82	12
50 mL/min				
BNL-CL2 - pEPO 02.01 0h	0.00	0.00	53.26	0
50 mL/min				
BNL-CL2 - pEPO 03.01 0h	0.00	0.00	77.91	0
BNL-CL2 - pEPO 03.02 1h	0.00	0.00	6.51	1
BNL-CL2 - pEPO 03.03 2h	0.00	0.00	2.99	2
25 mL/min				
BNL-CL2 - pEPO 04.01 1h	0.00	0.00	64.39	0
BNL-CL2 - pEPO 04.01 1h	3.50	17.50	64.95	1
BNL-CL2 - pEPO 04.02 2h	0.00	0.00	59.42	2
BNL-CL2 - pEPO 04.03 3h	0.00	0.00	52.38	3
BNL-CL2 - pEPO 04.04 4h	0.00	0.00	22.67	4
BNL-CL2 - pEPO 04.05 5h	0.00	0.00	16.26	5
BNL-CL2 - pEPO 04.06 6h	0.00	0.00	13.31	6
BNL-CL2 - pEPO 04.07 7h	0.00	0.00	5.32	7
BNL-CL2 - pEPO 04.08 8h	0.00	0.00	0.87	8
25 mL/min				
BNL-CL2 - pEPO 05.01 1h	0.00	0.00	55.89	1
BNL-CL2 - pEPO 05.02 3h	5.40	27.00	29.30	3
BNL-CL2 - pEPO 05.03 5h	0.00	0.00	5.53	5
BNL-CL2 - pEPO 05.04 7h	0.00	0.00	2.41	7

Table 5.2 – rhEPO concentration. cell area and time values from experiments 6 to 9

sample:	real [mU/mL] EPO value:	real [pg/mL] EPO concentration:	cell covered area [%]:	time elapsed [h]:
25 mL/min				
BNL-CL2 - pEPO 06.01 1h	4.60	23.00	77.09	1
BNL-CL2 - pEPO 06.02 2h	0.00	0.00	71.08	2
BNL-CL2 - pEPO 06.03 3h	3.00	15.00	65.37	3
BNL-CL2 - pEPO 06.04 4h	0.00	0.00	60.01	4
BNL-CL2 - pEPO 06.05 5h	4.20	21.00	61.31	5
BNL-CL2 - pEPO 06.06 6h	0.00	0.00	60.28	6
BNL-CL2 - pEPO 06.07 7h	3.00	15.00	57.61	7
BNL-CL2 - pEPO 06.08 9.5h	4.50	22.50	13.11	9.5
BNL-CL2 - pEPO 06.09 22h	2.60	13.00	0.72	22
BNL-CL2 - pEPO 06.10 23h	0.00	0.00	0.18	23
25 mL/min				
BNL-CL2 - pEPO 07.01 1h	3.00	15.00	74.95	1
BNL-CL2 - pEPO 07.02 2h	0.00	0.00	70.58	2
BNL-CL2 - pEPO 07.03 3h	0.00	0.00	4.98	3
BNL-CL2 - pEPO 07.04 4h	2.00	10.00	3.90	4
25 mL/min				
BNL-CL2 - pEPO 08.01 1h	0.00	0.00	67.40	1
BNL-CL2 - pEPO 08.02 2h	0.00	0.00	64.73	2
BNL-CL2 - pEPO 08.03 3h	3.50	17.50	59.51	3
BNL-CL2 - pEPO 08.04 4h	2.30	11.50	68.27	4
BNL-CL2 - pEPO 08.05 5h	2.10	10.50	63.49	5
BNL-CL2 - pEPO 08.06 6h	3.70	18.50	64.76	6
BNL-CL2 - pEPO 08.07 7h	1.50	7.50	69.09	7
BNL-CL2 - pEPO 08.08 8h	0.00	0.00	69.86	8
BNL-CL2 - pEPO 08.09 24h	6.30	31.50	56.73	24
BNL-CL2 - pEPO 08.10 26h	0.00	0.00	50.99	26
BNL-CL2 - pEPO 08.11 28h	1.40	7.00	49.65	28
BNL-CL2 - pEPO 08.12 30h	2.30	11.50	48.29	30
BNL-CL2 - pEPO 08.13 32h	2.10	10.50	43.68	32
BNL-CL2 - pEPO 08.14 48h	1.40	7.00	38.38	48
BNL-CL2 - pEPO 08.15 50h	1.70	8.50	19.15	50
25 mL/min				
BNL-CL2 - pEPO 09.01 1h	0.00	0.00	54.25	1
BNL-CL2 - pEPO 09.02 2h	0.00	0.00	51.17	2
BNL-CL2 - pEPO 09.03 3h	0.00	0.00	48.94	3
BNL-CL2 - pEPO 09.04 5h	2.30	11.50	53.64	5
BNL-CL2 - pEPO 09.05 8h	3.50	17.50	41.59	8
BNL-CL2 - pEPO 09.06 24h	2.40	12.00	25.56	24
BNL-CL2 - pEPO 09.07 26h	0.00	0.00	23.94	26
BNL-CL2 - pEPO 09.08 28h	0.00	0.00	21.63	28
BNL-CL2 - pEPO 09.09 30h	0.00	0.00	18.54	30
BNL-CL2 - pEPO 09.10 32h	0.00	0.00	17.16	32
BNL-CL2 - pEPO 09.11 48h	0.00	0.00	9.78	48

Table 5.3 – rhEPO concentration. cell area and time values from experiments 10 to 15

sample:	real [mU/mL] EPO value:	real [pg/mL] EPO concentration:	cell covered area [%]:	time elapsed [h]:
25 mL/min				
BNL-CL2 - pEPO 10.01 1h	1.90	9.50	68.17	1
BNL-CL2 - pEPO 10.02 2h	0.00	0.00	64.13	2
BNL-CL2 - pEPO 10.03 3h	0.00	0.00	54.49	3
BNL-CL2 - pEPO 10.04 4h	0.00	0.00	65.36	4
BNL-CL2 - pEPO 10.05 6h	1.60	8.00	51.23	6
BNL-CL2 - pEPO 10.07 24h	0.00	0.00	48.04	24
BNL-CL2 - pEPO 10.08 26h	1.40	7.00	40.21	26
BNL-CL2 - pEPO 10.09 28h	0.00	0.00	46.08	28
BNL-CL2 - pEPO 10.10 30h	1.40	7.00	34.76	30
BNL-CL2 - pEPO 10.11 32h	0.00	0.00	38.05	32
BNL-CL2 - pEPO 10.12 48h	1.20	6.00	19.56	48
25 mL/min				
BNL-CL2 - pEPO 11.01 1h	0.00	0.00	1.73	1
25 mL/min				
BNL-CL2 - pEPO 12.01 1h	0.00	0.00	0.00	1
BNL-CL2 - pEPO 12.02 3h	0.00	0.00	0.00	3
BNL-CL2 - pEPO 12.03 6h	0.00	0.00	0.00	6
BNL-CL2 - pEPO 12.04 8h	0.00	0.00	0.06	8
25 mL/min				
BNL-CL2 - pEPO 13.01 1h	0.00	0.00	0.40	1
25 mL/min				
BNL-CL2 - pEPO 14.01 1h	0.00	0.00	35.01	1
BNL-CL2 - pEPO 14.02 3h	0.00	0.00	26.65	3
BNL-CL2 - pEPO 14.03 5h	0.00	0.00	25.90	5
BNL-CL2 - pEPO 14.04 21h	0.00	0.00	16.16	21
BNL-CL2 - pEPO 14.05 23h	0.00	0.00	15.09	23
BNL-CL2 - pEPO 14.06 25h	0.00	0.00	14.96	25
BNL-CL2 - pEPO 14.07 27h	0.00	0.00	12.77	27
BNL-CL2 - pEPO 14.08 29h	0.00	0.00	13.97	29
BNL-CL2 - pEPO 14.09 45h	0.00	0.00	6.51	45
BNL-CL2 - pEPO 14.10 47h	0.00	0.00	5.27	47
25 mL/min				
BNL-CL2 - pEPO 15.01 1h	0.00	0.00	25.52	1
BNL-CL2 - pEPO 15.02 2h	0.00	0.00	16.41	2

Table 5.4 – rhEPO concentration. cell area and time values from experiments 16 and 17

sample:	real [mU/mL] EPO value:	real [pg/mL] EPO concentration:	cell covered area [%]:	time elapsed [h]:
25 mL/min				
BNL-CL2 - pEPO 16.01 1h	0.00	0.00	50.38	1
BNL-CL2 - pEPO 16.02 2h	0.00	0.00	52.61	2
BNL-CL2 - pEPO 16.03 4h	0.00	0.00	52.85	4
BNL-CL2 - pEPO 16.04 6h	0.00	0.00	53.07	6
BNL-CL2 - pEPO 16.05 22h	0.00	0.00	28.65	22
BNL-CL2 - pEPO 16.06 24h	0.00	0.00	25.42	24
BNL-CL2 - pEPO 16.07 26h	0.00	0.00	22.21	26
BNL-CL2 - pEPO 16.08 28h	0.00	0.00	20.64	28
BNL-CL2 - pEPO 16.09 31h	0.00	0.00	19.61	31
BNL-CL2 - pEPO 16.10 48h	0.00	0.00	4.40	48
25 mL/min				
BNL-CL2 - pEPO 17.01 1h	0.00	0.00	75.13	1
BNL-CL2 - pEPO 17.02 2h	0.00	0.00	72.27	2
BNL-CL2 - pEPO 17.03 4h	0.00	0.00	73.03	4
BNL-CL2 - pEPO 17.04 6h	0.00	0.00	76.36	6
BNL-CL2 - pEPO 17.05 8h	0.00	0.00	72.48	8
BNL-CL2 - pEPO 17.06 24h	0.00	0.00	75.50	24
BNL-CL2 - pEPO 17.07 26h	0.00	0.00	75.92	26
BNL-CL2 - pEPO 17.08 28h	0.00	0.00	76.16	28
BNL-CL2 - pEPO 17.09 30h	0.00	0.00	77.34	30
BNL-CL2 - pEPO 17.10 32h	0.00	0.00	68.93	32
BNL-CL2 - pEPO 17.11 34h	0.00	0.00	72.33	34
BNL-CL2 - pEPO 17.12 48h	0.00	0.00	50.89	48
BNL-CL2 - pEPO 17.13 50h	0.00	0.00	46.20	50

5.2 Experiments 18 to 35

Table 5.5 – Measured and calculated rhEPO values from experiments 18 to 20

sample:	measured [mU/mL] EPO value:	concentration factor:	real [mU/mL] EPO value:	real [pg/mL] EPO concentration:	half-life degradation [pg/mL]:	cell covered area [%]:	EPO release from detached cells [pg/mL]:	normalized [mU/mL] EPO value:	normalized [pg/mL] EPO value:	time elapsed [h]:
10 mL/min										
BNL-CL2 - pEPO 18.01 1h	0.00	5	0.00	0.00	0.00	53.78	4.14	0.00	0.00	1
BNL-CL2 - pEPO 18.02 2h	0.00	5	0.00	0.00	0.00	56.33	0.00	0.00	0.00	2
BNL-CL2 - pEPO 18.03 3h	0.00	5	0.00	0.00	0.00	53.40	0.26	0.00	0.00	3
BNL-CL2 - pEPO 18.04 4h	0.00	5	0.00	0.00	0.00	56.21	0.00	0.00	0.00	4
BNL-CL2 - pEPO 18.05 6h	6.63	5	1.33	6.63	0.00	32.19	2.15	2.22	4.47	6
BNL-CL2 - pEPO 18.06 8h	6.90	5	1.38	6.90	3.10	35.04	0.00	2.28	9.99	8
BNL-CL2 - pEPO 18.07 9.5h	0.00	5	0.00	0.00	2.60	32.46	0.23	0.00	2.37	9.5
BNL-CL2 - pEPO 18.08 24h	8.38	5	1.68	8.38	0.00	0.29	2.88	3.35	5.49	24
10 mL/min										
BNL-CL2 - pEPO 19.01 1h	0.00	5	0.00	0.00	0.00	75.38	2.21	0.00	0.00	1
BNL-CL2 - pEPO 19.02 2h	0.00	5	0.00	0.00	0.00	74.66	0.06	0.00	0.00	2
BNL-CL2 - pEPO 19.03 3h	6.83	5	1.37	6.83	0.00	58.17	1.48	1.94	5.36	3
BNL-CL2 - pEPO 19.04 4h	7.60	5	1.52	7.60	1.85	71.88	0.00	1.95	9.45	4
BNL-CL2 - pEPO 19.05 6h	9.48	5	1.90	9.48	3.55	69.55	0.21	2.47	12.83	6
BNL-CL2 - pEPO 19.06 8h	9.58	5	1.92	9.58	4.43	69.29	0.02	2.51	13.99	8
BNL-CL2 - pEPO 19.07 24h	8.75	5	1.75	8.75	9.52	51.32	1.61	2.60	16.66	24
BNL-CL2 - pEPO 19.08 25h	7.98	5	1.60	7.98	2.36	46.69	0.41	2.45	9.93	25
BNL-CL2 - pEPO 19.09 26h	7.90	5	1.58	7.90	2.16	43.79	0.26	2.47	9.79	26
BNL-CL2 - pEPO 19.10 27h	8.10	5	1.62	8.10	2.13	41.86	0.17	2.56	10.07	27
BNL-CL2 - pEPO 19.11 28h	7.29	5	1.46	7.29	2.19	47.22	0.00	2.23	9.48	28
BNL-CL2 - pEPO 19.12 30h	0.00	5	0.00	0.00	3.41	36.71	0.94	0.00	2.47	30
BNL-CL2 - pEPO 19.13 32h	8.58	5	1.72	8.58	0.00	33.39	0.30	2.86	8.29	32
BNL-CL2 - pEPO 19.14 48h	9.96	5	1.99	9.96	8.53	10.92	2.01	3.77	16.47	48
BNL-CL2 - pEPO 19.15 49h	9.88	5	1.98	9.88	2.69	7.09	0.34	3.81	12.22	49
BNL-CL2 - pEPO 19.16 50h	10.50	5	2.10	10.50	2.67	6.00	0.10	4.07	13.07	50
10 mL/min										
BNL-CL2 - pEPO 20.01 1h	3.00	5	0.60	3.00	0.00	68.99	2.78	0.79	0.22	1
BNL-CL2 - pEPO 20.02 2h	5.04	5	1.01	5.04	0.81	69.99	0.00	1.31	5.85	2
BNL-CL2 - pEPO 20.03 3h	2.79	5	0.56	2.79	1.36	65.14	0.43	0.75	3.72	3
BNL-CL2 - pEPO 20.04 4h	3.47	5	0.69	3.47	0.75	61.09	0.36	0.97	3.86	4
BNL-CL2 - pEPO 20.05 6h	2.84	5	0.57	2.84	1.62	54.10	0.63	0.83	3.84	6
BNL-CL2 - pEPO 20.06 8h	5.56	5	1.11	5.56	1.33	51.27	0.25	1.65	6.64	8
BNL-CL2 - pEPO 20.07 24h	6.33	5	1.27	6.33	5.53	49.69	0.14	1.90	11.72	24
BNL-CL2 - pEPO 20.08 25h	18.65	5	3.73	18.65	1.71	51.77	0.00	5.53	20.36	25
BNL-CL2 - pEPO 20.09 26h	8.65	5	1.73	8.65	5.04	54.85	0.00	2.51	13.69	26
BNL-CL2 - pEPO 20.10 27h	6.28	5	1.26	6.28	2.34	54.66	0.02	1.83	8.60	27
BNL-CL2 - pEPO 20.11 28h	6.65	5	1.33	6.65	1.70	54.50	0.01	1.93	8.33	28
BNL-CL2 - pEPO 20.12 30h	4.89	5	0.98	4.89	3.11	58.51	0.00	1.39	8.00	30
BNL-CL2 - pEPO 20.13 32h	16.37	5	3.27	16.37	2.29	58.17	0.03	4.64	18.63	32
BNL-CL2 - pEPO 20.14 48h	9.14	5	1.83	9.14	16.26	23.77	3.08	3.22	22.32	48
BNL-CL2 - pEPO 20.15 49h	6.12	5	1.22	6.12	2.47	13.23	0.94	2.29	7.65	49
BNL-CL2 - pEPO 20.16 50h	6.07	5	1.21	6.07	1.65	12.56	0.06	2.28	7.66	50

Table 5.6 – Measured and calculated rhEPO values from experiments 21 to 23

sample:	measured [mU/mL] EPO value:	concentration factor:	real [mU/mL] EPO value:	real [pg/mL] EPO concentration:	half-life degradation [pg/mL]:	cell covered area [%]:	EPO release from detached cells [pg/mL]:	normalized [mU/mL] EPO value:	normalized [pg/mL] EPO value:	time elapsed [h]:
10 mL/min										
BNL-CL2 - pEPO 21.01 1h	1.77	5	0.35	1.77	0.00	38.15	0.49	0.57	1.28	1
BNL-CL2 - pEPO 21.02 4h	2.40	5	0.48	2.40	1.08	28.36	0.22	0.83	3.27	4
BNL-CL2 - pEPO 21.03 6h	2.23	5	0.45	2.23	1.12	23.86	0.10	0.78	3.25	6
BNL-CL2 - pEPO 21.04 8h	4.39	5	0.88	4.39	1.04	22.81	0.02	1.55	5.40	8
BNL-CL2 - pEPO 21.05 10h	5.32	5	1.06	5.32	2.05	18.27	0.10	1.93	7.26	10
BNL-CL2 - pEPO 21.06 24h	12.70	5	2.54	12.70	5.25	10.95	0.16	4.80	17.79	24
BNL-CL2 - pEPO 21.07 26h	7.04	5	1.41	7.04	5.94	10.48	0.01	2.67	12.96	26
BNL-CL2 - pEPO 21.08 28h	7.12	5	1.42	7.12	3.29	9.00	0.03	2.72	10.38	28
BNL-CL2 - pEPO 21.09 30h	5.53	5	1.11	5.53	3.33	7.75	0.03	2.12	8.83	30
BNL-CL2 - pEPO 21.10 32h	4.02	5	0.80	4.02	2.58	8.00	0.00	1.54	6.60	32
BNL-CL2 - pEPO 21.11 48h	7.04	5	1.41	7.04	3.99	0.08	0.18	2.81	10.85	48
10 mL/min										
BNL-CL2 - pEPO 22.01 1h	3.47	5	0.69	3.47	0.00	6.10	0.53	1.35	2.94	1
BNL-CL2 - pEPO 22.02 2h	2.89	5	0.58	2.89	0.94	5.64	0.03	1.13	3.81	2
BNL-CL2 - pEPO 22.03 4h	1.35	5	0.27	1.35	1.35	5.08	0.03	0.53	2.67	4
BNL-CL2 - pEPO 22.06 6h	3.30	5	0.66	3.30	0.63	4.05	0.06	1.29	3.87	6
BNL-CL2 - pEPO 22.05 8h	3.12	5	0.62	3.12	1.54	3.95	0.01	1.22	4.66	8
BNL-CL2 - pEPO 22.06 24h	0.00	5	0.00	0.00	3.10	3.28	0.04	0.00	3.06	24
BNL-CL2 - pEPO 22.07 26h	6.21	5	1.24	6.21	0.00	3.28	0.00	2.44	6.21	26
BNL-CL2 - pEPO 22.08 28h	0.00	5	0.00	0.00	2.91	2.86	0.03	0.00	2.88	28
BNL-CL2 - pEPO 22.09 30h	0.00	5	0.00	0.00	0.00	2.59	0.02	0.00	0.00	30
BNL-CL2 - pEPO 22.10 32h	0.00	5	0.00	0.00	0.00	2.34	0.01	0.00	0.00	32
BNL-CL2 - pEPO 22.11 48h	0.00	5	0.00	0.00	0.00	2.08	0.02	0.00	0.00	48
20 mL/min										
BNL-CL2 - pEPO 23.01 1h	8.95	5	1.79	8.95	0.00	81.49	1.66	2.12	7.29	1
BNL-CL2 - pEPO 23.02 2h	7.09	5	1.42	7.09	2.42	85.90	0.00	1.62	9.51	2
BNL-CL2 - pEPO 23.03 3h	5.43	5	1.09	5.43	1.92	79.18	0.60	1.31	6.74	3
BNL-CL2 - pEPO 23.04 4h	6.05	5	1.21	6.05	1.47	84.07	0.00	1.40	7.52	4
BNL-CL2 - pEPO 23.05 6h	17.66	5	3.53	17.66	2.83	88.48	0.00	3.94	20.49	6
BNL-CL2 - pEPO 23.06 8h	8.50	5	1.70	8.50	8.26	88.59	0.00	1.89	16.76	8
BNL-CL2 - pEPO 23.07 24h	14.93	5	2.99	14.93	8.45	63.69	2.23	4.07	21.14	24
BNL-CL2 - pEPO 23.08 26h	16.18	5	3.24	16.18	6.98	53.29	0.93	4.75	22.23	26
BNL-CL2 - pEPO 23.09 28h	13.34	5	2.67	13.34	7.56	43.19	0.90	4.18	20.00	28
BNL-CL2 - pEPO 23.10 30h	9.18	5	1.84	9.18	6.24	34.15	0.81	3.04	14.60	30
BNL-CL2 - pEPO 23.11 32h	18.29	5	3.66	18.29	4.29	29.65	0.40	6.23	22.17	32
BNL-CL2 - pEPO 23.12 48h	14.30	5	2.86	14.30	18.17	2.76	2.41	5.64	30.06	48

Table 5.7 – Measured and calculated rhEPO values from experiments 24 to 26

sample:	measured [mU/mL] EPO value:	concentration factor:	real [mU/mL] EPO value:	real [pg/mL] EPO concentration:	half-life degradation [pg/mL]:	cell covered area [%]:	EPO release from detached cells [pg/mL]:	normalized [mU/mL] EPO value:	normalized [pg/mL] EPO value:	time elapsed [h]:
25 mL/min										
BNL-CL2 - pEPO 24.01 1h	3.36	5	0.67	3.36	0.00	77.65	2.00	0.82	1.36	1
BNL-CL2 - pEPO 24.02 2h	7.68	5	1.54	7.68	0.91	62.41	1.37	2.11	7.22	2
BNL-CL2 - pEPO 24.03 3h	8.18	5	1.64	8.18	2.08	54.78	0.68	2.38	9.57	3
BNL-CL2 - pEPO 24.04 4h	10.14	5	2.03	10.14	2.21	47.19	0.68	3.10	11.67	4
BNL-CL2 - pEPO 24.05 6h	8.46	5	1.69	8.46	4.74	45.17	0.18	2.62	13.02	6
BNL-CL2 - pEPO 24.06 8h	9.93	5	1.99	9.93	3.96	39.93	0.47	3.18	13.42	8
BNL-CL2 - pEPO 24.07 24h	13.82	5	2.76	13.82	9.86	21.05	1.69	4.95	21.99	24
BNL-CL2 - pEPO 24.08 26h	11.09	5	2.22	11.09	6.46	17.76	0.29	4.04	17.26	26
BNL-CL2 - pEPO 24.09 28h	11.95	5	2.39	11.95	5.18	14.70	0.27	4.43	16.86	28
BNL-CL2 - pEPO 24.10 30h	13.36	5	2.67	13.36	5.58	14.16	0.05	4.96	18.89	30
BNL-CL2 - pEPO 24.11 32h	26.54	5	5.31	26.54	6.24	11.96	0.20	9.98	32.58	32
BNL-CL2 - pEPO 24.12 48h	6.59	5	1.32	6.59	26.36	4.53	0.67	2.58	32.29	48
20 mL/min										
BNL-CL2 - pEPO 25.01 1h	7.89	5	1.58	7.89	0.00	73.46	2.38	2.00	5.52	1
BNL-CL2 - pEPO 25.02 2h	9.34	5	1.87	9.34	2.13	71.46	0.18	2.40	11.29	2
BNL-CL2 - pEPO 25.03 3h	12.20	5	2.44	12.20	2.52	65.41	0.54	3.28	14.18	3
BNL-CL2 - pEPO 25.04 4h	13.30	5	2.66	13.30	3.30	61.57	0.34	3.68	16.26	4
BNL-CL2 - pEPO 25.05 6h	11.98	5	2.40	11.98	6.22	55.92	0.51	3.45	17.69	6
BNL-CL2 - pEPO 25.06 8h	12.62	5	2.52	12.62	5.60	53.82	0.19	3.69	18.04	8
BNL-CL2 - pEPO 25.07 24h	11.17	5	2.23	11.17	12.54	11.71	3.77	4.21	19.94	24
BNL-CL2 - pEPO 25.08 26h	10.00	5	2.00	10.00	5.22	7.62	0.37	3.85	14.86	26
BNL-CL2 - pEPO 25.09 28h	16.47	5	3.29	16.47	4.67	5.67	0.17	6.40	20.97	28
BNL-CL2 - pEPO 25.10 30h	20.21	5	4.04	20.21	7.70	4.55	0.10	7.90	27.81	30
BNL-CL2 - pEPO 25.11 32h	13.21	5	2.64	13.21	9.45	3.86	0.06	5.18	22.59	32
BNL-CL2 - pEPO 25.12 48h	15.43	5	3.09	15.43	13.12	1.10	0.25	6.14	28.31	48
25 mL/min										
BNL-CL2 - pEPO 26.01 1h	2.47	5	0.49	2.47	0.00	15.20	3.63	0.91	0.00	1
BNL-CL2 - pEPO 26.02 2h	0.00	5	0.00	0.00	0.67	14.64	0.03	0.00	0.64	2
BNL-CL2 - pEPO 26.03 3h	0.00	5	0.00	0.00	0.00	12.06	0.14	0.00	0.00	3
BNL-CL2 - pEPO 26.04 4h	0.00	5	0.00	0.00	0.00	9.91	0.12	0.00	0.00	4
BNL-CL2 - pEPO 26.05 6h	0.00	5	0.00	0.00	0.00	9.68	0.01	0.00	0.00	6
BNL-CL2 - pEPO 26.06 8h	1.36	5	0.27	1.36	0.00	9.26	0.02	0.52	1.33	8
BNL-CL2 - pEPO 26.07 24h	2.36	5	0.47	2.36	1.35	3.44	0.33	0.93	3.38	24
BNL-CL2 - pEPO 26.08 26h	0.00	5	0.00	0.00	1.10	3.45	0.00	0.00	1.10	26
BNL-CL2 - pEPO 26.09 28h	2.72	5	0.54	2.72	0.00	3.24	0.01	1.07	2.71	28
BNL-CL2 - pEPO 26.10 30h	1.38	5	0.28	1.38	1.27	3.11	0.01	0.54	2.64	30
BNL-CL2 - pEPO 26.11 32h	0.00	5	0.00	0.00	0.64	3.16	0.00	0.00	0.64	32
BNL-CL2 - pEPO 26.12 48h	5.79	5	1.16	5.79	0.00	2.45	0.04	2.29	5.75	48

Table 5.8 – Measured and calculated rhEPO values from experiments 27 to 30

sample:	measured [mU/mL] EPO value:	concentration factor:	real [mU/mL] EPO value:	real [pg/mL] EPO concentration:	half-life degradation [pg/mL]:	cell covered area [%]:	EPO release from detached cells [pg/mL]:	normalized [mU/mL] EPO value:	normalized [pg/mL] EPO value:	time elapsed [h]:
20 mL/min										
BNL-CL2 - pEPO 27.01 1h	4.66	5	0.93	4.66	0.00	69.30	0.60	1.22	4.06	1
BNL-CL2 - pEPO 27.02 2h	5.87	5	1.17	5.87	1.26	67.78	0.09	1.55	7.04	2
BNL-CL2 - pEPO 27.03 3h	6.26	5	1.25	6.26	1.59	65.68	0.12	1.68	7.73	3
BNL-CL2 - pEPO 27.04 4h	5.79	5	1.16	5.79	1.69	67.86	0.00	2.11	7.49	4
BNL-CL2 - pEPO 27.05 6h	7.02	5	1.40	7.02	2.71	64.54	0.19	1.85	9.54	6
BNL-CL2 - pEPO 27.06 8h	12.00	5	2.40	12.00	3.28	60.11	0.25	3.36	15.03	8
BNL-CL2 - pEPO 27.07 24h	11.42	5	2.28	11.42	11.92	30.47	1.66	3.87	21.68	24
BNL-CL2 - pEPO 27.08 26h	9.49	5	1.90	9.49	5.34	27.35	0.17	3.28	14.65	26
BNL-CL2 - pEPO 27.09 28h	10.42	5	2.08	10.42	4.44	22.74	0.26	3.69	14.59	28
BNL-CL2 - pEPO 27.10 30h	4.28	5	0.86	4.28	4.87	1.31	1.20	1.70	7.95	30
BNL-CL2 - pEPO 27.11 32h	3.94	5	0.79	3.94	2.00	0.89	0.02	1.57	5.92	32
BNL-CL2 - pEPO 27.12 48h	8.92	5	1.78	8.92	3.92	0.33	0.03	3.56	12.81	48
25 mL/min										
BNL-CL2 - pEPO 28.01 1h	9.74	5	1.95	9.74	0.00	65.15	0.39	2.63	9.34	1
BNL-CL2 - pEPO 28.02 2h	10.15	5	2.03	10.15	2.63	63.66	0.06	2.77	12.72	2
BNL-CL2 - pEPO 28.03 3h	6.83	5	1.37	6.83	2.74	55.67	0.32	1.97	9.25	3
BNL-CL2 - pEPO 28.04 4h	10.74	5	2.15	10.74	1.85	50.54	0.20	3.21	12.38	4
BNL-CL2 - pEPO 28.05 6h	6.21	5	1.24	6.21	5.02	29.92	0.82	2.11	10.42	6
BNL-CL2 - pEPO 28.06 8h	7.66	5	1.53	7.66	2.91	12.65	0.69	2.87	9.87	8
BNL-CL2 - pEPO 28.07 24h	9.04	5	1.81	9.04	7.61	5.20	0.30	3.52	16.35	24
BNL-CL2 - pEPO 28.08 26h	7.79	5	1.56	7.79	4.23	5.61	0.00	3.03	12.01	26
BNL-CL2 - pEPO 28.09 28h	7.84	5	1.57	7.84	3.64	5.64	0.00	3.05	11.48	28
BNL-CL2 - pEPO 28.10 30h	8.40	5	1.68	8.40	3.67	4.77	0.03	3.28	12.03	30
BNL-CL2 - pEPO 28.11 32h	9.00	5	1.80	9.00	3.93	3.95	0.03	3.53	12.89	32
BNL-CL2 - pEPO 28.12 48h	8.86	5	1.77	8.86	8.94	1.87	0.08	3.51	17.72	48
10 mL/min										
BNL-CL2 - pEPO 29.01 1h	7.61	5	1.52	7.61	0.00	63.01	0.95	2.09	6.66	1
BNL-CL2 - pEPO 29.02 2h	9.31	5	1.86	9.31	2.06	61.00	0.11	2.59	11.26	2
BNL-CL2 - pEPO 29.03 3h	8.67	5	1.73	8.67	2.52	65.32	0.00	2.34	11.19	3
BNL-CL2 - pEPO 29.04 4h	8.49	5	1.70	8.49	2.34	62.03	0.18	2.34	10.65	4
BNL-CL2 - pEPO 29.05 6h	9.91	5	1.98	9.91	3.97	57.19	0.27	2.83	13.61	6
BNL-CL2 - pEPO 29.06 8h	8.89	5	1.78	8.89	4.63	55.91	0.07	2.56	13.45	8
BNL-CL2 - pEPO 29.07 24h	15.39	5	3.08	15.39	8.83	5.70	2.81	5.98	21.40	24
BNL-CL2 - pEPO 29.08 26h	13.11	5	2.62	13.11	7.19	4.41	0.07	5.13	20.23	26
BNL-CL2 - pEPO 29.09 28h	11.21	5	2.24	11.21	6.13	4.03	0.02	4.40	17.32	28
10 mL/min										
BNL-CL2 - pEPO 30.01 1h	9.41	5	1.88	9.41	0.00	84.06	1.43	2.18	7.98	1
BNL-CL2 - pEPO 30.02 2h	8.34	5	1.67	8.34	2.54	80.05	0.36	2.00	10.52	2
BNL-CL2 - pEPO 30.03 4h	7.59	5	1.52	7.59	3.90	72.56	0.67	1.93	10.82	4
BNL-CL2 - pEPO 30.04 6h	6.68	5	1.34	6.68	3.55	64.84	0.69	1.81	9.53	6
BNL-CL2 - pEPO 30.01 8h	8.23	5	1.65	8.23	3.12	60.36	0.40	2.30	10.95	8
BNL-CL2 - pEPO 30.02 24h	8.37	5	1.67	8.37	8.17	42.42	1.61	2.64	14.94	24
BNL-CL2 - pEPO 30.03 26h	4.40	5	0.88	4.40	3.91	38.19	0.38	1.43	7.94	26
BNL-CL2 - pEPO 30.04 28h	10.09	5	2.02	10.09	2.06	32.61	0.50	3.38	11.65	28
BNL-CL2 - pEPO 30.01 30h	9.09	5	1.82	9.09	4.72	28.40	0.38	3.12	13.43	30
BNL-CL2 - pEPO 30.02 32h	4.72	5	0.94	4.72	4.25	26.79	0.14	1.63	8.82	32
BNL-CL2 - pEPO 30.03 48h	10.65	5	2.13	10.65	4.69	14.42	1.11	3.95	14.23	48

Table 5.9 – Measured and calculated rhEPO values from experiments 31 to 33

sample:	measured [mU/mL] EPO value:	concentration factor:	real [mU/mL] EPO value:	real [pg/mL] EPO concentration:	half-life degradation [pg/mL]:	cell covered area [%]:	EPO release from detached cells [pg/mL]:	normalized [mU/mL] EPO value:	normalized [pg/mL] EPO value:	time elapsed [h]:
30 mL/min										
BNL-CL2 - pEPO 31.01 1h	9.07	5	1.81	9.07	0.00	85.62	1.29	2.08	7.78	1
BNL-CL2 - pEPO 31.02 2h	11.02	5	2.20	11.02	2.45	82.71	0.26	2.58	13.21	2
BNL-CL2 - pEPO 31.03 4h	11.50	5	2.30	11.50	5.15	78.96	0.34	2.78	16.31	4
BNL-CL2 - pEPO 31.04 6h	10.66	5	2.13	10.66	5.38	79.94	0.00	2.56	16.04	6
BNL-CL2 - pEPO 31.05 8h	13.45	5	2.69	13.45	4.98	83.79	0.00	3.13	18.43	8
BNL-CL2 - pEPO 31.06 10h	12.45	5	2.49	12.45	6.29	84.40	0.00	2.88	18.73	10
BNL-CL2 - pEPO 31.07 12h	17.59	5	3.52	17.59	5.82	88.05	0.00	3.94	23.41	12
BNL-CL2 - pEPO 31.08 24h	12.25	2.8	4.38	21.88	17.19	83.41	0.42	5.10	38.65	24
BNL-CL2 - pEPO 31.09 26h	19.46	5	3.89	19.46	10.23	82.07	0.12	4.59	29.57	26
BNL-CL2 - pEPO 31.10 28h	13.61	5	2.72	13.61	9.10	78.46	0.32	3.31	22.38	28
BNL-CL2 - pEPO 31.11 30h	13.41	5	2.68	13.41	6.36	76.10	0.21	3.32	19.56	30
BNL-CL2 - pEPO 31.12 32h	15.88	5	3.18	15.88	6.27	75.23	0.08	3.96	22.07	32
BNL-CL2 - pEPO 31.13 34h	25.30	5	5.06	25.30	7.42	73.19	0.18	6.42	32.54	34
BNL-CL2 - pEPO 31.14 36h	13.21	5	2.64	13.21	11.83	69.53	0.33	3.45	24.72	36
BNL-CL2 - pEPO 31.15 48h	16.38	5	3.28	16.38	12.91	18.10	4.61	5.96	24.68	48
30 mL/min										
BNL-CL2 - pEPO 32.01 1h	8.89	5	1.78	8.89	0.00	83.12	1.51	2.08	7.38	1
BNL-CL2 - pEPO 32.02 12h	13.70	5	2.74	13.70	8.61	74.09	0.81	3.45	21.50	12
BNL-CL2 - pEPO 32.03 14h	11.20	5	2.24	11.20	6.40	74.70	0.00	2.81	17.60	14
BNL-CL2 - pEPO 32.04 16h	11.50	5	2.30	11.50	5.23	69.82	0.44	2.99	16.30	16
BNL-CL2 - pEPO 32.05 18h	12.25	5	2.45	12.25	5.38	73.17	0.00	3.11	17.63	18
BNL-CL2 - pEPO 32.06 20h	13.00	5	2.60	13.00	5.73	69.23	0.35	3.40	18.37	20
BNL-CL2 - pEPO 32.07 22h	12.95	5	2.59	12.95	6.08	67.53	0.15	3.43	18.87	22
BNL-CL2 - pEPO 32.08 24h	17.05	5	3.41	17.05	6.05	65.53	0.18	4.59	22.93	24
BNL-CL2 - pEPO 32.09 36h	15.13	5	3.03	15.13	16.66	47.24	1.64	4.62	30.15	36
BNL-CL2 - pEPO 32.10 38h	13.55	5	2.71	13.55	7.07	47.78	0.00	4.13	20.62	38
BNL-CL2 - pEPO 32.11 40h	12.64	5	2.53	12.64	6.34	43.75	0.36	3.95	18.62	40
BNL-CL2 - pEPO 32.12 42h	13.84	5	2.77	13.84	5.91	40.39	0.30	4.42	19.45	42
BNL-CL2 - pEPO 32.13 44h	21.43	5	4.29	21.43	6.47	0.41	3.58	8.55	24.32	44
BNL-CL2 - pEPO 32.14 46h	17.39	5	3.48	17.39	10.02	0.22	0.02	6.95	27.39	46
30 mL/min										
BNL-CL2 - pEPO 33.01 1h	6.81	5	1.36	6.81	0.00	84.23	1.41	1.58	5.40	1
BNL-CL2 - pEPO 33.02 2h	8.77	5	1.75	8.77	1.84	84.05	0.02	2.03	10.59	2
BNL-CL2 - pEPO 33.03 4h	13.26	5	2.65	13.26	4.10	83.99	0.01	3.08	17.35	4
BNL-CL2 - pEPO 33.04 6h	19.62	5	3.92	19.62	6.20	83.83	0.01	4.56	25.80	6
BNL-CL2 - pEPO 33.05 8h	14.45	5	2.89	14.45	9.17	81.74	0.19	3.42	23.43	8
BNL-CL2 - pEPO 33.06 10h	17.79	5	3.56	17.79	6.75	82.30	0.00	4.19	24.54	10
BNL-CL2 - pEPO 33.07 12h	16.36	5	3.27	16.36	8.32	78.74	0.32	3.97	24.36	12
BNL-CL2 - pEPO 33.08 24h	16.13	5	3.23	16.13	15.99	51.12	2.47	4.80	29.64	24
BNL-CL2 - pEPO 33.09 26h	25.15	5	5.03	25.15	7.54	48.81	0.21	7.60	32.48	26
BNL-CL2 - pEPO 33.10 28h	20.38	5	4.08	20.38	11.76	43.42	0.48	6.38	31.66	28
BNL-CL2 - pEPO 33.11 30h	15.68	5	3.14	15.68	9.53	41.64	0.16	4.97	25.05	30
BNL-CL2 - pEPO 33.12 32h	18.77	5	3.75	18.77	7.33	37.78	0.35	6.09	25.75	32
BNL-CL2 - pEPO 33.13 34h	16.21	5	3.24	16.21	8.77	34.89	0.26	5.35	24.73	34
BNL-CL2 - pEPO 33.14 36h	21.64	5	4.33	21.64	7.58	29.89	0.45	7.36	28.77	36
BNL-CL2 - pEPO 33.15 48h	18.13	5	3.63	18.13	10.12	5.07	2.22	7.07	26.02	48

Table 5.10 – Measured and calculated rhEPO values from experiments 34 and 35

sample:	measured [mU/mL] EPO value:	concentration factor:	real [mU/mL] EPO value:	real [pg/mL] EPO concentration:	half-life degradation [pg/mL]:	cell covered area [%]:	EPO release from detached cells [pg/mL]:	normalized [mU/mL] EPO value:	normalized [pg/mL] EPO value:	time elapsed [h]:
30 mL/min										
BNL-CL2 - pEPO 34.01 1h	19.68	5	3.94	19.68	0.00	80.87	1.71	4.69	17.97	1
BNL-CL2 - pEPO 34.02 12h	22.58	5	4.52	22.58	19.07	75.86	0.45	5.61	41.20	12
BNL-CL2 - pEPO 34.03 14h	20.56	5	4.11	20.56	10.56	70.74	0.46	5.32	30.66	14
BNL-CL2 - pEPO 34.04 16h	17.26	5	3.45	17.26	9.61	64.70	0.54	4.67	26.33	16
BNL-CL2 - pEPO 34.05 18h	21.68	5	4.34	21.68	8.07	58.60	0.55	6.13	29.21	18
BNL-CL2 - pEPO 34.06 20h	14.77	5	2.95	14.77	10.14	48.17	0.93	4.49	23.97	20
BNL-CL2 - pEPO 34.07 22h	20.47	5	4.09	20.47	6.91	38.61	0.86	6.61	26.52	22
BNL-CL2 - pEPO 34.08 24h	22.74	5	4.55	22.74	9.57	24.61	1.25	7.98	31.05	24
BNL-CL2 - pEPO 34.09 36h	26.95	5	5.39	26.95	22.22	1.52	2.07	10.70	47.10	36
BNL-CL2 - pEPO 34.10 38h	18.12	5	3.62	18.12	12.60	0.16	0.12	7.24	30.60	38
BNL-CL2 - pEPO 34.11 40h	20.12	5	4.02	20.12	8.47	0.16	0.00	8.04	28.59	40
BNL-CL2 - pEPO 34.12 42h	15.35	5	3.07	15.35	9.41	0.06	0.01	6.14	24.75	42
30 mL/min										
BNL-CL2 - pEPO 35.01 1h	13.19	5	2.64	13.19	0.00	78.12	1.96	3.22	11.23	1
BNL-CL2 - pEPO 35.02 12h	19.83	5	3.97	19.83	12.78	73.01	0.46	5.04	32.15	12
BNL-CL2 - pEPO 35.03 14h	19.32	5	3.86	19.32	9.27	69.25	0.34	5.05	28.25	14
BNL-CL2 - pEPO 35.04 16h	20.28	5	4.06	20.28	9.03	66.41	0.25	5.42	29.05	16
BNL-CL2 - pEPO 35.05 18h	22.09	5	4.42	22.09	9.48	59.52	0.62	6.21	30.95	18
BNL-CL2 - pEPO 35.06 20h	20.06	5	4.01	20.06	10.32	55.96	0.32	5.78	30.07	20
BNL-CL2 - pEPO 35.07 22h	19.36	5	3.87	19.36	9.38	49.03	0.62	5.85	28.12	22
BNL-CL2 - pEPO 35.08 24h	14.98	5	3.00	14.98	9.05	43.65	0.48	4.68	23.55	24
BNL-CL2 - pEPO 35.09 36h	7.15	5	1.43	7.15	14.64	34.11	0.85	2.37	20.93	36
BNL-CL2 - pEPO 35.10 38h	13.23	5	2.65	13.23	3.34	34.06	0.01	4.39	16.57	38
BNL-CL2 - pEPO 35.11 40h	12.43	5	2.49	12.43	6.19	33.29	0.07	4.14	18.54	40
BNL-CL2 - pEPO 35.12 42h	14.85	5	2.97	14.85	5.81	33.19	0.01	4.95	20.65	42
BNL-CL2 - pEPO 35.13 44h	13.36	5	2.67	13.36	6.94	34.00	0.00	4.44	20.30	44
BNL-CL2 - pEPO 35.14 46h	14.53	5	2.91	14.53	6.25	32.89	0.10	4.86	20.68	46
BNL-CL2 - pEPO 35.15 48h	14.64	5	2.93	14.64	6.79	33.01	0.00	4.89	21.43	48
BNL-CL2 - pEPO 35.16 60h	9.04	5	1.81	9.04	14.30	32.69	0.03	3.03	23.32	60

References

1. Macleod, J.N.; Tetreault, J.W.; Lorschy, K.A.S.; and Gu, D.N.; Expression and bioactivity of recombinant canine erythropoietin; *American Journal of Veterinary Research* (1998) 59, 1144-1148.

2. Kutschera, C.; Muhr, A.; and Khinast, J.; Vorrichtung zur Entnahme von Proben aus einem Reaktor- oder Kesselsystem, insbesondere Bioreaktoren oder Rührkessel; (2010) CH 29.12.09, 01988/09.

3. Muhr, A.; Richter, U.; Kutschera, C.; and Khinast, J.; Objekthalterung für Lichtmikroskop; (2010) DE G02B 21/26 (2006.01), DE 20 2009 017 583 U1.

4. Godoy-Silva, R.; Chalmers, J.J.; Casnocha, S.A.; Bass, L.A.; and Ma, N.N.; Physiological Responses of CHO Cells to Repetitive Hydrodynamic Stress; *Biotechnology and Bioengineering* (2009) 103, 1103-1117.

5. Godoy-Silva, R.; Mollet, M.; and Chalmers, J.J.; Evaluation of the Effect of Chronic Hydrodynamical Stresses on Cultures of Suspensed CHO-6E6 Cells; *Biotechnology and Bioengineering* (2009) 102, 1119-1130.

6. Xing, Z.Z.; Kenty, B.N.; Li, Z.J.; and Lee, S.S.; Scale-Up Analysis for a CHO Cell Culture Process in Large-Scale Bioreactors; *Biotechnology and Bioengineering* (2009) 103, 733-746.

7. Titchener-Hooker, N.J.; Dunnill, P.; and Hoare, M.; Micro biochemical engineering to accelerate the design of industrial-scale downstream processes for biopharmaceutical proteins; *Biotechnology and Bioengineering* (2008) 100, 473-487.

8. Henzler, H.J. and Biedermann, A.; Model studies on particle stress in reactors; *Chemie Ingenieur Technik* (1996) 68, 1546-1561.

9. Cherry, R.S. and Hulle, C.T.; Cell-death in the thin-films of bursting bubbles; *Biotechnology Progress* (1992) 8, 11-18.

10. Meier, S.J.; Hatton, T.A.; and Wang, D.I.C.; Cell death from bursting bubbles: Role of cell attachment to rising bubbles in sparged reactors; *Biotechnology and Bioengineering* (1999) 62, 468-478.

11. Mardikar, S.H. and Niranjan, K.; Observations on the shear damage to different animal cells in a concentric cylinder viscometer; *Biotechnology and Bioengineering* (2000) 68, 697-704.

12. Mollet, M.; Godoy-Silva, R.; Berdugo, C.; and Chalmers, J.J.; Acute hydrodynamic forces and apoptosis: A complex question; *Biotechnology and Bioengineering* (2007) 98, 772-788.

13. Murhammer, D.W. and Goochee, C.F.; Sparged animal-cell bioreactors - Mechanism of cell-damage and pluronic F-68 protection; *Biotechnology Progress* (1990) 6, 391-397.

14. Bluestein, M. and Mockros, L.F.; Hemolytic Effects of Energy Dissipation in Flowing Blood; *Medical & Biological Engineering* (1969) 7, 1-&.

15. Mollet, M.; Ma, N.N.; Zhao, Y.; Brodkey, R.; Taticek, R.; and Chalmers, J.J.; Bioprocess equipment: Characterization of energy dissipation rate and its potential to damage cells; *Biotechnology Progress* (2004) 20, 1437-1448.

16. Hoerl, W.H. and Wannder, C.; Dialyseverfahren in Klinik und Praxis: Technik und Klinik; (2003) 6,

17. Jelkmann, W.; Erythropoietin - Structure, Control of Production, and Function; *Physiological Reviews* (1992) 72, 449-489.

18. Qiao, L. and Farrell, G.C.; The effects of cell density, attachment substratum and dexamethasone on spontaneous apoptosis of rat hepatocytes in primary culture; *In Vitro Cellular & Developmental Biology-Animal* (1999) 35, 417-424.

19. Narhi, L.O.; Arakawa, T.; Aoki, K.H.; Elmore, R.; Rohde, M.F.; Boone, T.; and Strickland, T.W.; The Effect of Carbohydrate on the Structure and Stability of Erythropoietin; *Journal of Biological Chemistry* (1991) 266, 23022-23026.

20. Al-Fageeh, M.B.; Marchant, R.J.; Carden, M.J.; and Smales, C.M.; The cold-shock response in cultured mammalian cells: Harnessing the response for the improvement of recombinant protein production; *Biotechnology and Bioengineering* (2006) 93, 829-835.

21. Amicone, L.; Spagnoli, F.M.; Spath, G.; Giordano, S.; Tommasini, C.; Bernardini, S.; DeLuca, V.; DellaRocca, C.; Weiss, M.C.; Comoglio, P.M.; and Tripodi, M.; Transgenic expression in the liver of truncated Met blocks apoptosis and permits immortalization of hepatocytes; *Embo Journal* (1997) 16, 495-503.

22. Wang, Y.S. and Fan, O.Y.; Bead-to-bead transfer of Vero cells in microcarrier culture; *Cytotechnology* (1999) 31, 221-224.

23. Aggeler, J.; Kapp, L.N.; Tseng, S.C.G.; and Werb, Z.; Regulation of Protein Secretion in Chinese-Hamster Ovary Cells by Cell-Cycle Position and Cell-Density - Plasminogen-Activator, Procollagen and Fibronectin; *Experimental Cell Research* (1982) 139, 275-283.

24. Yokota, M. and Tanji, Y.; Analysis of cell-cycle-dependent production of tissue plasminogen activator analogue (pamiteplase) by CHO cells; *Biochemical Engineering Journal* (2008) 39, 297-304.

25. Keane, J.T.; Ryan, D.; and Gray, P.P.; Effect of shear stress on expression of a recombinant protein by Chinese hamster ovary cells; *Biotechnol. Bioeng.* (2003) 81, 211-220.

26. Croughan, M.S.; Hamel, J.F.; and Wang, D.I.C.; Hydrodynamic effects on animal cells grown in microcarrier cultures; *Biotechnology and Bioengineering* (2006) 95, 295-305.

27. Hochleitner, B.W.; Hochleitner, E.O.; Obrist, P.; Eberl, T.; Amberger, A.; Xu, Q.B.; Margreiter, R.; and Wick, G.; Fluid shear stress induces heat shock protein 60 expression in endothelial cells in vitro and in vivo; *Arteriosclerosis Thrombosis and Vascular Biology* (2000) 20, 617-623.

28. Tsao, E.I.; Bohn, M.A.; Numsuwan, V.; Omstead, D.R.; and Munster, M.J.; Effects of heat-shock on the production of human erythropoietin from recombinant CHO cells; *Biotechnology and Bioengineering* (1992) 40, 1190-1196.

29. Marks, D.M.; Equipment design considerations for large scale cell culture; *Cytotechnology* (2003) 42, 21-33.

Figures

Tables

Part D

Future aspects

1 Further investigations of stressed mammalian cells

Further investigations with higher flow rates should be conducted, to complete the understanding of the influence of shear stress on mammalian cells. Also the results with different adherent mammalian cell lines and / or different recombinant protein products would strongly increase the understanding of stress levels influencing production. For these approaches the system [(1)] would be available to start the experiments as soon as the desired cells are available.

The process setup itself however, should also be appropriate to investigate a wide variety of phenomena, e.g., the examination of the glycosylation shift at low EDR [(2)]. Furthermore, mechanical stress induces heat shock protein (HSP) production [(3)], and HSPs have a definite influence on protein production [(4)]. Yet another topic will be the study of protein expression as a function of cyclic environmental conditions, e.g., periodic variations in the shear stress. All these studies are important for the design scale-up and optimization of cell culture bioreactors, by determining the relevant factor(s) for a specific mammalian production cell line.

These are the topics that could be examined rather easily with the available process setup. The experimental setup could be adopted for other topics from this field, to achieve a deeper scientific understanding of the influence of mechanical stress on the production of therapeutic proteins. This would enable the design of appropriate scale-up bioreactors rather than trying to fit existing setups to the demand of mammalian cell cultures. Moreover, it could be a step towards designing whole processes and setups ahead of the production.

2 Fixation of living cells by temporary pH-value shift

Experiment 36 was conducted under different settings but opened new possible ways in designing further experiments. An incident during an experiment, which data has not been used, occurred due to a stuck stirrer. The bioreactor control unit tried to maintain pH-value 7.2 ± 0.4 by adding 0.5 M HCl and NaOH, ending up at a pH-value of approximately 3. Surprisingly, cells remained in the collagen IV coated Ibidi™ µ-Slide $I^{0.4}$ Luer. After fixing the stirrer and manually adjusting the pH-value to the correct range, the cells were further observed. They were not only still active but even secreted rhEPO to some extent. Furthermore, the cell number remained nearly constant for up to 60 hours.

Considering, that the cells were being stuck to the collagen IV, a literature research revealed that collagen fibrils tend to tighten to globular structures at pH-values around 3.5 and reform fibrils at pH-values around 7 [(4)]. With this information, the BNL-CL.2 cells for the experiment 36 were seeded overnight in a collagen IV coated Ibidi™ µ-Slide $I^{0.4}$ Luer and treated with pH-value 3.4 for 1 hour at a flow rate of 20 mL/min and 47°C prior to the experiment. Afterwards, the pH-value was restored to 7.2 and the experiment was started keeping the flow rate at 20 mL/min. The further experiment was conducted with the following settings (Table 2.1):

Table 2.1 – Time period, stress level and bioreactor settings for experiment 36

eapsed time:	flow rate (adjusted at peristaltic pump)	EDR (calculated for µ-Slide $I^{0.4}$)	temperature (adjusted at bioreactor)	pH-value (adjusted at bioreactor)	agitation: (adjusted at bioreactor)
Up to 8 hours	20 mL/min	6.25 x 10^3 W/m^3	47°C ± 0.5°C	7.2 ± 0.4	100 rpm
8 to 16 hours	25 mL/min	9.77 x 10^3 W/m^3	44°C ± 0.5°C	7.2 ± 0.4	100 rpm
16 to 24 hours	30 mL/min	1.41 x 10^4 W/m^3	42°C ± 0.5°C	7.2 ± 0.4	100 rpm
24 to 32 hours	35 mL/min	1.91 x 10^4 W/m^3	40°C ± 0.5°C	7.2 ± 0.4	100 rpm
32 to 40 hours	40 mL/min	2.50 x 10^4 W/m^3	37°C ± 0.5°C	7.2 ± 0.4	100 rpm
40 to 48 hours	45 mL/min	3.16 x 10^4 W/m^3	37°C ± 0.5°C	7.2 ± 0.4	100 rpm
48 to 50 hours	50 mL/min	3.91 x 10^4 W/m^3	37°C ± 0.5°C	7.2 ± 0.4	100 rpm

The digital microscope pictures proofed the assumption of strong adherence (Figure 2.1). Even after 50 hours with improving hydrodynamic forces surpassing all previously tested flow rates, most of the cells still remained adherent.

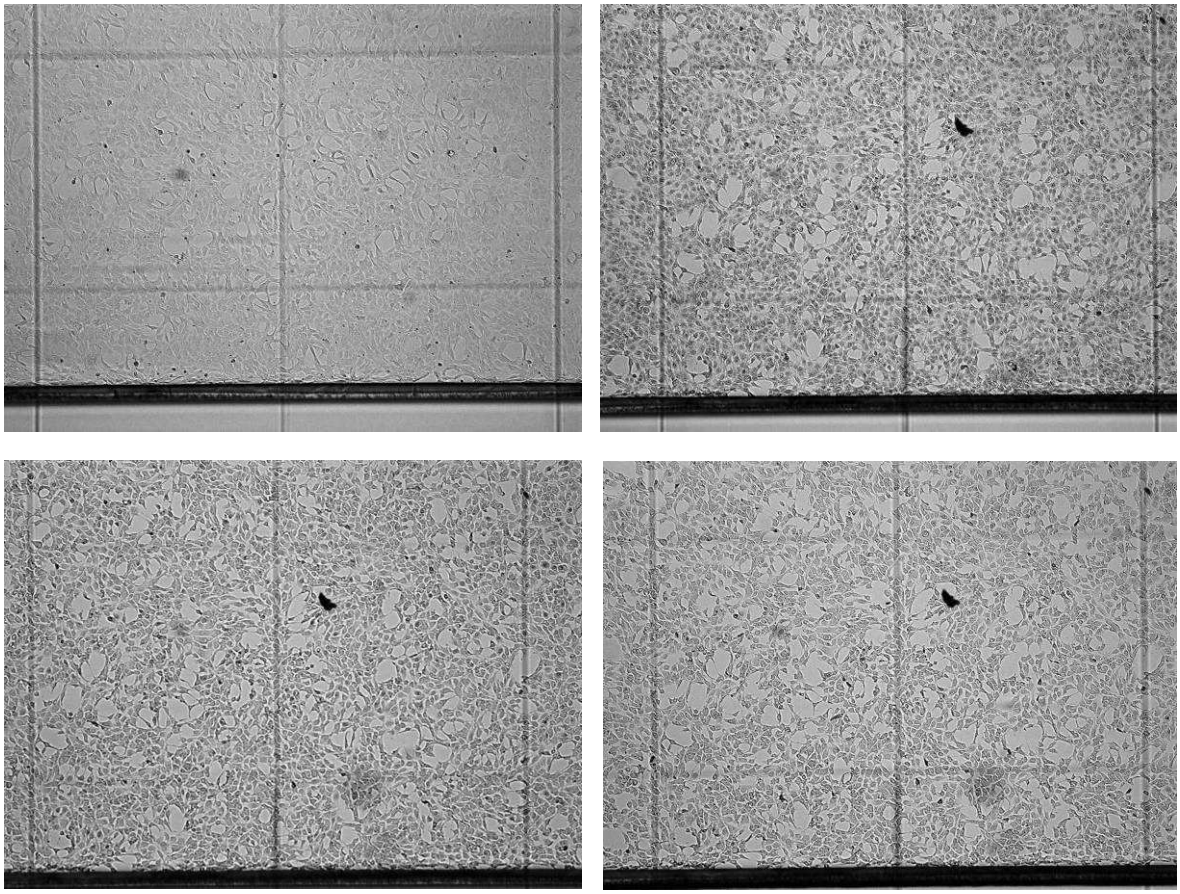

Figure 2.1 – BNL-CL.2 cells prior to pH-value fixation, afterwards and after 26 and 50 hours

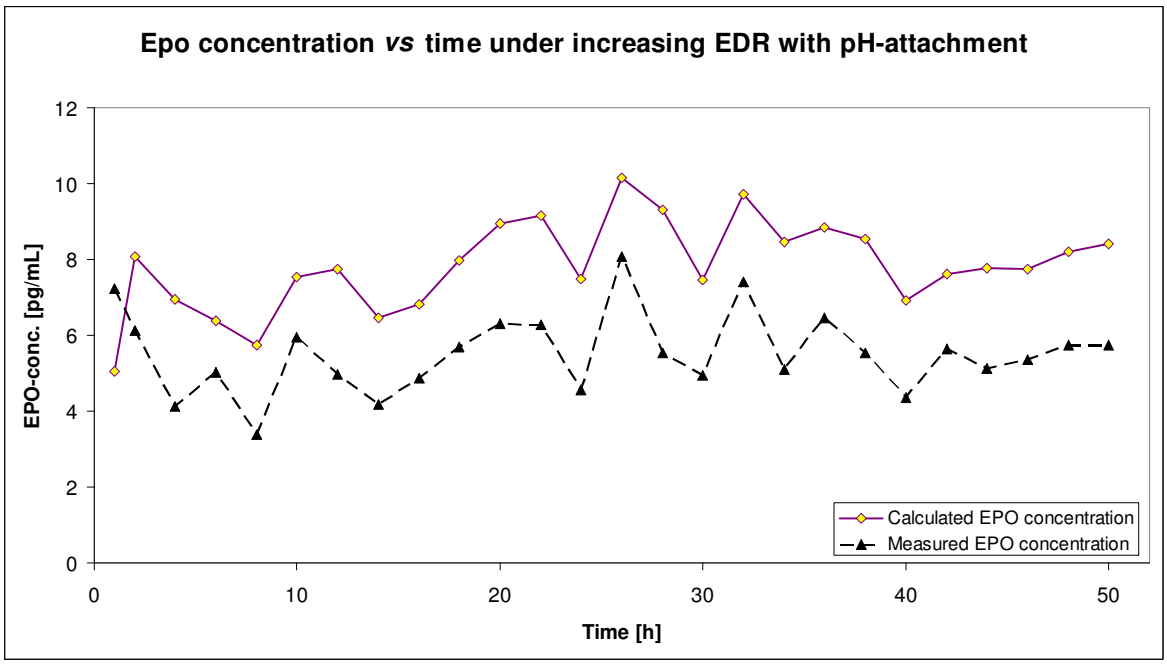

Figure 2.2 – rhEPO concentration [pg/mL] graphed versus time at increasing flow rates

But not only adherence was working far stronger than before, rhEPO measurements also displayed functional secretion of recombinant proteins (Figure 2.2). Compared to the previous results, the output was equal to the experiments with 10 mL/min, but at a slow but quite stable increase after recovery from the pH-value treatment. The generation time had a much lower impact in this experiment than in all others. The raw and calculated data are displayed in Table 2.2.

Of course this is just a first step towards verified results, but the tool of fixation of adherent cells by a temporary pH-value shift might be very convenient for experiments with cells that have lesser adherence than BNL-CL.2 cells. It might even be of interest for the fixation of adherent cells on microcarriers after thorough examination of the production behaviour.

Table 2.2 – Measured and calculated rhEPO values from experiment 36

sample:	measured [mU/mL] EPO value:	concentration factor:	real [mU/mL] EPO value:	real [pg/mL] EPO concentration:	half-life degradation [pg/mL]:	cell covered area [%]:	EPO release from detached cells [pg/mL]:	normalized [mU/mL] EPO value:	normalized [pg/mL] EPO value:	time elapsed [h]:
increasing mL/min										
BNL-CL2 - pEPO 36.02 1h	7.23	5	1.45	7.23	0.00	75.63	2.18	1.80	5.05	1
BNL-CL2 - pEPO 36.03 2h	6.12	5	1.22	6.12	1.95	75.75	0.00	1.52	8.08	2
BNL-CL2 - pEPO 36.04 4h	4.12	5	0.82	4.12	2.86	75.45	0.03	1.03	6.96	4
BNL-CL2 - pEPO 36.05 6h	5.04	5	1.01	5.04	1.93	69.12	0.57	1.32	6.40	6
BNL-CL2 - pEPO 36.06 8h	3.39	5	0.68	3.39	2.35	75.83	0.00	0.84	5.74	8
BNL-CL2 - pEPO 36.07 10h	5.95	5	1.19	5.95	1.58	76.51	0.00	1.47	7.53	10
BNL-CL2 - pEPO 36.08 12h	4.98	5	1.00	4.98	2.78	76.19	0.03	1.23	7.73	12
BNL-CL2 - pEPO 36.09 14h	4.18	5	0.84	4.18	2.33	75.84	0.03	1.04	6.47	14
BNL-CL2 - pEPO 36.10 16h	4.88	5	0.98	4.88	1.95	76.24	0.00	1.21	6.83	16
BNL-CL2 - pEPO 36.11 18h	5.68	5	1.14	5.68	2.28	76.62	0.00	1.40	7.96	18
BNL-CL2 - pEPO 36.12 20h	6.30	5	1.26	6.30	2.66	77.63	0.00	1.54	8.96	20
BNL-CL2 - pEPO 36.13 22h	6.28	5	1.26	6.28	2.94	76.77	0.08	1.55	9.15	22
BNL-CL2 - pEPO 36.14 24h	4.56	5	0.91	4.56	2.94	77.03	0.00	1.12	7.50	24
BNL-CL2 - pEPO 36.15 26h	8.07	5	1.61	8.07	2.13	76.41	0.06	1.99	10.15	26
BNL-CL2 - pEPO 36.16 28h	5.53	5	1.11	5.53	3.77	76.74	0.00	1.36	9.30	28
BNL-CL2 - pEPO 36.17 30h	4.95	5	0.99	4.95	2.58	75.88	0.08	1.23	7.45	30
BNL-CL2 - pEPO 36.18 32h	7.40	5	1.48	7.40	2.31	76.44	0.00	1.83	9.72	32
BNL-CL2 - pEPO 36.19 34h	5.11	5	1.02	5.11	3.46	75.35	0.10	1.27	8.47	34
BNL-CL2 - pEPO 36.20 36h	6.46	5	1.29	6.46	2.39	75.35	0.00	1.61	8.84	36
BNL-CL2 - pEPO 36.21 38h	5.53	5	1.11	5.53	3.02	75.56	0.00	1.38	8.54	38
BNL-CL2 - pEPO 36.22 40h	4.37	5	0.87	4.37	2.58	75.14	0.04	1.09	6.91	40
BNL-CL2 - pEPO 36.23 42h	5.65	5	1.13	5.65	2.04	74.16	0.09	1.42	7.60	42
BNL-CL2 - pEPO 36.24 44h	5.14	5	1.03	5.14	2.64	74.89	0.00	1.29	7.78	44
BNL-CL2 - pEPO 36.25 46h	5.37	5	1.07	5.37	2.40	74.64	0.02	1.35	7.75	46
BNL-CL2 - pEPO 36.26 48h	5.74	5	1.15	5.74	2.51	74.12	0.05	1.44	8.20	48
BNL-CL2 - pEPO 36.27 50h	5.75	5	1.15	5.75	2.68	73.70	0.04	1.45	8.40	50

References

1. Muhr, A.; Kutschera, C.; and Khinast, J.; Steriles invitro Messverfahren für adhärente Säugetierzellen; (2011) A 266/2011, pending.

2. Godoy-Silva, R.; Chalmers, J.J.; Casnocha, S.A.; Bass, L.A.; and Ma, N.N.; Physiological Responses of CHO Cells to Repetitive Hydrodynamic Stress; *Biotechnology and Bioengineering* (2009) 103, 1103-1117.

3. Hochleitner, B.W.; Hochleitner, E.O.; Obrist, P.; Eberl, T.; Amberger, A.; Xu, Q.B.; Margreiter, R.; and Wick, G.; Fluid shear stress induces heat shock protein 60 expression in endothelial cells in vitro and in vivo; *Arteriosclerosis Thrombosis and Vascular Biology* (2000) 20, 617-623.

4. Jiang, F.Z.; Horber, H.; Howard, J.; and Muller, D.J.; Assembly of collagen into microribbons: effects of pH and electrolytes; *Journal of Structural Biology* (2004) 148, 268-278.

Figures

Tables